



International Agreement Report

Assessment of RELAP5/MOD2 Critical Flow Model Using Marviken Test Data 15 and 24

Prepared by
K. Kim, H.-J. Kim

Korea Institute of Nuclear Safety
Safety Analysis Department
P.O. Box 16, Daeduk-Danji
Taejeon, Korea

Office of Nuclear Regulatory Research
U.S. Nuclear Regulatory Commission
Washington, DC 20555

April 1992

Prepared as part of
The Agreement on Research Participation and Technical Exchange
under the International Thermal-Hydraulic Code Assessment
and Application Program (ICAP)

Published by
U.S. Nuclear Regulatory Commission

92060500B2 920430
PDR NUREG
IA-0086 R PDR

NOTICE

This report was prepared under an international cooperative agreement for the exchange of technical information.* Neither the United States Government nor any agency thereof, or any of their employees, makes any warranty, expressed or implied, or assumes any legal liability or responsibility for any third party's use, or the results of such use, of any information, apparatus product or process disclosed in this report, or represents that its use by such third party would not infringe privately owned rights.

Available from

Superintendent of Documents
U.S. Government Printing Office
P.O. Box 37082
Washington, D.C. 20013-7082

and

National Technical Information Service
Springfield, VA 22161



International Agreement Report

Assessment of RELAP5/MOD2 Critical Flow Model Using Marviken Test Data 15 and 24

Prepared by
K. Kim, H.-J. Kim

Korea Institute of Nuclear Safety
Safety Analysis Department
P.O. Box 16, Daeduk-Danji
Taejeon, Korea

Office of Nuclear Regulatory Research
U.S. Nuclear Regulatory Commission
Washington, DC 20555

April 1992

Prepared as part of
The Agreement on Research Participation and Technical Exchange
under the International Thermal-Hydraulic Code Assessment
and Application Program (ICAP)

Published by
U.S. Nuclear Regulatory Commission

NOTICE

This report is based on work performed under the sponsorship of The Korea Advanced Energy Institute of Korea. The information in this report has been provided to the USNRC under the terms of an information exchange agreement between the United States and Korea (Agreement on Thermal-Hydraulic Research between the United States Nuclear Regulatory Commission and The Korea Advanced Energy Research Institute, May 1, 1985). Korea has consented to the publication of this report as a USNRC document in order that it may receive the widest possible circulation among the reactor safety community. Neither the United States Government nor Korea or any agency thereof, or any of their employees, makes any warranty, expressed or implied, or assumes any legal liability of responsibility for any third party's use, or the results of such use, or any information, apparatus, product or process disclosed in this report or represents that its use by such third party would not infringe privately owned rights.

ICAP

Assessment of RELAP5/MOD2 Critical Flow Model Using Marviken

Test Data 15 and 24

ABSTRACT

The simulations of Marviken CFT 15 and 24 have been performed using RELAP5/MOD2. For the modeling of a nozzle as a pipe, the results of simulations and the CFT 15 test data are in good agreement, but the simulations underpredict by about 5 to 10 % in transition region between subcooled and two-phase. In the two phase region, there happens the fluctuations of the calculated mass flowrate for the case of using the critical flow model in RELAP5/MOD3. It seems that the improvement of the critical flow model in RELAP5 during the transition period is necessary. RELAP5 critical flow model underpredicts the CFT 24 data by 10 to 20 % in two phase choked flow region, while its predictions are in good agreement with subcooled choked flowrate data. The modeling of a nozzle as a pipe in the case of CFT 24 may give rise of unreasonable results in subcooled critical flow region.

LIST OF CONTENTS	PAGE
ABSTRACT	iii
EXECUTIVE SUMMARY	xi
ACKNOWLEDGEMENT	xiii
1. Introduction	1
2. Facility And Test Description	3
2.1. Test Facility	3
2.2. Test Description	4
3. Code And Model Description	9
3.1. Code Features	9
3.2. Input Description	10
4. Results and Discussion	14
4.1. Critical Flow Test 15	14
4.2. Critical Flow Test 24	18
4.3. Evaluation of the Model in RELAP5/MOD3	21
5. Computational Efficiency	64
6. Conclusions	66
References	68
APPENDIX A - RELAP5 INPUT DECK FOR CFT 15	69
APPENDIX B - RELAP5 INPUT DECK FOR CFT 24	76

List of Tables

Table 2-1	Dimensions of test nozzles	4
Table 2-2	Summary of initial and final conditions in test 15 and 24	5
Table 3-1	Summary of case study	12
Table 5-1	Run statistics for CFT 15 simulations	64
Table 5-2	Run statistics for CFT 24 simulations	65

List of Figures

Fig. 2-1	Diagram of the facility, including flow path during the CFT	6
Fig. 2-2	Diagram of discharge pipe, including measurements	7
Fig. 2-3	Dimensions of the test nozzles used from test 15 onwards	8
Fig. 3-1	Nodalization of Marviken facility	13
Fig. 4-1	Comparison of calculated and measured mass flowrate for CFT 15(CASE 1)	23
Fig. 4-2	Comparison of calculated and measured pressure at nozzle inlet for CFT 15(CASE 1)	23
Fig. 4-3	Comparison of calculated and measured void fraction at nozzle inlet for CFT 15(CASE 1)	24
Fig. 4-4	Comparison of calculated and measured density at discharge pipe for CFT 15(CASE 1)	24
Fig. 4-5	Void fraction and quality at break for CFT 15(CASE 1)	25
Fig. 4-6	Critical velocity at break junction for CFT 15(CASE 1)	25
Fig. 4-7	Liquid temperature at nozzle for CFT 15(CASE 1)	26
Fig. 4-8	Comparison of calculated and measured mass flowrate for CFT 15(CASE 2)	27

Fig. 4-9 Comparison of calculated and measured pressure at nozzle inlet for CFT 15(CASE 2)	27
Fig. 4-10 Comparison of calculated and measured void fraction at nozzle inlet for CFT 15(CASE 2)	28
Fig. 4-11 Comparison of calculated and measured density at discharge pipe for CFT 15(CASE 2)	28
Fig. 4-12 Void fraction and quality at break for CFT 15(CASE 2)	29
Fig. 4-13 Critical velocity at break junction for CFT 15(CASE 2)	29
Fig. 4-14 Comparison of calculated and measured mass flowrate for CFT 15(CASE 3)	30
Fig. 4-15 Comparison of calculated and measured pressure at nozzle inlet for CFT 15(CASE 3)	30
Fig. 4-16 Comparison of calculated and measured void fraction at nozzle inlet for CFT 15(CASE 3)	31
Fig. 4-17 Comparison of calculated and measured density at discharge pipe for CFT 15(CASE 3)	31
Fig. 4-18 Void fraction and quality at break for CFT 15(CASE 3)	32
Fig. 4-19 Critical velocity at break junction for CFT 15(CASE 3)	32
4-20 Liquid temperature at nozzle for CFT 15(CASE 3)	33
4-21 Comparison of calculated and measured mass flowrate for CFT 15(CASE 4)	34
Fig. 4-22 Comparison of calculated and measured pressure at nozzle inlet for CFT 15(CASE 4)	34
Fig. 4-23 Comparison of calculated and measured void fraction at nozzle inlet for CFT 15(CASE 4)	35
Fig. 4-24 Comparison of calculated and measured density at discharge pipe for CFT 15(CASE 4)	35
Fig. 4-25 Void fraction and quality at break for CFT 15(CASE 4)	36
Fig. 4-26 Critical velocity at break junction for CFT 15(CASE 4)	36

Fig. 4-27 Comparison of mass flowrate for case 1 and case 7 of CFT 15	37
Fig. 4-28 Comparison of mass flowrate for case 2 and case 8 of CFT 15	37
Fig. 4-29 Comparison of calculated and measured mass flowrate for CFT 24(CASE 1)	38
Fig. 4-30 Comparison of calculated and measured pressure at nozzle inlet for CFT 24(CASE 1)	38
Fig. 4-31 Comparison of calculated and measured void fraction at nozzle inlet for CFT 24(CASE 1)	39
Fig. 4-32 Comparison of calculated and measured density at discharge pipe for CFT 24(CASE 1)	39
Fig. 4-33 Void fraction and quality at break for CFT 24(CASE 1)	40
Fig. 4-34 Critical velocity at break junction for CFT 24(CASE 1)	40
Fig. 4-35 Liquid temperature at nozzle for CFT 24(CASE 1)	41
Fig. 4-36 Comparison of calculated and measured mass flowrate for CFT 24(CASE 2)	42
Fig. 4-37 Comparison of calculated and measured pressure at nozzle inlet for CFT 24(CASE 2)	42
Fig. 4-38 Comparison of calculated and measured void fraction at nozzle inlet for CFT 24(CASE 2)	43
Fig. 4-39 Comparison of calculated and measured density at discharge pipe for CFT 24(CASE 2)	43
Fig. 4-40 Void fraction and quality at break for CFT 24(CASE 2)	44
Fig. 4-41 Critical velocity at break junction for CFT 24(CASE 2)	44
Fig. 4-42 Liquid temperature at nozzle for CFT 24(CASE 2)	45
Fig. 4-43 Comparison of calculated and measured mass flowrate for CFT 24(CASE 3)	46
Fig. 4-44 Comparison of calculated and measured pressure at nozzle inlet for CFT 24(CASE 3)	46

Fig. 4-45 Comparison of calculated and measured void fraction at nozzle inlet for CFT 24(CASE 3)	47
Fig. 4-46 Comparison of calculated and measured density at discharge pipe for CFT 24(CASE 3)	47
Fig. 4-47 Void fraction and quality at break for CFT 24(CASE 3)	48
Fig. 4-48 Critical velocity at break junction for CFT 24(CASE 3)	48
Fig. 4-49 Liquid temperature at nozzle for CFT 24(CASE 3)	49
Fig. 4-50 Comparison of calculated and measured mass flowrate for CFT 24(CASE 5)	50
Fig. 4-51 Comparison of calculated and measured pressure at nozzle inlet for CFT 24(CASE 5)	50
Fig. 4-52 Comparison of calculated and measured void fraction at nozzle inlet for CFT 24(CASE 5)	51
Fig. 4-53 Comparison of calculated and measured density at discharge pipe for CFT 24(CASE 5)	51
Fig. 4-54 Void fraction and quality at break for CFT 24(CASE 5)	52
Fig. 4-55 Critical velocity at break junction for CFT 24(CASE 5)	52
Fig. 4-56 Liquid temperature at nozzle for CFT 24(CASE 5)	53
Fig. 4-57 Comparison of calculated and measured mass flowrate for CFT 15(CASE5-MOD3)	54
Fig. 4-58 Comparison of calculated and measured pressure at nozzle inlet for CFT 15(CASE5-MOD3)	54
Fig. 4-59 Comparison of calculated and measured void fraction nozzle inlet for CFT 15(CASE5-MOD3)	55
Fig. 4-60 Comparison of calculated and measured density at discharge pipe for CFT 15(CASE5-MOD3)	55
Fig. 4-61 Void fraction and quality at break for CFT 15(CASE5-MOD3)	56
Fig. 4-62 Critical velocity at break junction for CFT 15(CASE5-MOD3)	56

Fig. 4-63 Liquid temperature at nozzle for CFT 15(CASE5-MOD3)	57
Fig. 4-64 Comparison of calculated and measured mass flowrate for CFT 15(CASE6-MOD3)	58
Fig. 4-65 Comparison of calculated and measured pressure at nozzle inlet for CFT 15(CASE6-MOD3)	58
Fig. 4-66 Comparison of calculated and measured void fraction at nozzle inlet for CFT 15(CASE6-MOD3)	59
Fig. 4-67 Comparison of calculated and measured density at discharge pipe for CFT 15(CASE6-MOD3)	59
Fig. 4-68 Void fraction and quality at break for CFT 15(CASE6-MOD3)	60
Fig. 4-69 Critical velocity at break junction for CFT 15(CASE6-MOD3)	60
Fig. 4-70 Comparison of calculated and measured mass flowrate for CFT 24(CASE4-MOD3)	61
Fig. 4-71 Comparison of calculated and measured pressure at nozzle inlet for CFT 24(CASE4-MOD3)	61
Fig. 4-72 Comparison of calculated and measured void fraction at nozzle inlet for CFT 24(CASE4-MOD3)	62
Fig. 4-73 Comparison of calculated and measured density at discharge pipe for CFT 24(CASE4-MOD3)	62
Fig. 4-74 Void fraction and quality at break for CFT 24(CASE4-MOD3)	63
Fig. 4-75 Critical velocity at break junction for CFT 24(CASE4-MOD3)	63

EXECUTIVE SUMMARY

The assessment of RELAP5/MOD2 critical flow model has been carried out using Marviken critical flow test 15 and 24. The purpose of this assessment is to identify the code or model deficiencies, and to improve the capability of the RELAP5 for the prediction of critical flowrate.

Marviken critical flow tests were conducted between 1977 and 1979 as a multi-national project at the Marviken Power Station. The Marviken test facility consisted of a vessel of 5.2 m in diameter and 22 m high, a discharge pipe with a ball valve, a nozzle containing ruptured discs and a containment. Through the Marviken test program, the 27 CFT experiments, together with the test procedures, equipments and measurement techniques were produced.

To assess the capability of RELAP5/MOD2 critical flow model, our concern is focused on the nodalization of a nozzle, the time step of calculation, and the computational efficiency.

For CFT 15 with a L/D of 3.6, which is one of the largest among 27 tests, the simulations are performed with changing the modeling of a nozzle as a pipe having 3 cells or one cell. While the simulation predicts test data inappropriately in the case of modeling of a discharge pipe of 3 cells, the results of simulation are in good agreement with test data for modeling of a discharge pipe of 6 cells uniformly.

For CFT 24 with a L/D of 0.6, smallest among 27 tests, the simulations are also performed with varying the modeling of a nozzle as a single junction or a pipe having 2 cells or one cell. However, the results of simulation with modeling of a nozzle as a pipe are not in good agreement with test data. For the modeling of a nozzle as a single junction, the simulation predicts well subcooled critical flowrate, but underpredicts two phase critical flowrate by 10 to 20 %.

It is found that the success of simulation depends how a nozzle is modeled according to a L/D of nozzle.

Acknowledgement

This report was completed under the sponsorship of the Korean Ministry of Science and Technology. Dr. Sang Hoon Lee, President of the Korea Institute of Nuclear Safety, contributed significantly to the project administration.

Authors expressed a great appreciation to professors K. C. Park, E. C. Lee in Seoul National University and professors M. H. Chun, H. C. No in Korea Advanced Institute of Science and Technology for their in-depth technical reviews in Korea.

1. Introduction

In RELAP5, the mass discharge from the system through a pipe break or a nozzle is calculated primarily by a critical flow model consisted of the Lienard-Alamgir-Jones(LAJ) model for subcooled choking and the model developed by Ranson and Trapp for two-phase choking. In the critical flow model of RELAP5, the critical velocity of flow is calculated using the upstream properties as the second relation, which may represent incorrect prediction of the choking phenomena at throat.

It is well-known, that choking occurs when the flow velocity exceeds or equal to local pressure propagation velocity, and that the critical velocity of single-phase flow is same as the sound speed. However, the choked conditions of two-phase flow are different from those of single-phase flow, and the critical velocity of two-phase flow can not be characterized as the sound speed. Even though the liquid in system is subcooled enough, the discharge flow from the system may vary from subcooled liquid to two-phase mixture passing through a pipe break or a nozzle. Many researches have been studied on the critical two-phase flow and many critical flow models for two-phase flow have been generated. However, there are still exist many uncertainties and inconsistencies in the two-phase critical flow model, because of the difficulties to solve a critical

flow mechanisms completely for two-phase flow using only field equations. In RELAP5, the thermal equilibrium assumption with phase slip is used as the basis for the critical flow criterion.

As a part of the International Thermal-Hydraulic Code Assessment and Applications Program (ICAP), the assessment of the RELAP5 for the critical flow model has been carried out. The purpose of this assessment is to evaluate the capability of RELAP5 to simulate a critical flow, and to improve the nodalizations for a pipe break or a nozzle. In addition, the assessment is carried out to evaluate the adequacy of the critical flow model improved in RELAP5/MOD3. For this assessment, Marviken critical flow test facility is simulated. And the critical flow results from the RELAP5 are compared with the experimental data of Marviken critical flow test number 15 and 24.

A brief description of Marviken facility and tests is provided in section 2. The critical flow model in RELAP5 and the input deck used to simulate the experiments are described in section 3. Section 4 describes the results and discussion of the calculations for nodalization. Computational efficiency is discussed in section 5. Conclusions are presented in section 6.

2. Facility And Test Description

2.1 Test Facility

The Marviken Full Scale Critical Flow Tests(CFTs) were conducted between mid-1977 and Dec. 1979 as a multi-national project at the Marviken Power Station, which had produced the twenty-seven CFT experiments. The tests were conducted by discharging water and steam water mixtures from a full sized reactor vessel through a large diameter discharge pipe that supplied the flow to the test nozzle and mounted on the bottom of a vessel.

Vertical cross-sectional views of the test facility and of the discharge pipe, test nozzle are shown in figures 2-1 and 2-2. The major components of the facility are the pressure vessel having net-volume of 425 cubic-meter, the discharge pipe consisting of the ball valve and pipe spools, the test nozzle and rupture disc assemblies, and the containment and exhaust pipe. The nozzles ranged in length from 166 to 1809 mm and in diameter from 200 to 500 mm, which have similarity to the pipe of broken loop at large break LOCA in nuclear power plant.

Tests 15 through 27 were conducted using a constant diameter test nozzle section of 500 mm and length to diameter ratio(L/D) of 0.3 and 3.7 to provide full scale critical flow data at LBLOCA for operational nuclear power plants. For the tests 15 and 24, the

dimensions of the test nozzle section are summarized in table 2-1 and are shown in figure 2-3.

Table 2-1 Dimensions of Test Nozzles

Test Number	D (mm)	L (mm)	L/D	L1 (mm)	L2 (mm)	L3 (mm)	L4 (mm)	R (mm)
15	500	1809	3.6	0	181	156	241	250
24	500	166	0.3	0	225	225	250	250

2.2 Test Description

The test matrix of Marviken CFT is classified as category I, II and III according to initial subcooling. Category I tests were conducted with water initially subcooled 15 °C or more, and category III is the group of tests initially subcooled less than 5 °C. Both test 15 and test 24 are belong to category II tests, which conducted with a modified vessel temperature profiles and with water subcooled 30 °C or more. The test conditions are listed in table 2-2. The test objective of test 15 is to examine the effect of new initial temperature profiles of category II tests. And the test 24 is for the definition of short L/D in category II condition. Both CFT 15 and CFT 24 were conducted under similar initial conditions, but nozzle geometry and initial temperature at nozzle inlet. Initial

temperature at nozzle inlet is meaningless, because the liquid in nozzle is discharged simultaneously with the start of test. The results of these CFI's could show the effect of L/D on the critical flow.

Table 2-2 Summary of Initial and Final Conditions in Test 15 and 24

1	Test Number	15	24
2	Date of Test Performance	11-01, '78	03-29, '79
3	Steam Dome Pressure (MPa)	5.04	4.96
4	Saturation Temperature (°C)	264	263
5	Degree of Nominal Subcooling in the Lower Vessel (°C)	31	33
6	Minimum Fluid Temperature in the Vessel (°C)	233	230
7	Initial Temperature at Nozzle Inlet (°C)	177	27
8	Mass of Water and Steam (Mg) (Include the Water in Discharge Pipe)	327	330
9	Mass of Steam (Mg)	0.6	0.63
10	Mass of Saturated Water (Mg)	73.1	39.4
11	Initial Level in the Vessel (m)	19.93	19.88
12	Final Level in the Vessel (m)	< 0.74	< 0.74
13	Nominal Elevation of Tr ₁ Δz_{10} (m) ± 0.5	12.5-14	15.5-17
14	Oxygen Content Obtained after stabilization at 3 MPa (mole ratio x E6)	0.8	0.5
15	Test Period (seconds)	55	54

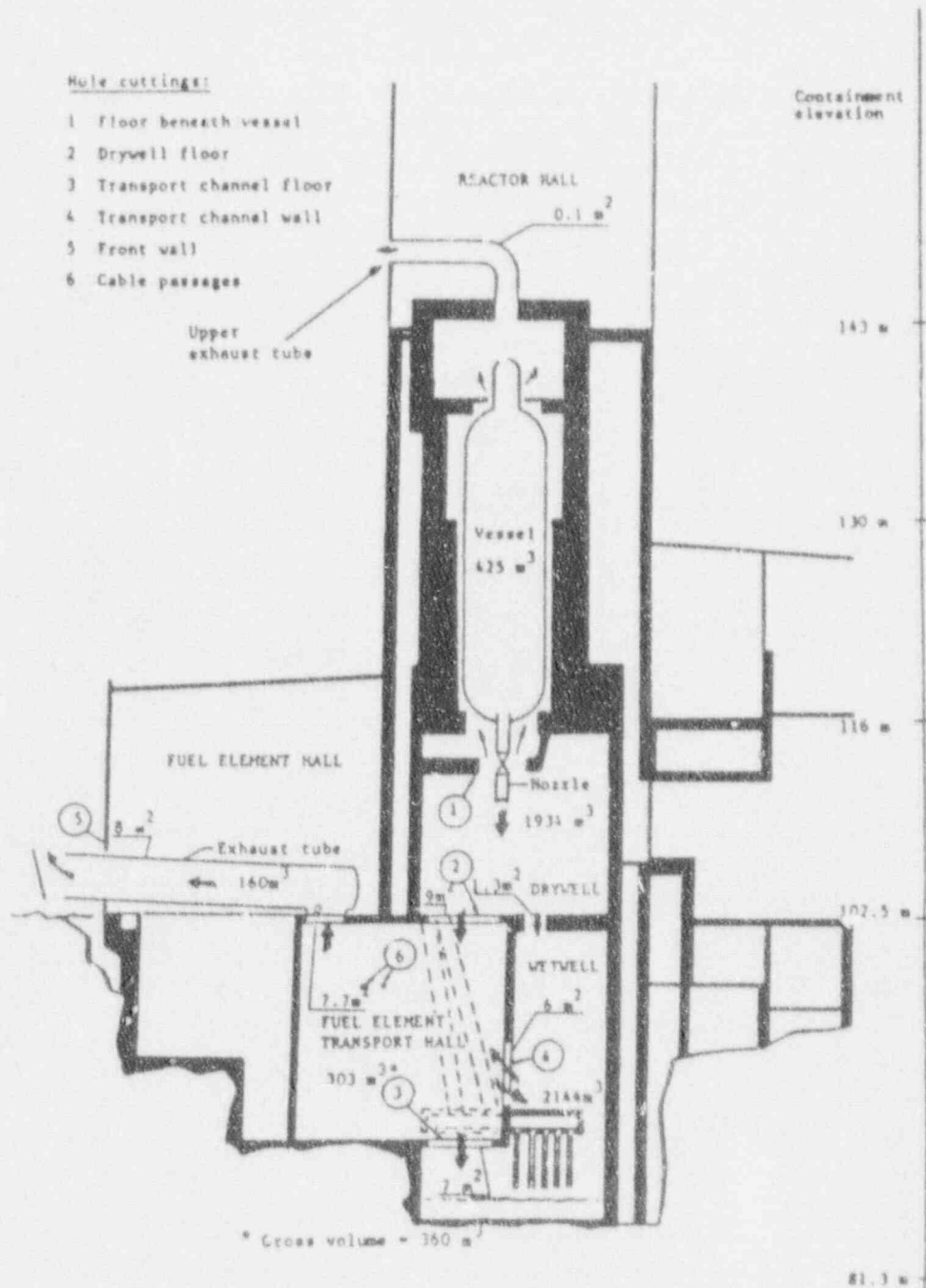


Fig. 2-1 Diagram of the Facility, including Flow Path during the CFT

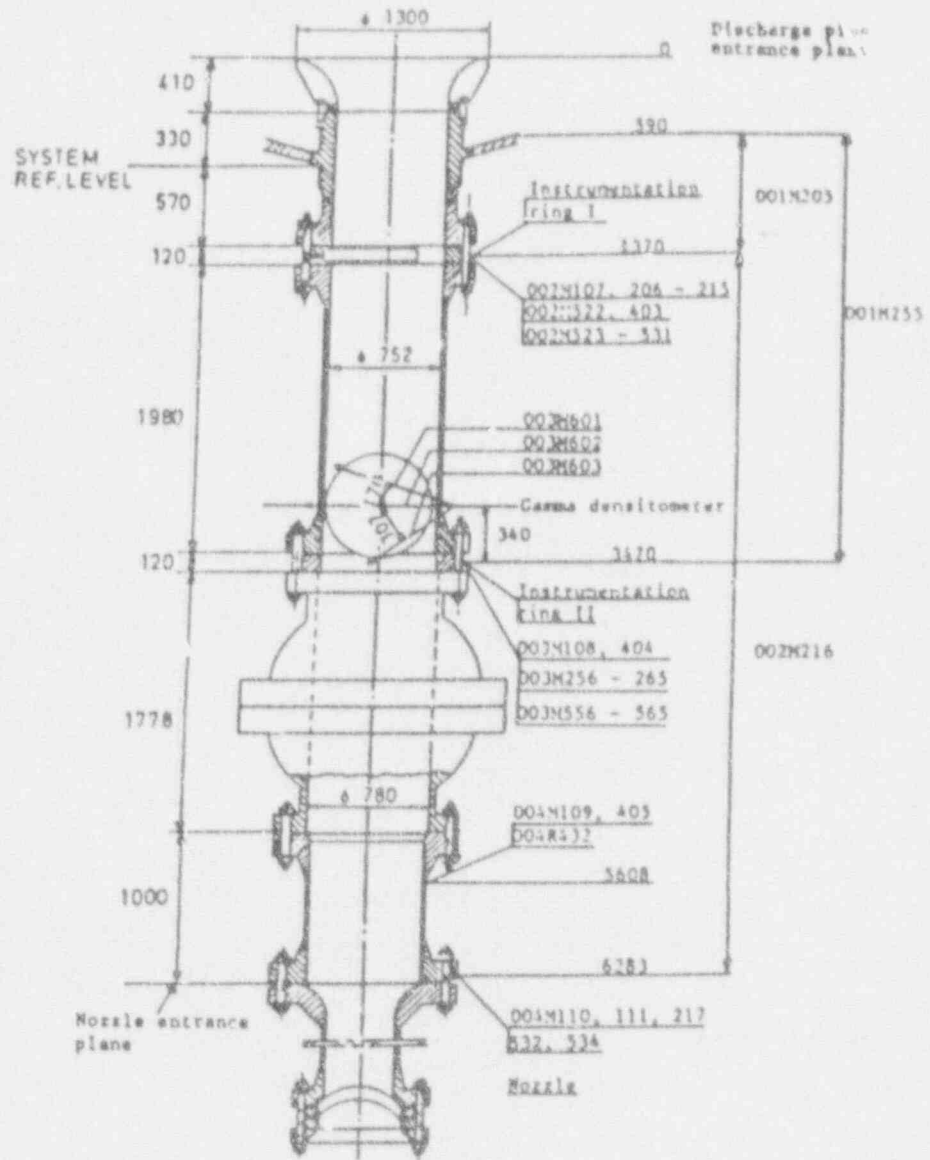


Fig. 2-2 Diagram of Discharge pipe, including measurements

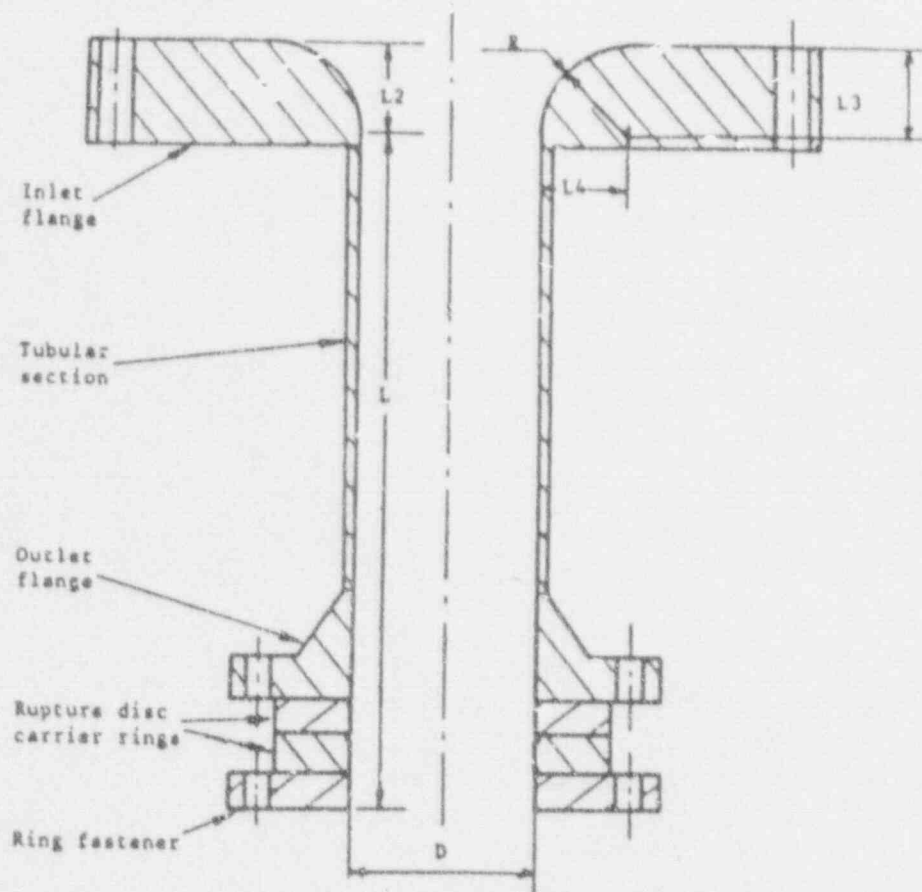


Fig. 2-3 Dimensions of the test nozzles used from Test 15 onwards

3. Code And Model Description

3.1 Code Features

RELAP5 has two types of critical flow models. One is for subcooled critical flow model and the other is for two-phase critical flow model. Both models are applied only at junctions.

The subcooled critical flow model used in RELAP5 is similar conceptually to the model proposed by Burnell and is designed to reflect the physics occurring during the break flow process. The RELAP5 subcooled critical flow model assumes the Bernoulli expansion to the point of vapor inception at the choke plane.

The two-phase critical flow model in RELAP5 is based on the model by Trapp and Ransom for non-homogeneous, non-equilibrium flow. In this model, the analytic choking criteria was determined by a characteristic analysis of a two-fluid model that included relative phasic acceleration terms and derivative dependent mass transfer. Although both frozen flow and thermal equilibrium assumptions were employed to test the analytic criteria during the implement of this model, the thermal equilibrium assumption was proved to be appropriate by comparisons to experimental data. Because the application of the two-phase choking criterion has not been fully explored, an approximate criterion has been applied extensively through the good code and data comparisons.

The critical flow model in RELAP5/MOD3 has been modified to correct or mitigate the effects of several deficiencies identified previously during the assessments of RELAP5/MOD2 as part of the ICAP. The deficiencies were identified as the computation of the throat mixture internal energy, and the prediction of the throat state and the transition between two states of subcooled and two-phase.

3.2 Input Description

To assess the critical flow model in RELAP5, the Marviken CFT 15 and 24 are simulated. Both test conditions belong to category I7, but are different in L/Ds, 3.6 and 0.3.

The nodalization of Marviken facility consists of a vessel, a discharge pipe, a nozzle and a containment, as shown in figure 3-1. The vessel is modeled by a PIPE component with thirty-nine cells(nodes) and is connected with a discharge pipe by SNGLJUN component where the smooth area change option is used to exclude undesired pressure drop. A vessel is subdivided into many cells to provide the correct distribution of pressure and temperature in a vessel during transient, instead of modelling as a TMDPVOL. For the sensitivity analysis of nodalization, the discharge pipe is modeled by a PIPE component having three or six cells, and is connected a

nozzle by SNGLJUN component. Also, a nozzle is modeled as a PIPE component or a VALVE component which is applied to simulation of CFT 24 having small L/D. The cell number of a discharge pipe and a nozzle is summarized in table 3-1. A nozzle is connected to a containment, and the junction or valve attached to the bottom of a nozzle opens simultaneously at the start of transient. A containment is represented by a TMDPVOL component filled with pure vapor in atmospheric conditions.

Because of the negligible effect of the heat transfer from vessel to containment on the CFT modelling, the heat structures of a vessel, a discharge pipe and a nozzle are not considered.

In order to establish the initial conditions of tests, the steady state simulation is performed. By means of attaching a TMDPVOL component to the top of vessel, the pressures and temperatures at vessel and discharge pipe are obtained appropriately. The water level of vessel is determined by adjusting the fluid qualities in vessel.

The time step is set up minutely up to twenty seconds from the start of test because of complex critical flow phenomena at the inception and transition. And the transient is simulated up to sixty seconds similar to the test period.

Table 3-1. Summary of Case Study

Test No.	Case	Code	Number of Nodes		Remark
			Nozzle	Discharge	
CFT #15 L/D =3.6	Case 1	MOD2	3	5	* Application of choking option at only break
	Case 2	"	1	6	
	Case 3	"	3	3	
	case 4	"	1	3	
	Case 5	MOD3	3	6	* For comparison with RELAP5/MOD3
	Case 6	"	1	3	
	Case 7	MOD2	3	6	* Application of
	case 8	"	1	6	choking option at every junctions
CFT #24 L/D =0.3	Case 1	MOD2	0	6	* Choking option at only break.
	Case 2	"	2	6	
	Case 3	"	0	3	
	Case 4	MOD3	0	6	
	Case 5	MOD2	1	6	* Choking option at every junctions

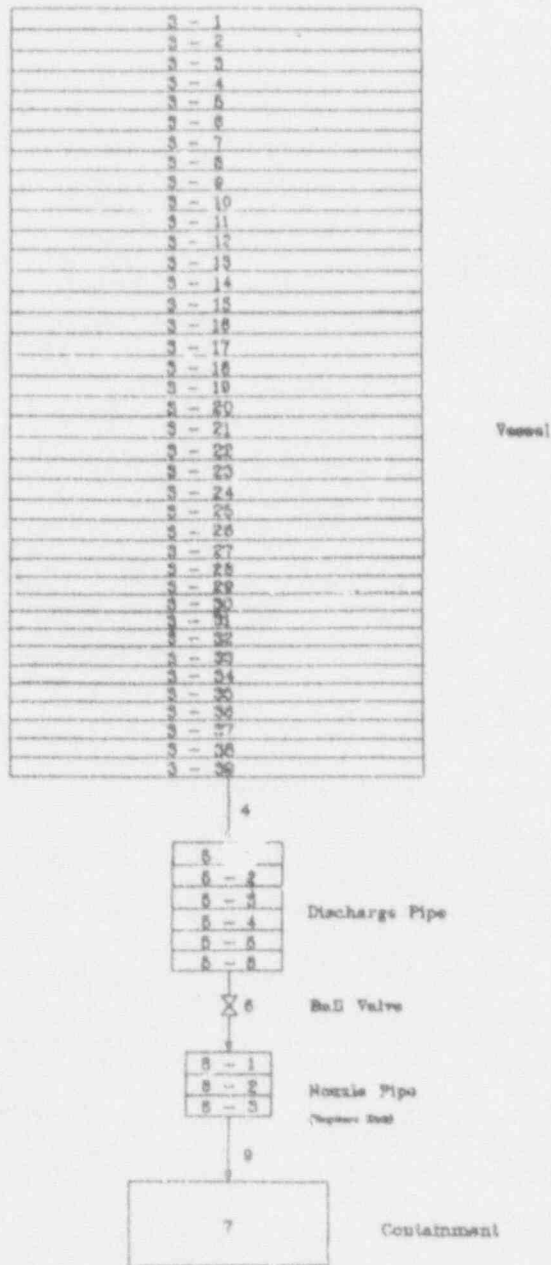


Fig. 3-1 Nodalization of Marviken Facility

4. Results and Discussion

4.1 Critical Flow Test 15

For the CFT 15 with a relatively long nozzle, it is important that how to simulate a nozzle is adequate and what cell number of of a nozzle is optimal. Thus, a nozzle is modelled as a PIPE component with 3 cells or as a SINGVOL component. Additionally, the nodalization of a discharge pipe is evaluated. The cell numbers of a nozzle and a discharge pipe are summarized in table 3-1. The transient input deck is prepared with the results from the steady state calculation to obtain the initial conditions for CFT 15. The calculations proceed up to sixty seconds as in the case of actual test periods. There are some problems during the transient calculation when the choking option is used at every junctions. These problems may be caused by the critical flow inadequately occurred at upper junction of a nozzle, which may restrict the flow toward nozzle outlet. Hence, the calculations are carried out using the choking option at only throat and compared with other cases.

To study the sensitivity to the nodalization for the case of CFT 15 (CASE 1), the nozzle is modeled with 3 cells considering a nozzle shape. That is, first cell as a nozzle inlet, second and third cells as the remainder are modeled. In the CASE 1, the discharge pipe has 6 cells and a smooth area change option is used

in the junction connecting a discharge pipe and a nozzle inlet. At only nozzle outlet junction, i.e. single junction, choking option is used. The results of CASE 1 are compared with test data for mass flowrate, pressure and void fraction at nozzle inlet, etc., as shown in figure 4-1 through 4-7. The mass flowrate calculated by RELAP5 is compared with test data in figure 4-1. In subcooled choked flow region, the calculated mass flowrate agrees well with experimental data. Also, the calculated pressure behavior agrees well in this region, as shown in figure 4-2. However, the calculated mass flowrate is underestimated by about 6 % relative to experimental data between subcooled and two-phase choked flow region. Thus, from the point where the mismatching of mass flowrate occurs, the system pressure is slightly overpredicted due to the gravitational effect of remaining liquid in vessel. From the inception of void fraction at discharge pipe the calculated mass flowrate agrees well with test data, without the correction of the discharge coefficient. The behavior of system pressure has similar trend of test data but maintains as high value as the overpredicted value during subcooled choked flow region. Because higher calculated pressure suppress the growth of void in discharge pipe, the prediction of inception of void fraction at nozzle inlet is late as shown in figure 4-3. However, the mass flowrate in two-phase region agrees well with test data in spite of higher calculated pressure. Therefore, it is considered that the critical mass flowrate model for two-phase in RELAP5 is not sensitive to upstream pressure.

As second sensitivity calculation for nodalization study (CASE 2), the nozzle is modeled with a single volume without changing nodalization of discharge pipe. A smooth area change option is used in the junction connecting a discharge pipe and a nozzle inlet. As shown in figure 4-8 through 4-13, in general, the calculated mass flowrate has good agreement with test data in the whole region. The results of this case are almost same as those of case 1. Also, the inception time of void fraction at nozzle inlet is nearly the same as CASE 1. Thus, the cell numbers of a nozzle do not effect the predictions.

As third sensitivity calculation for nodalization of discharge pipe (CASE 3), a nozzle is modeled with 3 cells as same as CASE 1, and a discharge pipe is divided 3 cells. The results of this case compared with test data, are presented in figures 4-14 through 4-20. As shown in figure 4-14, the fluctuation of the calculated mass flowrate occurs in the period of transition choked flow region. It is considered this fluctuation is oriented from low junction velocity calculated by two-phase critical model, because the quality in a nozzle determines incorrectly the choking criterion. As shown in figure 4-18, because the quality in a nozzle exists on the bound of choking criterion, the small perturbation of the quality can cause incorrect determination of choking criterion. The upstream pressure is overestimated as shown in figure 4-15, that is because the pressure is calculated as an average of the pressure at upstream and downstream when volumes are lumped in a large volume.

In fourth sensitivity calculation (CASE 4), a nozzle is modeled as same as CASE 2 and a discharge pipe as same as CASE 3. The results of CASE 4 compared with test data are presented in figures 4-21 through 4-26. As shown in figure 4-21, however, the calculated mass flowrate fluctuates in the period of two-phase choked flow region, which is influenced by strong fluctuation of the void fraction at break junction, as shown in figure 4-25, because oscillated void fraction in discharge pipe is amplified at a nozzle as shown in figure 4-23.

As the sensitivity study for internal choking (CASE 7 and CASE 8), the choking option is used at every junctions for inputs of CASE 1 and CASE 2, respectively. The comparisons of mass flowrate are presented as shown in figures 4-27 and 4-28. In CASE 7 and CASE 8, undesirable fluctuations occur due to the restriction of flow at previous junction.

For the nozzle with a L/D of 3.6, the appropriate nodalization of nozzle as a pipe may present good simulation results. Lumped volumes of a nozzle and a discharge pipe may predict incorrectly the variables related to the volume. Also internal choking may generated undesirable fluctuations for critical mass flowrate. With more than 3 cells the simulation was failed because the mismatch between fast flow and short nozzle length causes the water properties errors. In the transition period of very low void fraction at nozzle from subcooled choked flow region to two phase region, RELAP5 critical flow model does not agree well with test data.

4.2 Critical Flow Test 24

The transient input for the CASE 1 is also prepared from the results obtained by steady state calculation that gives the initial conditions for CFT 24. Because the CFT 24 has a relatively short nozzle, a nozzle is modelled as a junction or a PIPE component with 2 cells or a SNGLVOL component. Additionally, the nodalization of a discharge pipe is evaluated. The cell numbers of a nozzle and a discharge pipe is summarized in table 3-1. The simulation time is sixty seconds as in the case of the actual test periods.

In CASE 1, the nodalization of a nozzle is represented by single junction and a discharge pipe is directly connected to a containment of TMDPVOL. There happens to be no problem during the transient calculation of sixty seconds. The results of CASE 1 calculation are shown in figures 4-29 to 4-35. The mass flowrate calculated by RELAP5 is compared with test data in figure 4-29. In subcooled choked flow region, the calculated mass flowrate agrees well with the experimental data except for a moment following the opening of the break. Also, the calculated pressure underestimates due to the release of relatively large mass at the opening of break as shown in figure 4-30. For a moment following the opening of the break, RELAP5 does not simulate the actual system experiencing a pressure undershoot and can not calculate the mass flowrate reduction according to a pressure

undershoot. In two-phase choked flow region, the calculated mass flowrate underestimates by about 15 %. In this region, the calculated pressure overpredicts due to the underestimated mass flowrate. The discharge coefficient used for this region is one as same as for subcooled choked flow region.

As a sensitivity calculation for nodalization study of CFT 24 (CASE 2), the nozzle is modeled by a PIPE having 2 cells. That is, first cell as a nozzle inlet, second cell as the remainder are modeled. A smooth area change option is used in the junction connecting a discharge pipe and a nozzle inlet, and choking option is used at only break junction. The results of CASE 2 are compared with test data and base case as shown in figures 4-36 through 4-42. As shown in figure 4-36, the calculated mass flowrate is underestimated by 15 to 20 % compared to experimental data in subcooled choked flow region, and the system pressure is overpredicted as shown in figure 4-37. In two phase choked flow region, the calculated mass flowrate is underpredicted smoothly by 10 % relative to test data, and is not better than CASE 1. And, the prediction of inception of void fraction at nozzle inlet is somewhat faster.

In CASE 3, the nodalization of nozzle is represented by a single junction and a discharge pipe is modelled with 3 cells pipe. The results of CASE 3 calculation are shown in figures 4-43 to 4-49. The mass flowrate calculated by RELAP5 is compared with test data in figure 4-43. In subcooled choked flow region, the calculated mass

flowrate agrees well with the experimental data as in the case of CASE 1. following opening of the break. However, the calculated pressure overestimates because the pressure at lumping volume in a discharge pipe is calculated as averaged in spite of the pressure decrease due to relatively large mass release at opening of break as shown in figures 4-44. At the initiation of two-phase choked flow region, the calculated mass flowrate is very low due to the generation of high void fraction, and is underestimated by about 15 % during two-phase region. In this region, the calculated pressure overpredictes due to the underestimated mass flowrate. Thus, rough subdivision of upstream region may give incorrect information needed to calculation critical flow criterion and conditions.

As a sensitivity calculation for nodalization study of CFT 24 (CASE 5), the nozzle is modeled with single volume. A smooth area change option is used in the junction connecting a discharge pipe and a nozzle inlet. In this case choking option is used at each junction in discharge pipe. The results of CASE 5 are compared with test data for mass flowrate, pressure at nozzle inlet and void fraction, etc, as shown in figures 4-50 through 4-56. As shown in figure 4-50, the calculated mass flowrate is underestimated by 10 to 20 % compared to experimental data in subcooled choked flow region. Thus the system pressure is overpredicted as shown in figure 4-51. In two phase choked flow region, the calculated mass flowrate is underpredicted with high fluctuation. This fluctuation is caused by internal choking

problem. And, the prediction of inception of void fraction at nozzle inlet is similar to that of CASE 2, but the variation of void fraction fluctuates strongly. Except the oscillation, the trends of results from CASE5 are similar to those of CASE2. Therefore, there is no effect of the cell number of a nozzle on the of critical flow behavior.

For the nozzle with a L/D of 0.3, the nodalization of nozzle as a pipe may not give better simulation results than as a SNGLJUN component. With more than 2 cells the simulation has been failed because the mismatch between fast flow and short nozzle length causes the water properties errors.

4.3 Evaluation of the Model in RELAP5/MOD3

The adquacy of the critical flow model improved in RELAP5/MOD3 is assessed. The items of the assessment are two for CFT 15 and one for CFT 24. Firstly, the assessment is carried out with the same input as CASE 1 of CFT 15 (CASE 5), as shown in figure 4-57 through 4-63. As shown in figure 4-57, mass flowrate is compared with experimental data. From transition region, mass flowrate is underpredicted by about 10 % relative to experimental data. And, the fluctuation of mass flowrate is found during two-phase region. Because the critical flow criterion depends on the void fraction at the break junction in the critical flow model of RELAP5/MOD3, instantaneous fluctuation of

void fraction at the break junction may change critical velocity which results in the feedback to oscillation of void fraction, and subsequently, amplify the oscillation of critical mass flowrate, as shown in figure 4-61.

Secondly, the assessment is carried out with same input as CASE 4 of CFT 15 (CASE 6), as shown in figure 4-64 through figure 4-69. As shown in figure 4-64, mass flowrate is compared with experimental data. From transition region, mass flowrate is underpredicted by about 10 % relative to experimental data. Also, the fluctuation of mass flowrate is found during two-phase region, but the range of fluctuation is reduced than the case of RELAP5/MOD2. Rather, the trends of results for this case are similar to those of CASE 5.

In RELAP5/MOD3, instantaneous fluctuation of void fraction at break junction may amplify the oscillation of critical mass flowrate. On the whole, the model in RELAP5/MOD3 may be not effected by nodalization and may be not improved successfully to predict the critical flow behavior for CFT 15.

Thirdly, the assessment is carried out with same input as CASE 1 of CFT 24 (CASE 4), as shown in figures 4-70 through 4-75. In general, the trends of results for CASE 4 are similar to those of CASE 1 for CFT 24. Similar to the case of CFT 15, the fluctuation due to amplification of void fraction occurs in two-phase region.

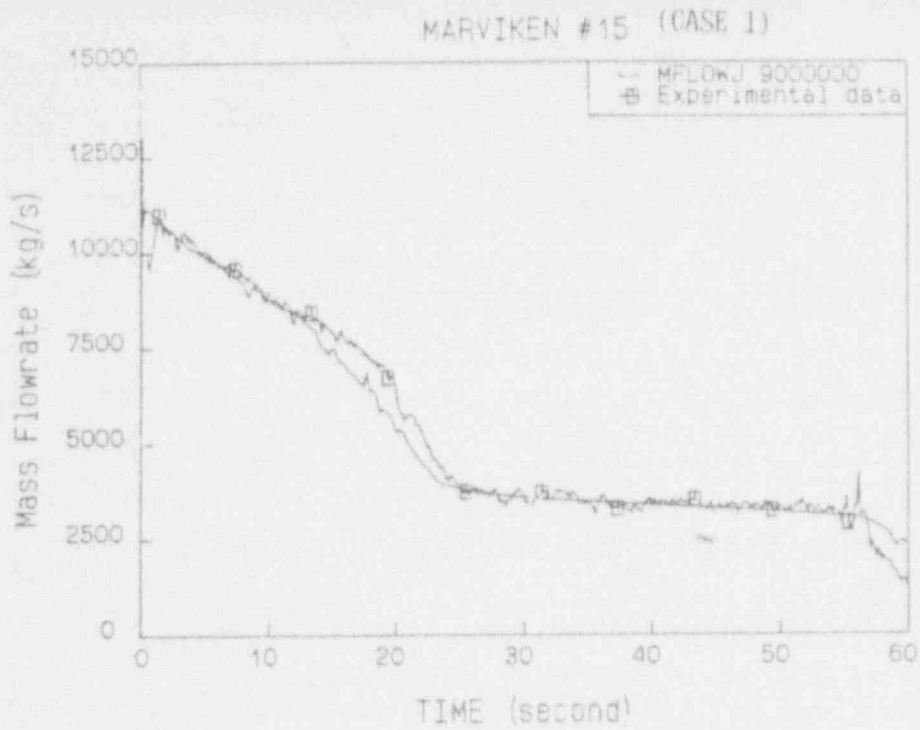


Fig. 4-2 Comparison of calculated and measured pressure at nozzle inlet for CFT 15(CASE 1)

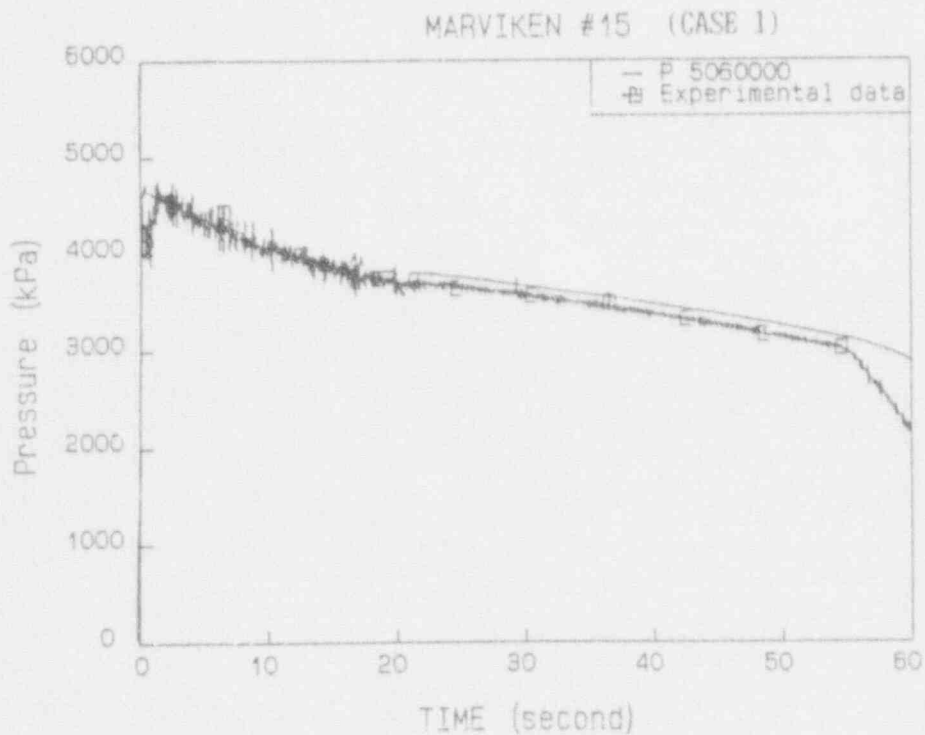


Fig. 4-1 Comparison of calculated and measured mass flowrate for CFT 15(CASE 1)

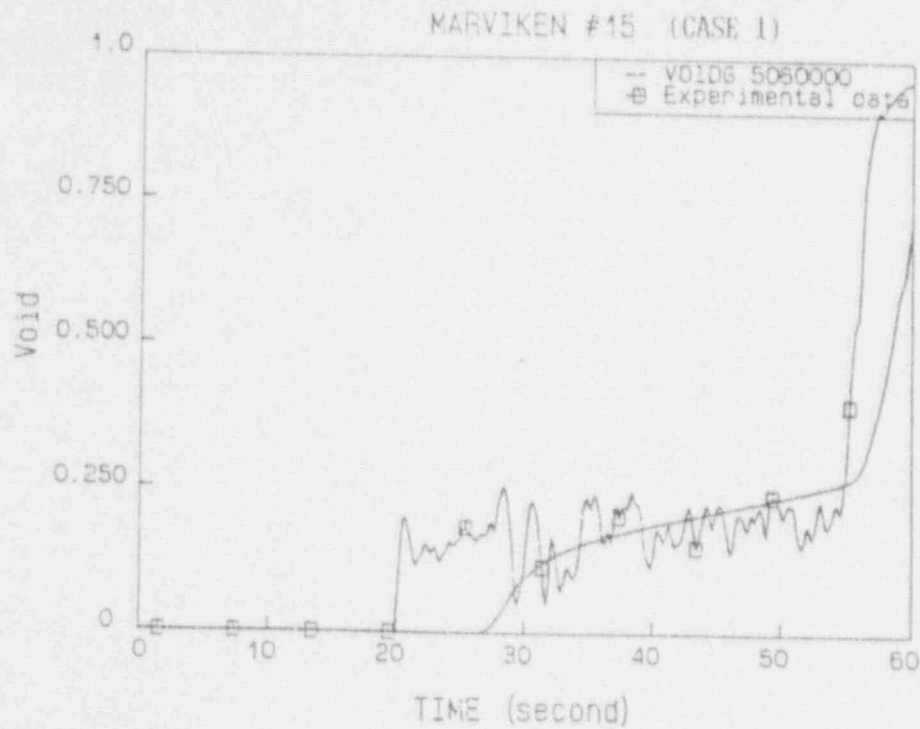


Fig. 4-3 Comparison of calculated and measured void fraction at nozzle inlet for CFT 15(CASE 1)

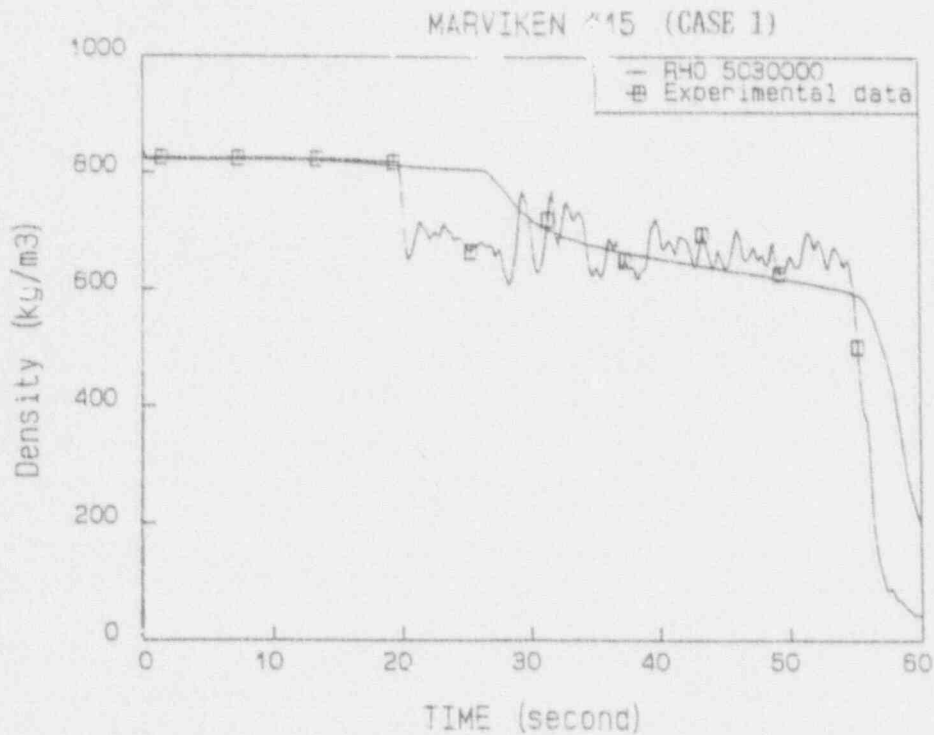


Fig. 4-4 Comparison of calculated and measured density at discharge pipe for CFT 15(CASE 1)

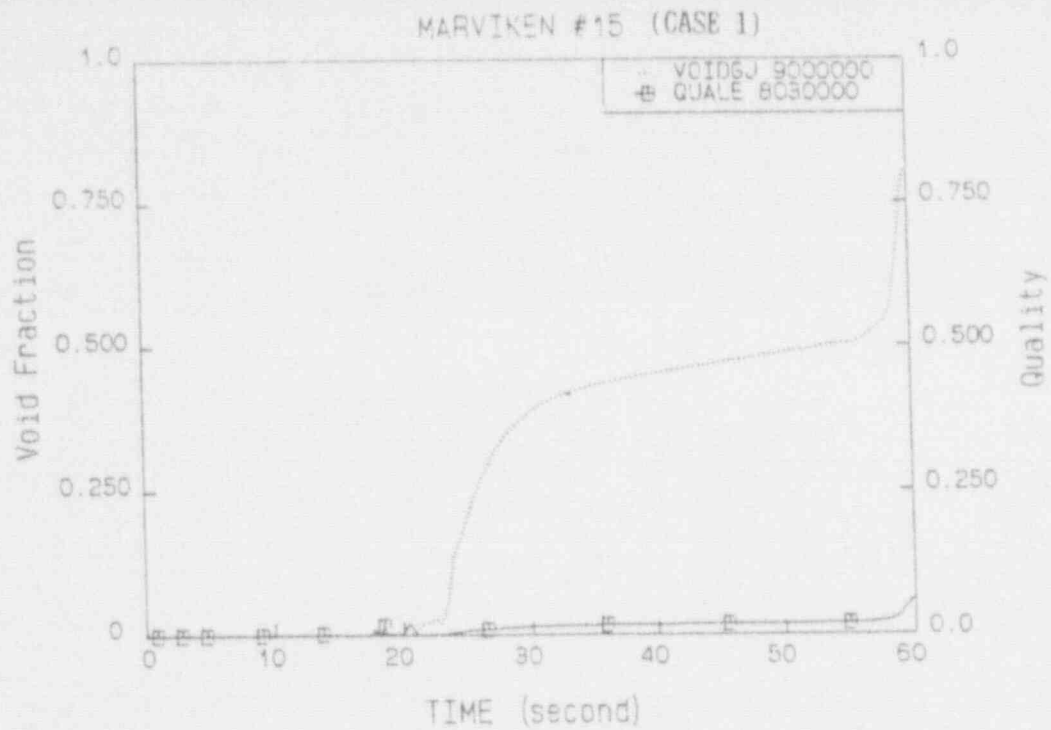


Fig. 4-5 Void fraction and quality at break for CFT 15(CASE 1)

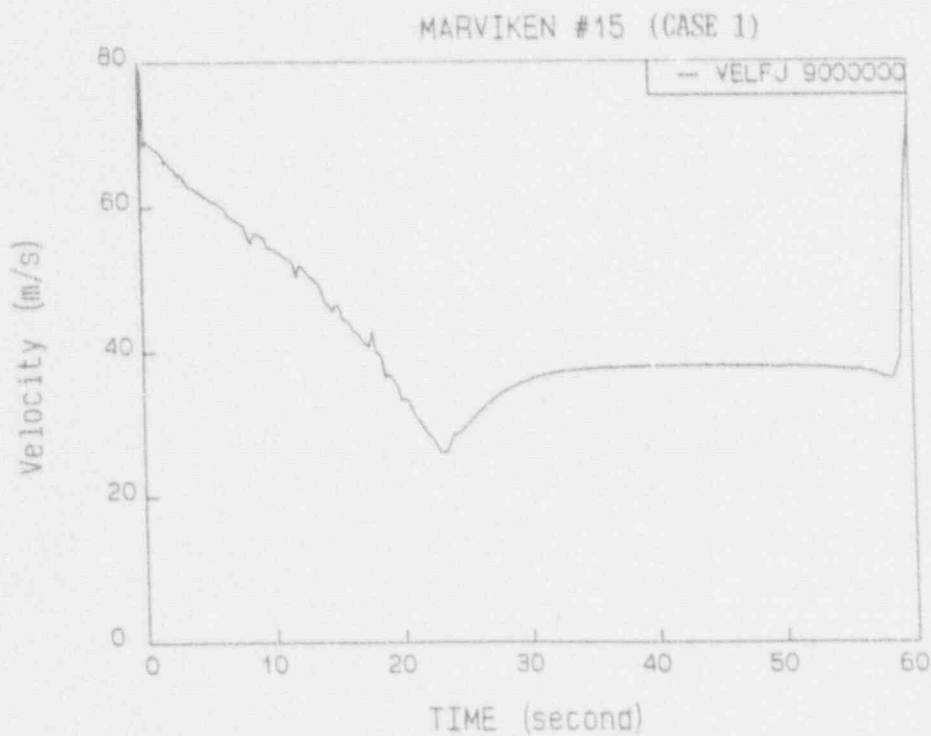


Fig. 4-6 Critical velocity at break junction for CFT 15(CASE 1)

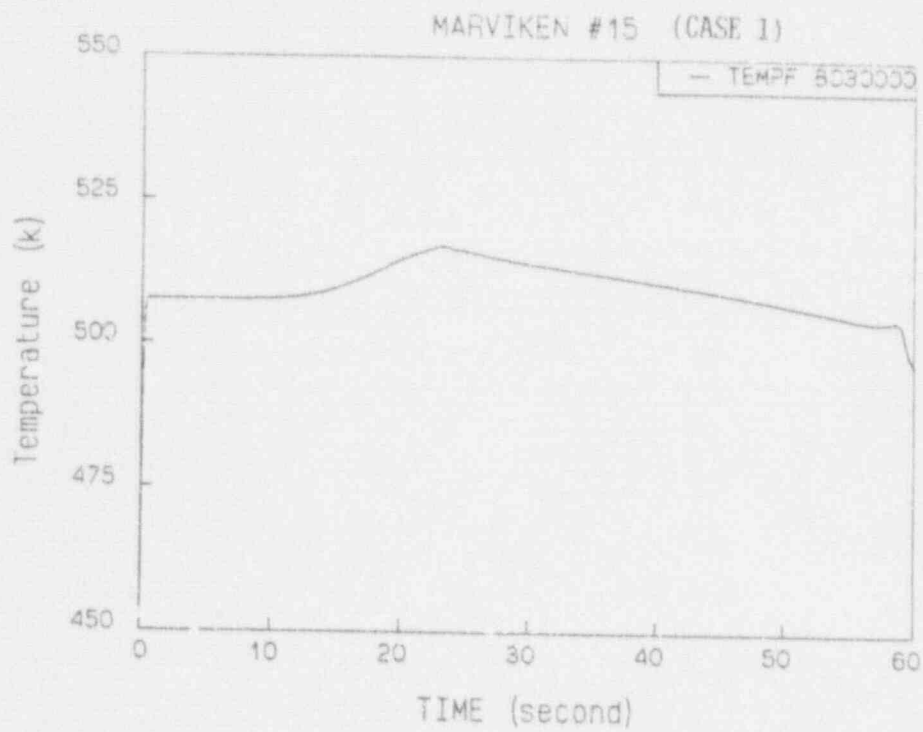


Fig. 4-7 Liquid temperature at nozzle

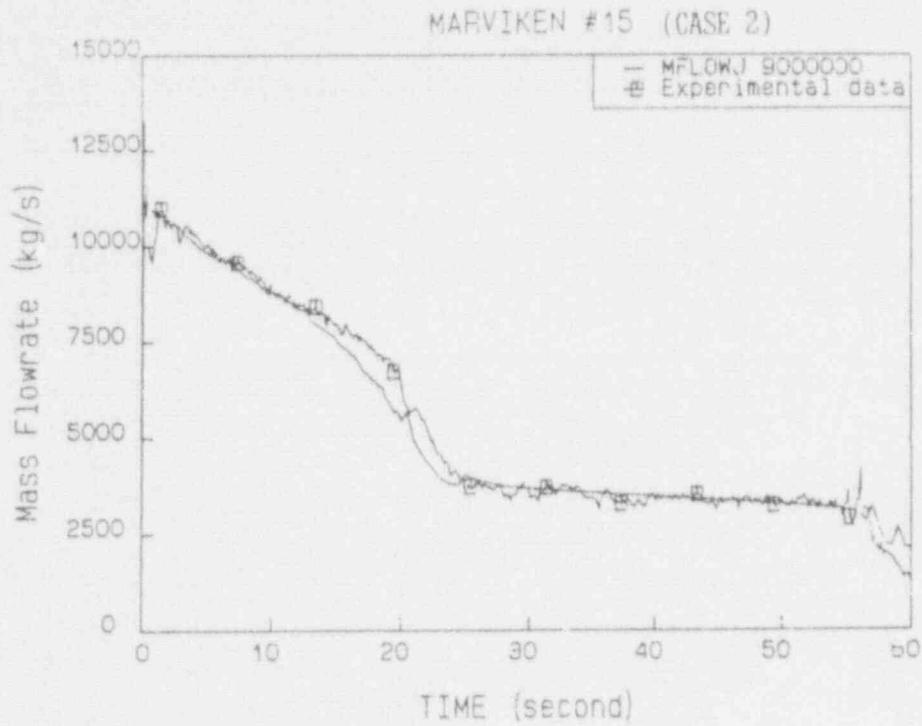


Fig. 4-8 Comparison of calculated and measured mass flowrate for CFT 15(CASE 2)

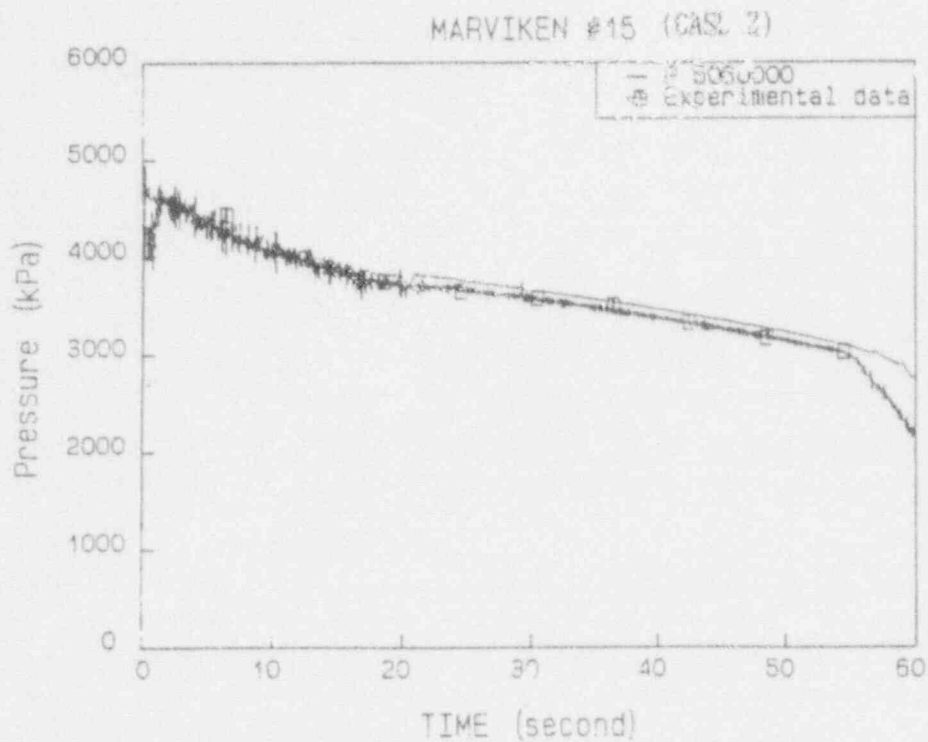


Fig. 4-9 Comparison of calculated and measured pressure at nozzle inlet for CFT 15(CASE 2)

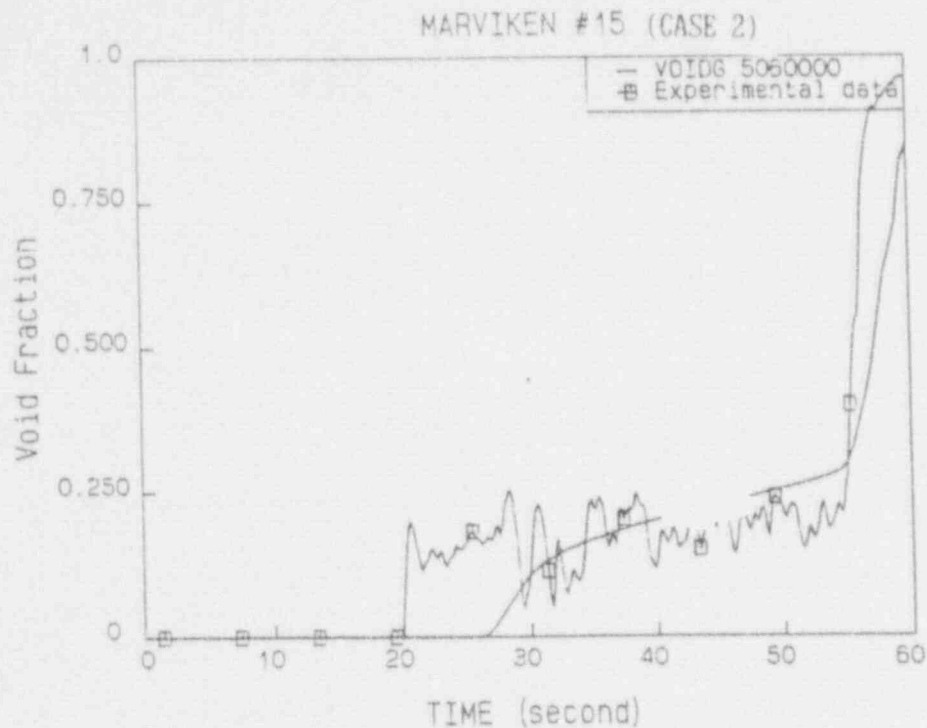


Fig. 4-10 Comparison of calculated and measured void fraction at nozzle inlet for CFT 15(CASE 2)

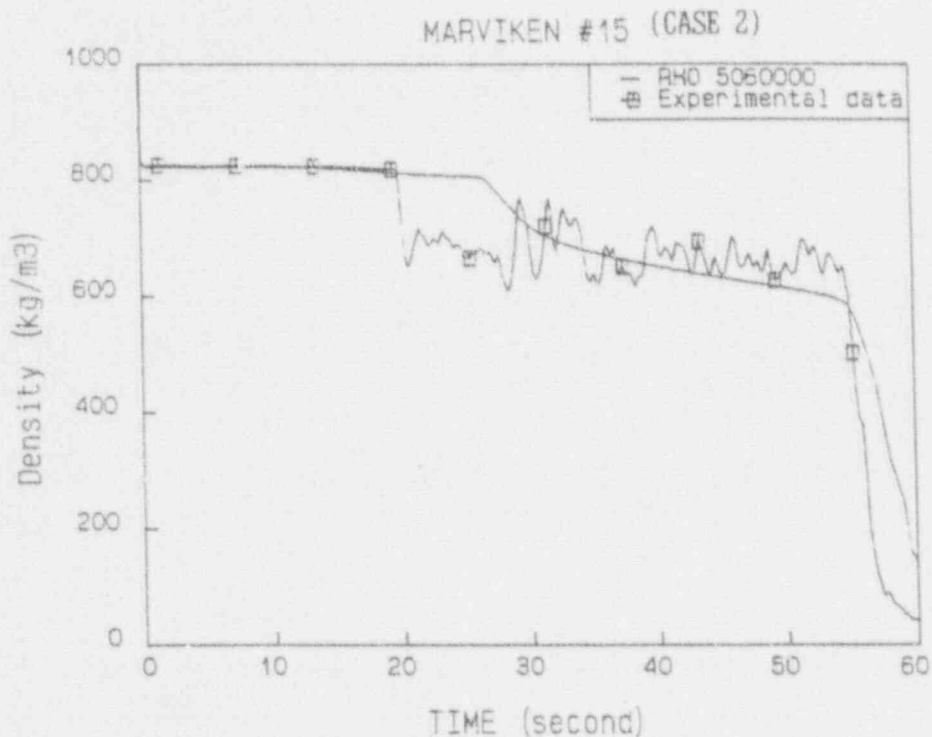


Fig. 4-11 Comparison of calculated and measured density at discharge pipe for CFT 15(CASE 2)

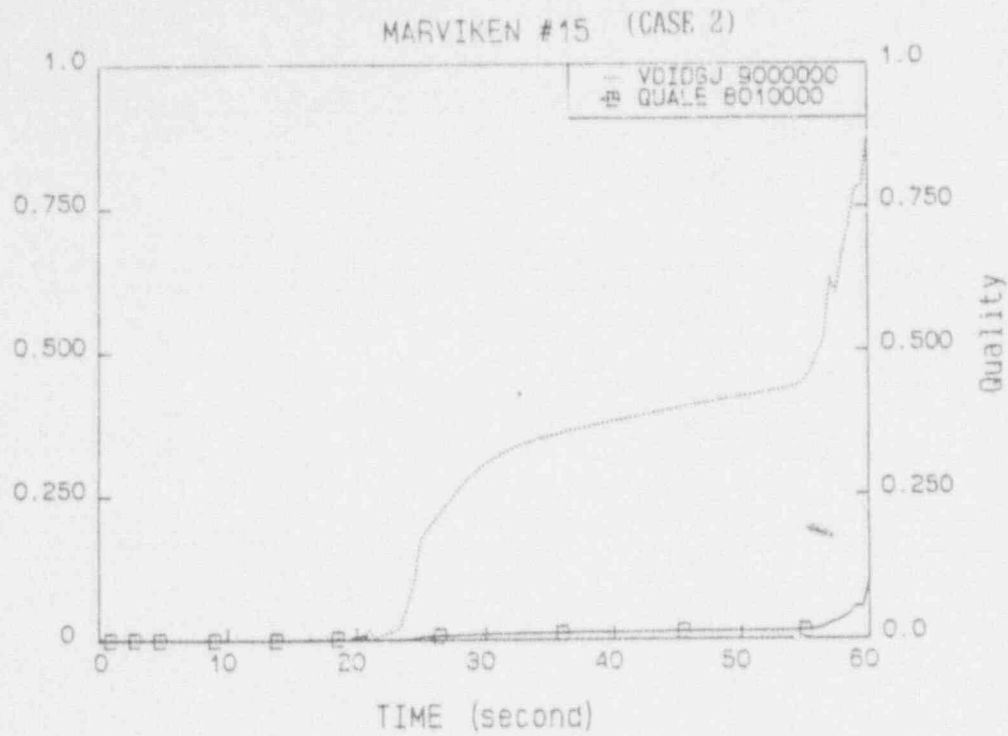


Fig. 4-12 Void fraction and quality at break for CFT 15(CASE 2)

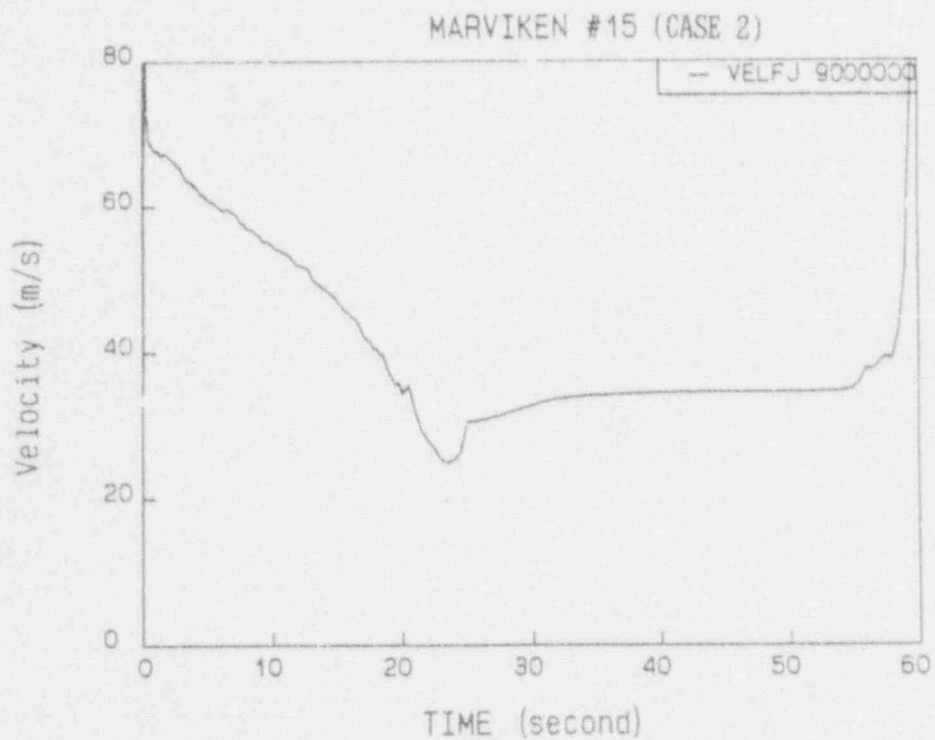


Fig. 4-13 Critical velocity at break junction for CFT 15(CASE 2)

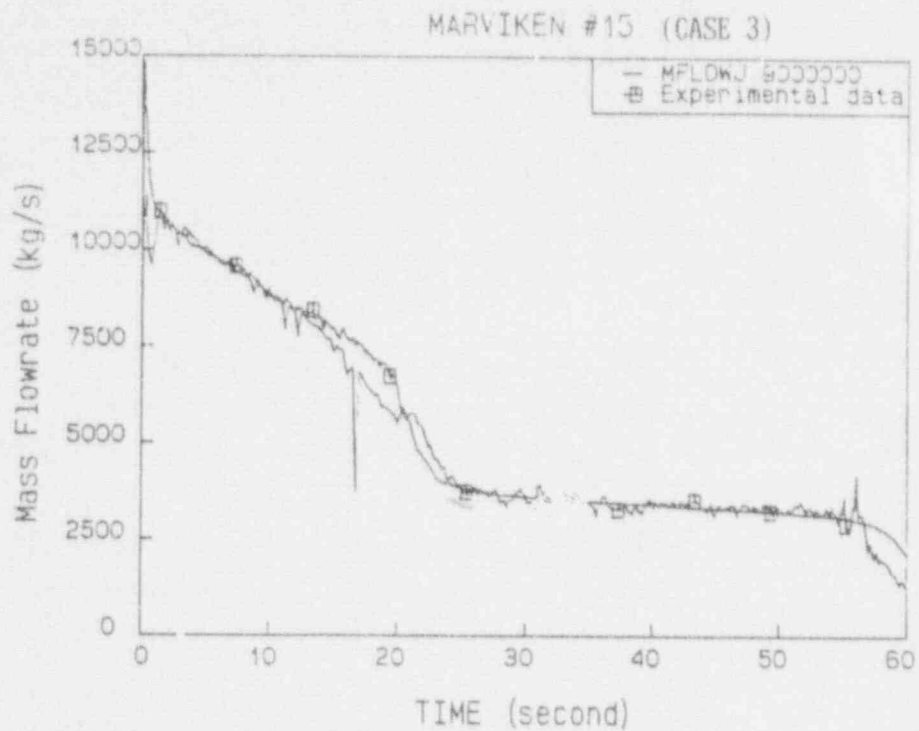


Fig. 4-14 Comparison of calculated and measured mass flowrate for CFT 15(CASE 3)

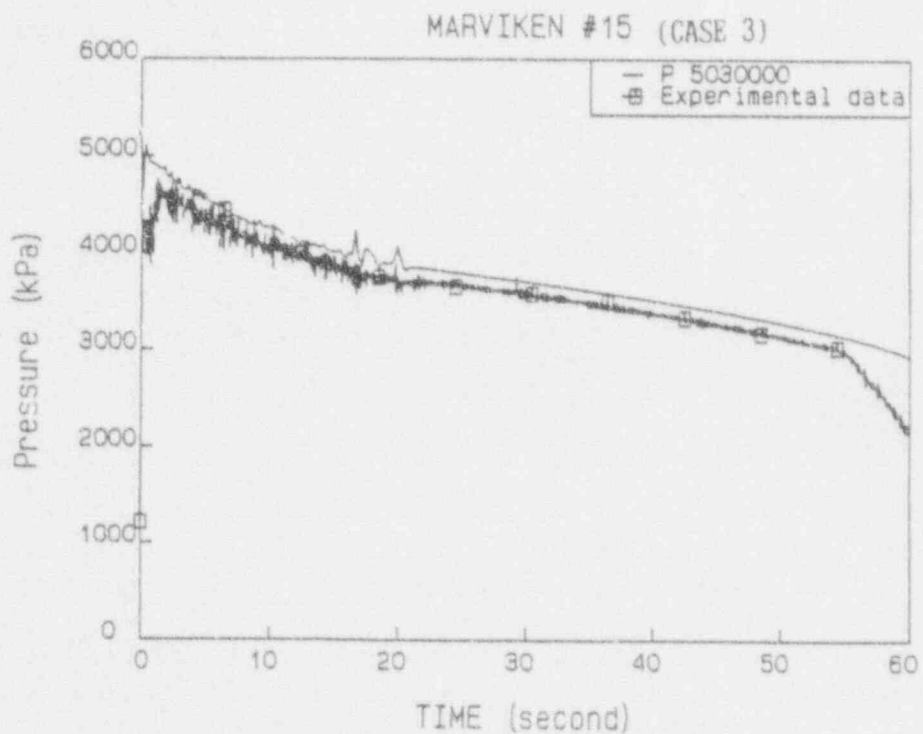


Fig. 4-15 Comparison of calculated and measured pressure at nozzle inlet for CFT 15(CASE 3)

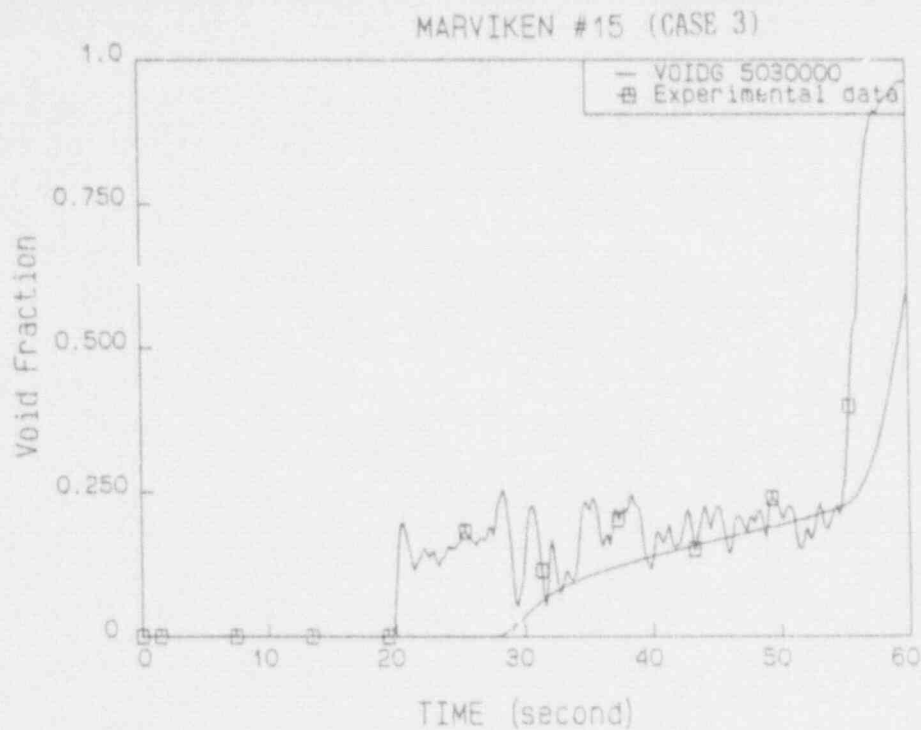


Fig. 4-16 Comparison of calculated and measured void fraction at nozzle inlet for CFT 15(CASE 3)

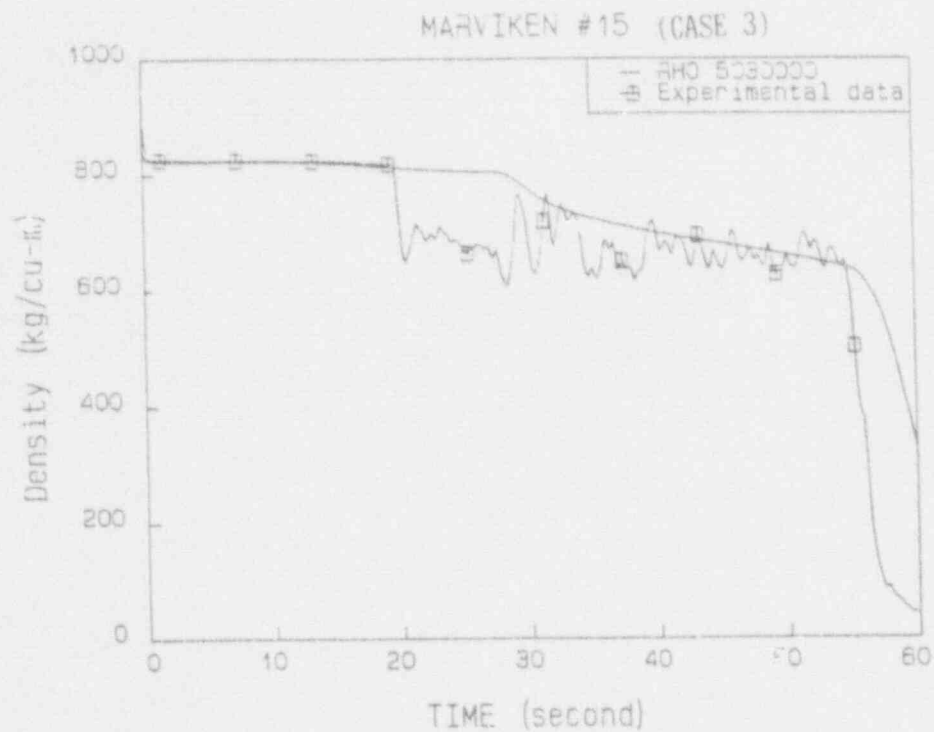


Fig. 4-17 Comparison of calculated and measured density at discharge pipe for CFT 15(CASE 3)

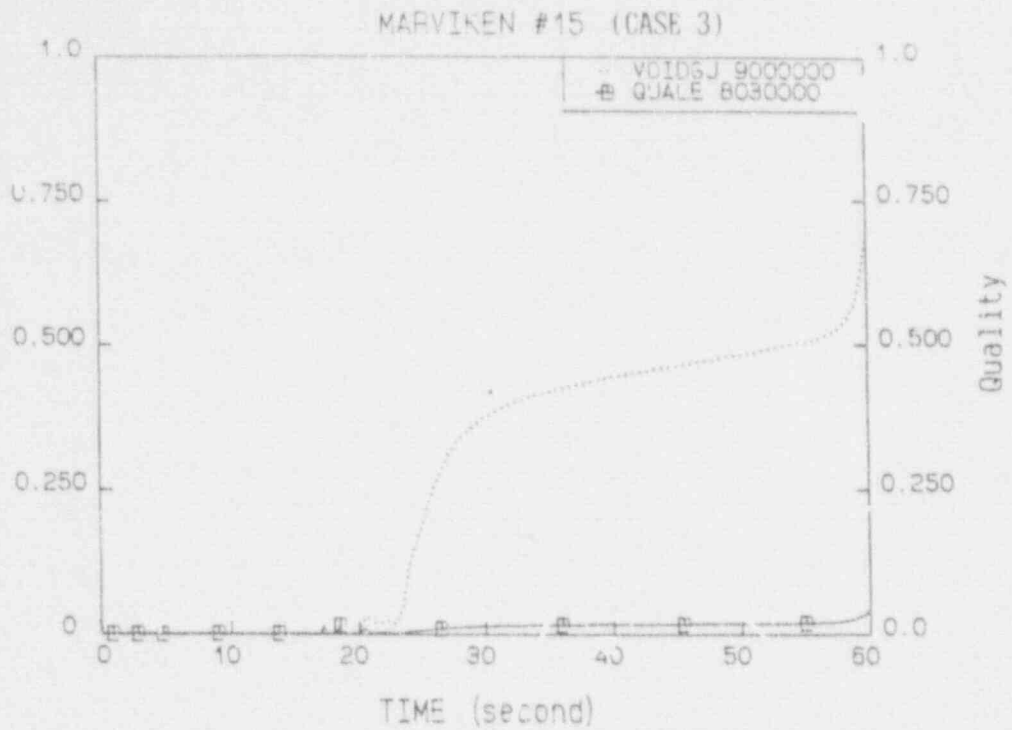


Fig. 4-18 Void fraction and quality at break for CFT 15(CASE 3)

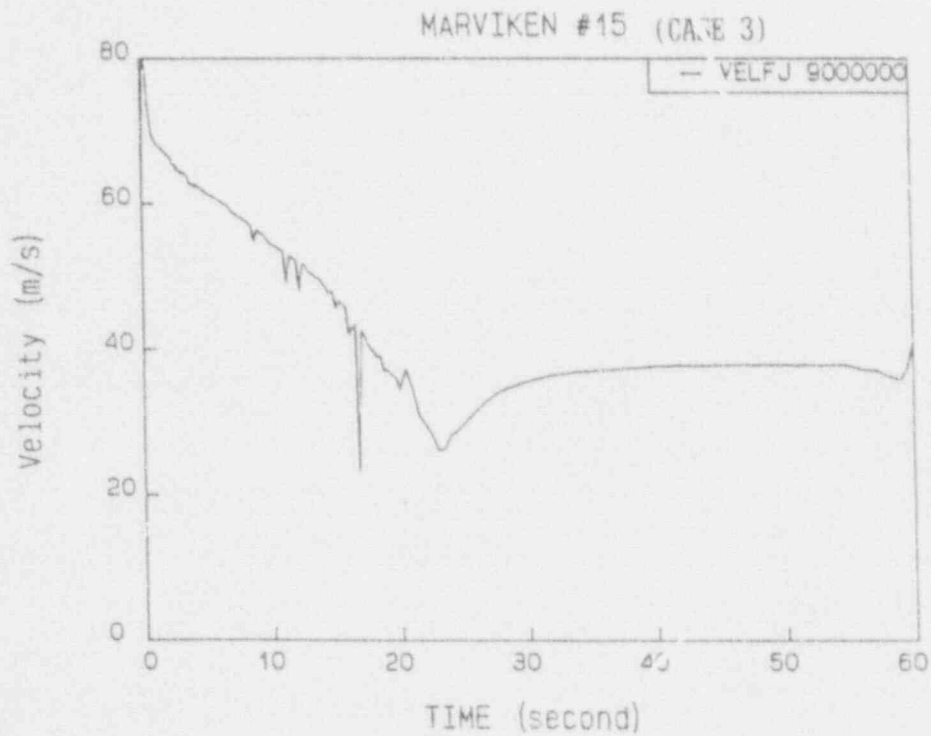


Fig. 4-19 Critical velocity at break junction for CFT 15(CASE 3)

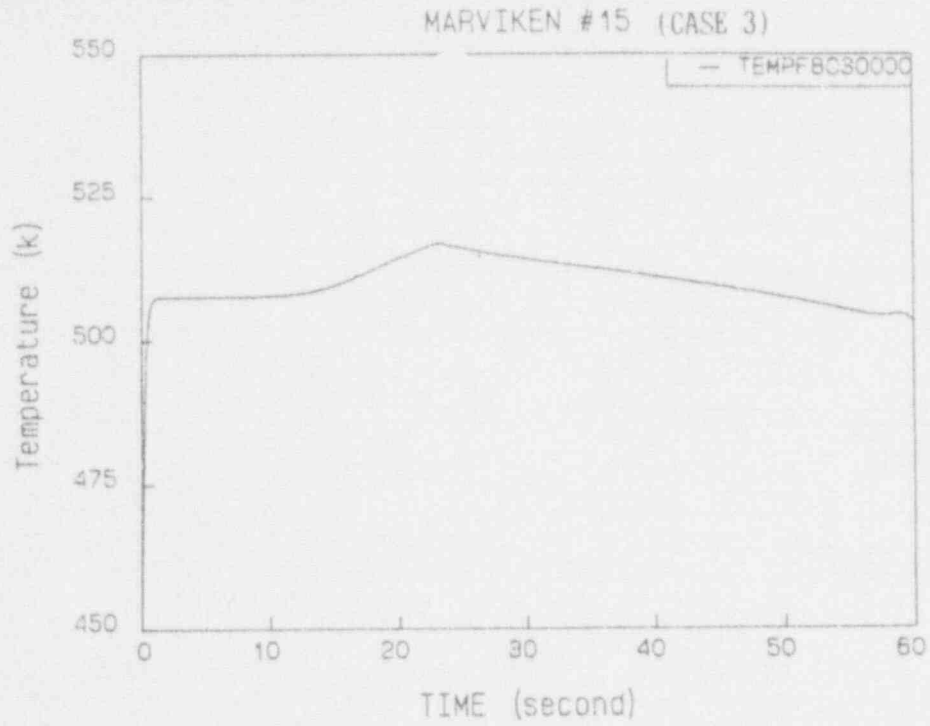


Fig. 4-20 Liquid temperature at nozzle for CPT 15(CASE 3)

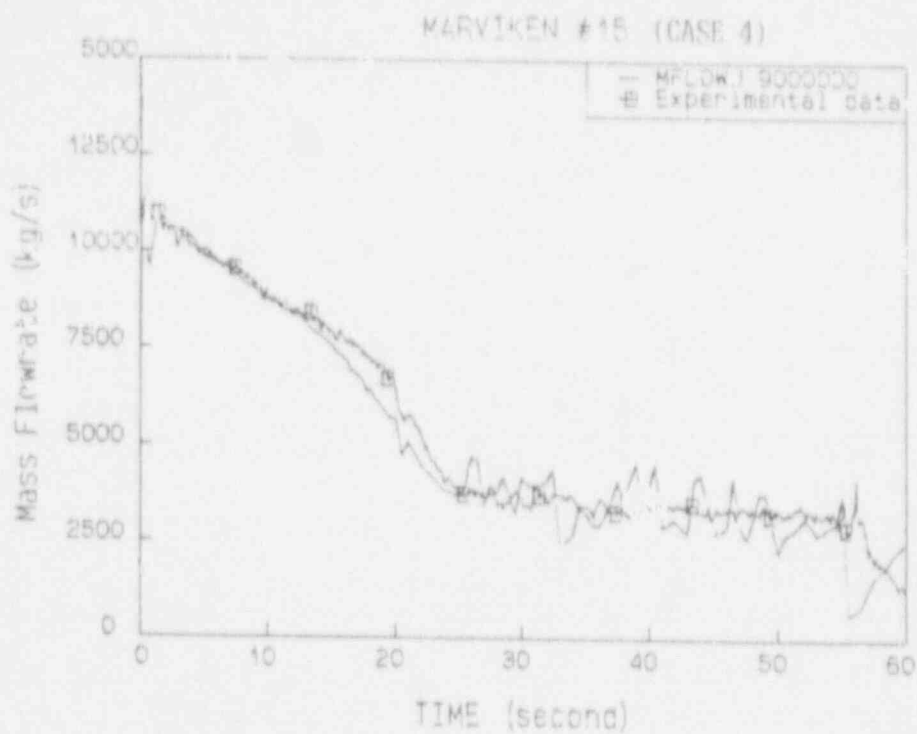


Fig. 4-21 Comparison of calculated and measured mass flowrate for CFI 15(CASE 4)

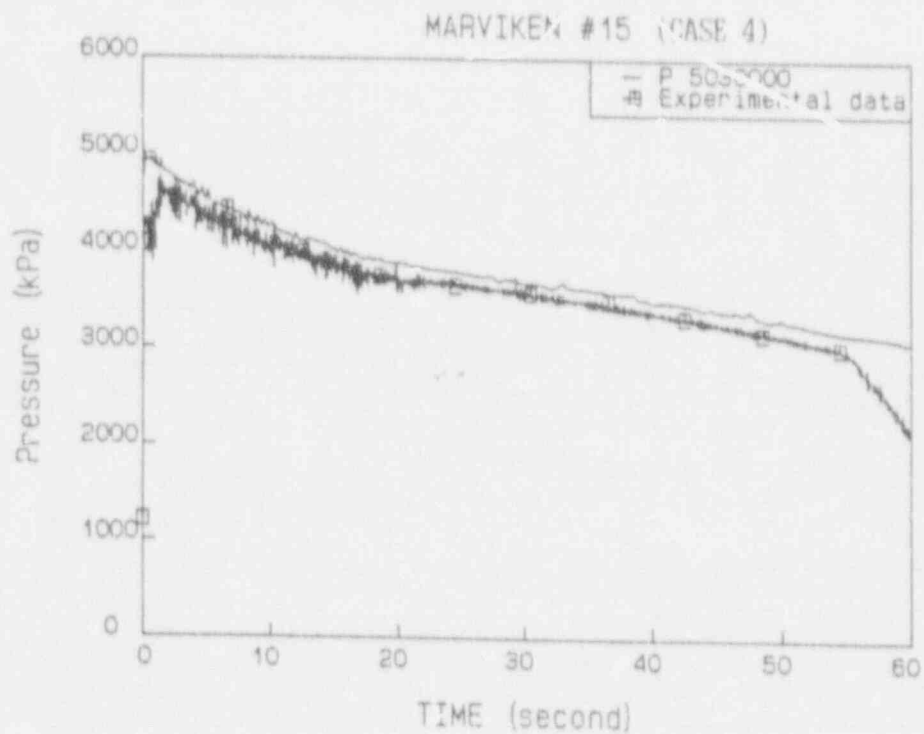


Fig. 4-22 Comparison of calculated and measured pressure at nozzle inlet for CFI 15(CASE 4)

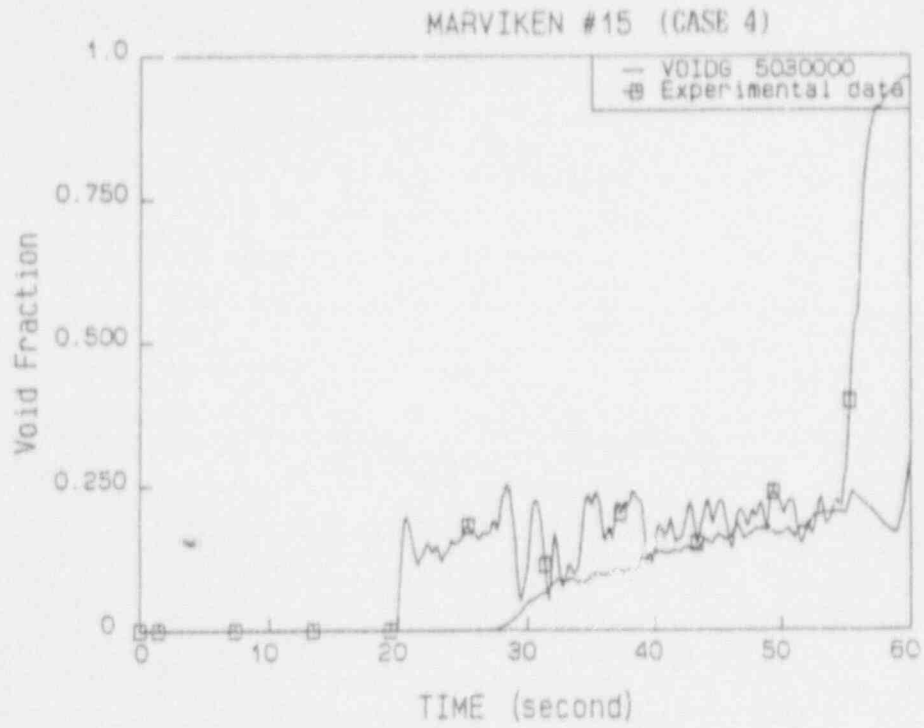


Fig. 4-23 Comparison of calculated and measured void fraction at nozzle inlet for CFT 15(CASE 4)

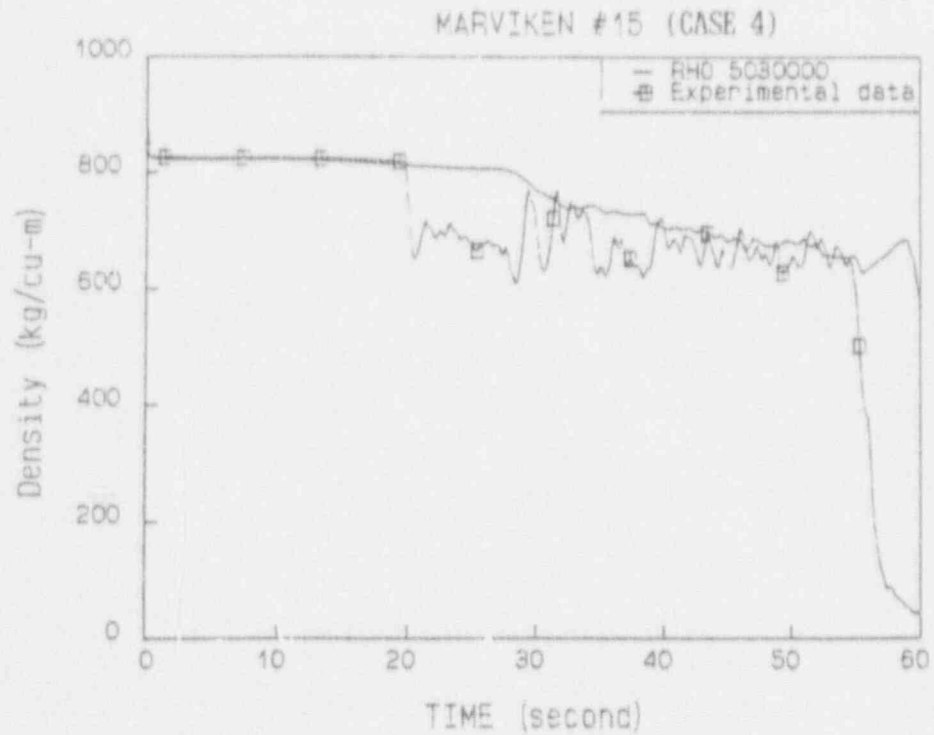


Fig. 4-24 Comparison of calculated and measured density at discharge pipe for CFT 15(CASE 4)

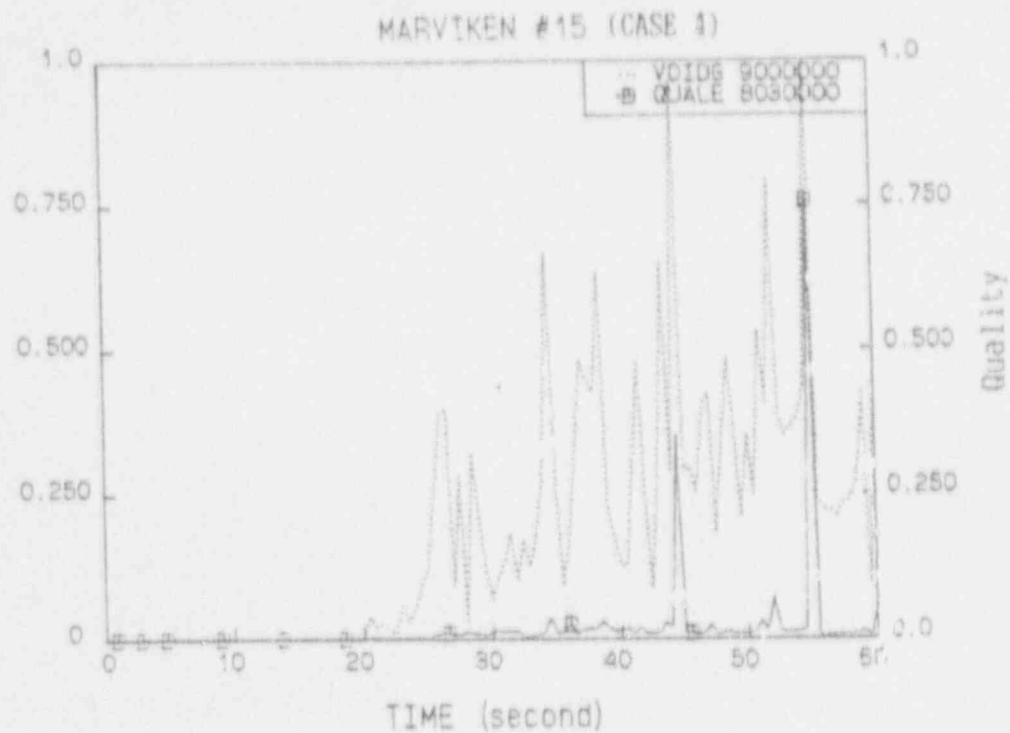


Fig. 4-25 Void fraction and quality at break for CFT 15(CASE 4)

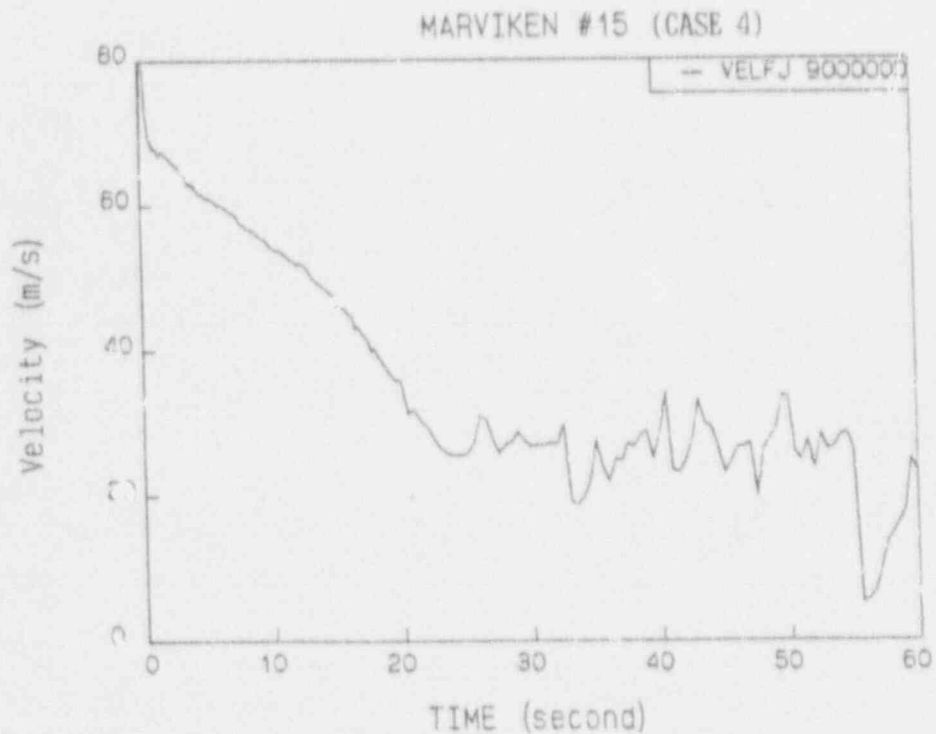


Fig. 4-26 Critical velocity at break junction for CFT 15(CASE 4)

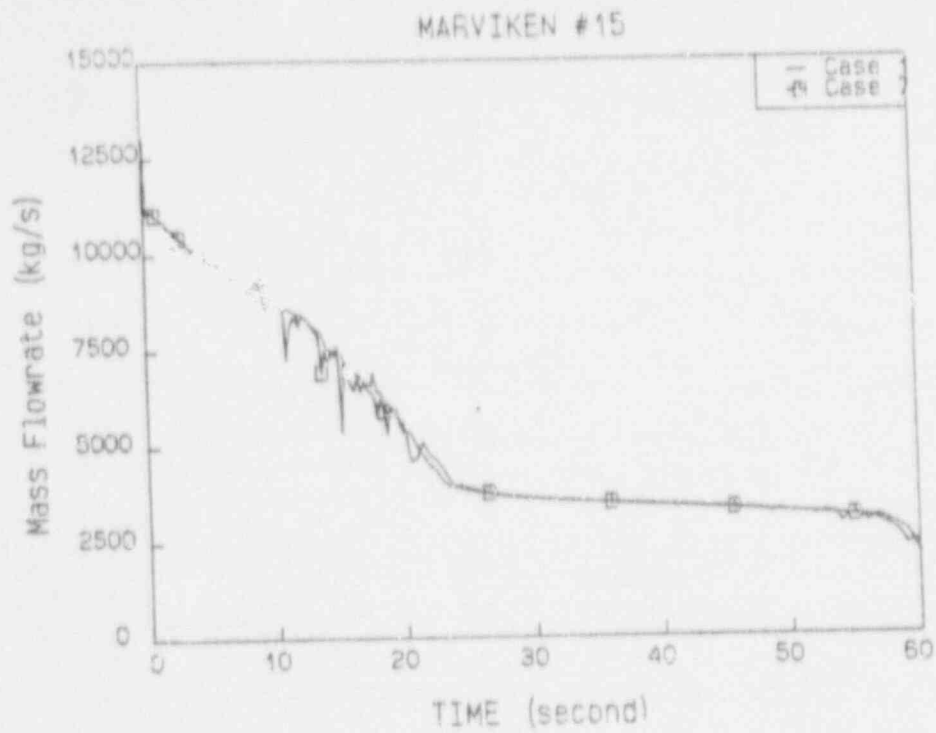


Fig. 4-27 Comparison of mass flowrate for case 1 and case 7 of CFT 15

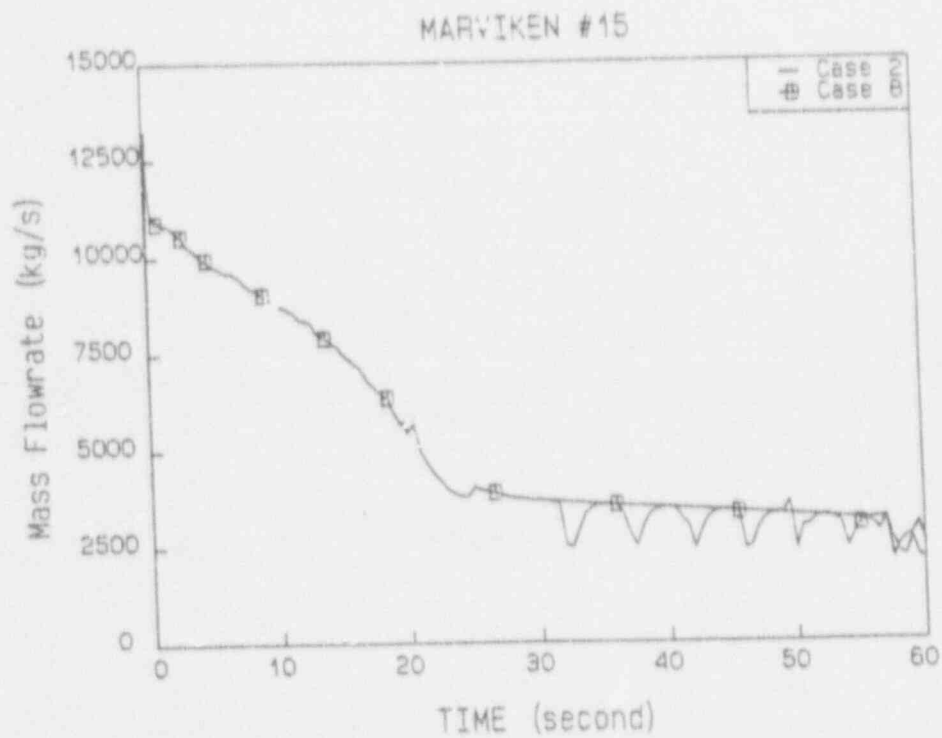


Fig. 4-28 Comparison of mass flowrate for case 2 and case 8 of CFT 15

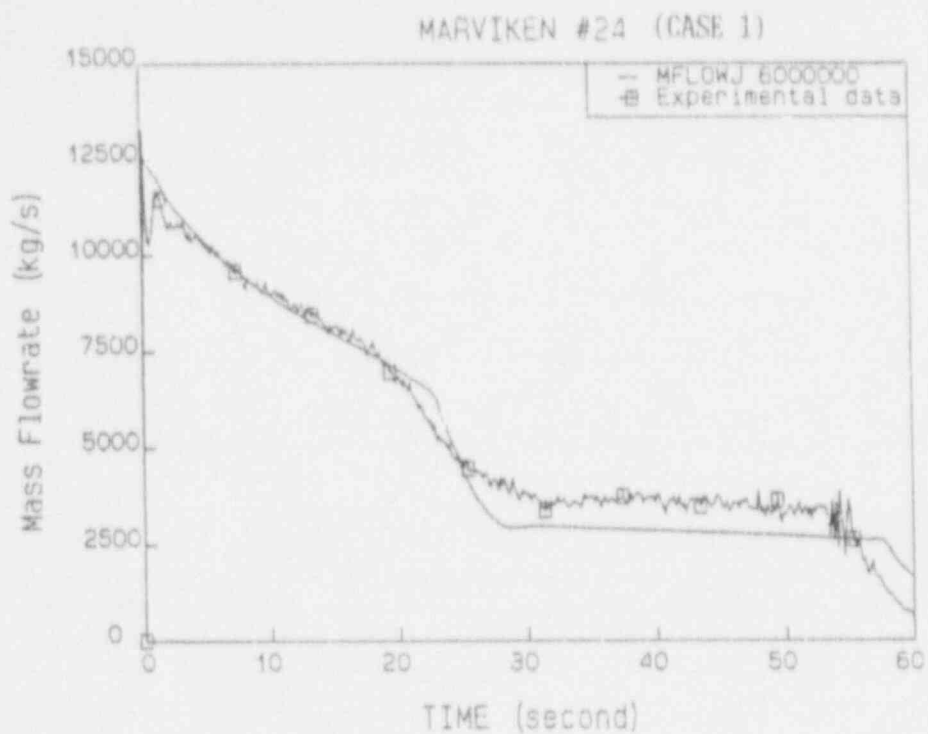


Fig. 4-29 Comparison of calculated and measured mass flowrate for CFT 24(CASE 1)

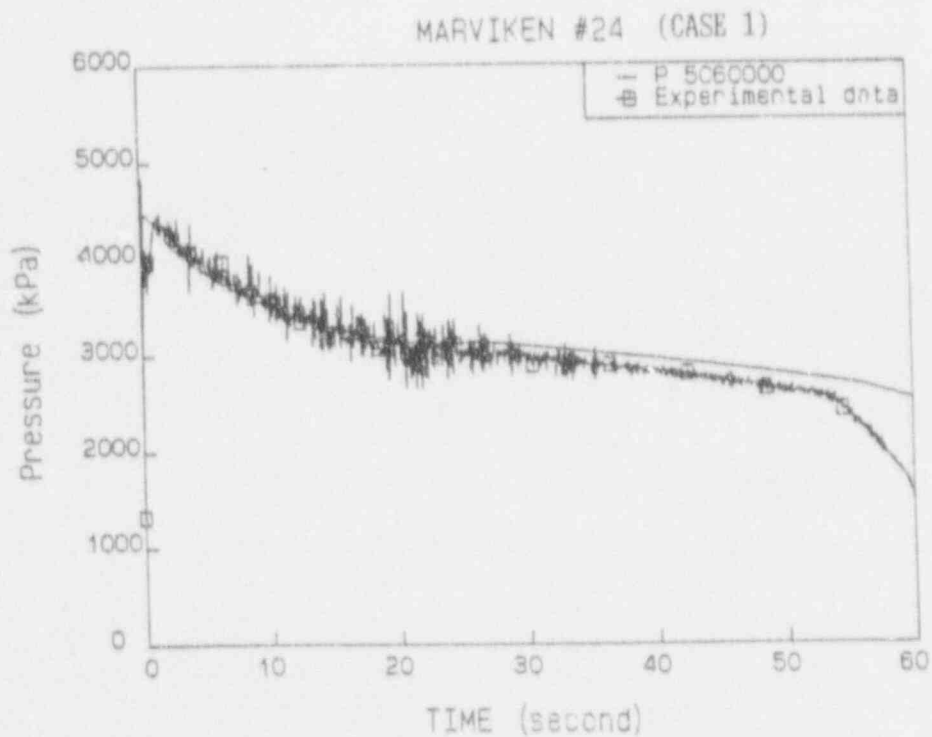


Fig. 4-30 Comparison of calculated and measured pressure at nozzle inlet for CFT 24(CASE 1)

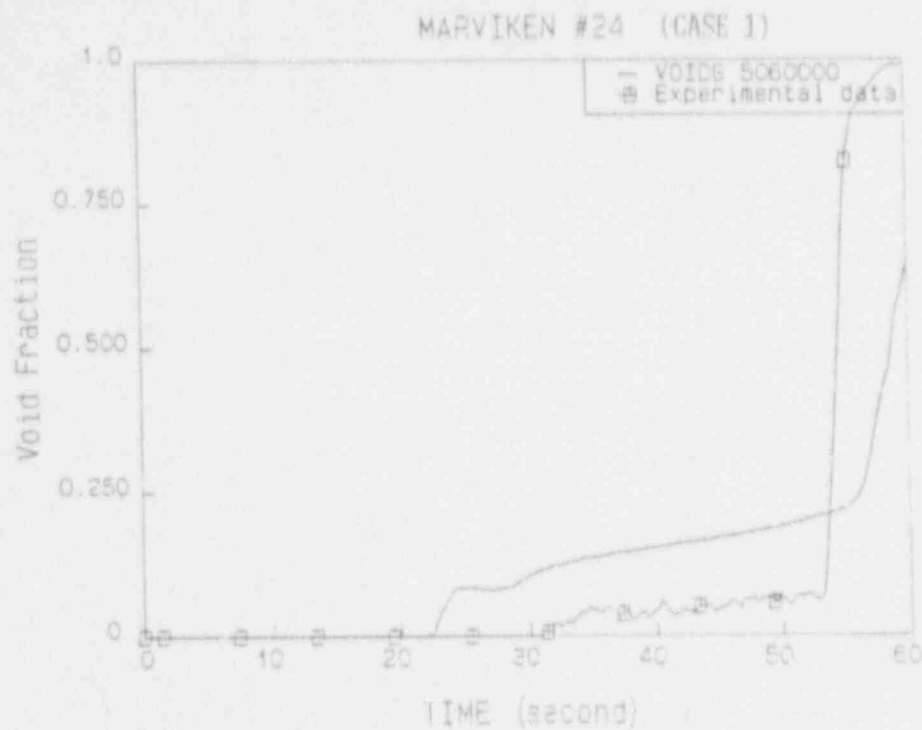


Fig. 4-31 Comparison of calculated and measured void fraction at nozzle inlet for CFT 24(CASE 1)

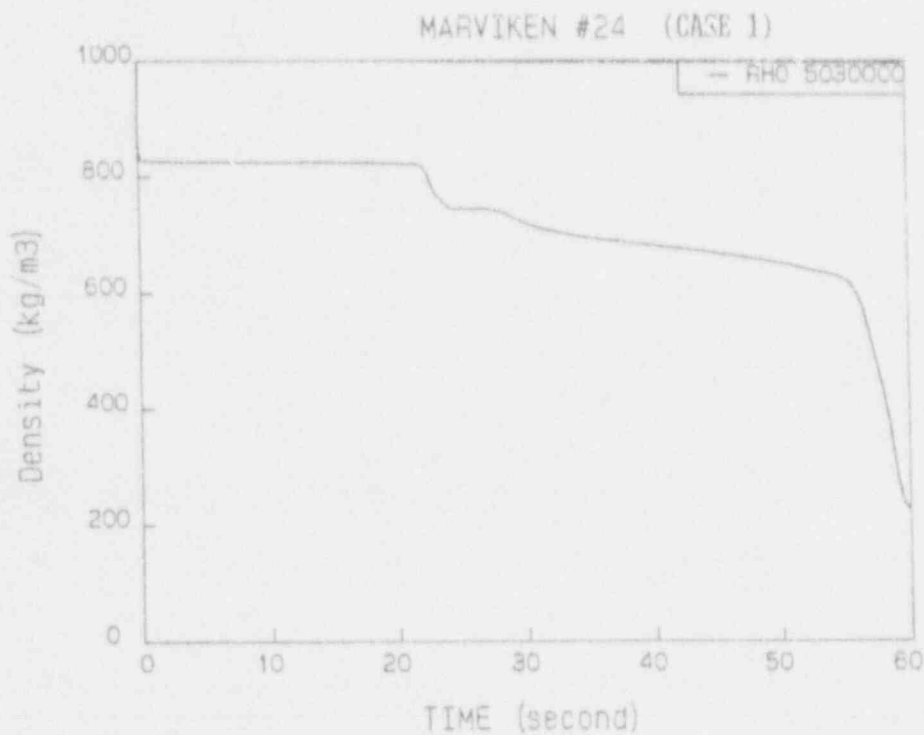


Fig. 4-32 Comparison of calculated and measured density at discharge pipe for CFT 24(CASE 1)

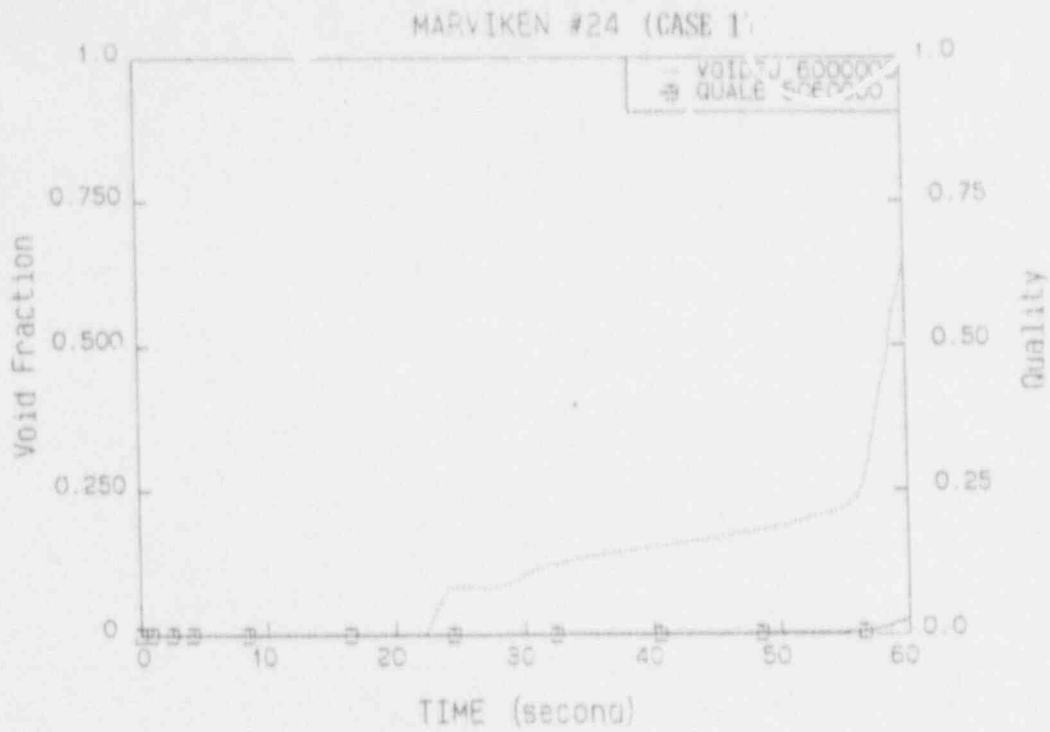


Fig. 4-33 Void fraction and quality at break for CFT 24(CASE 1)

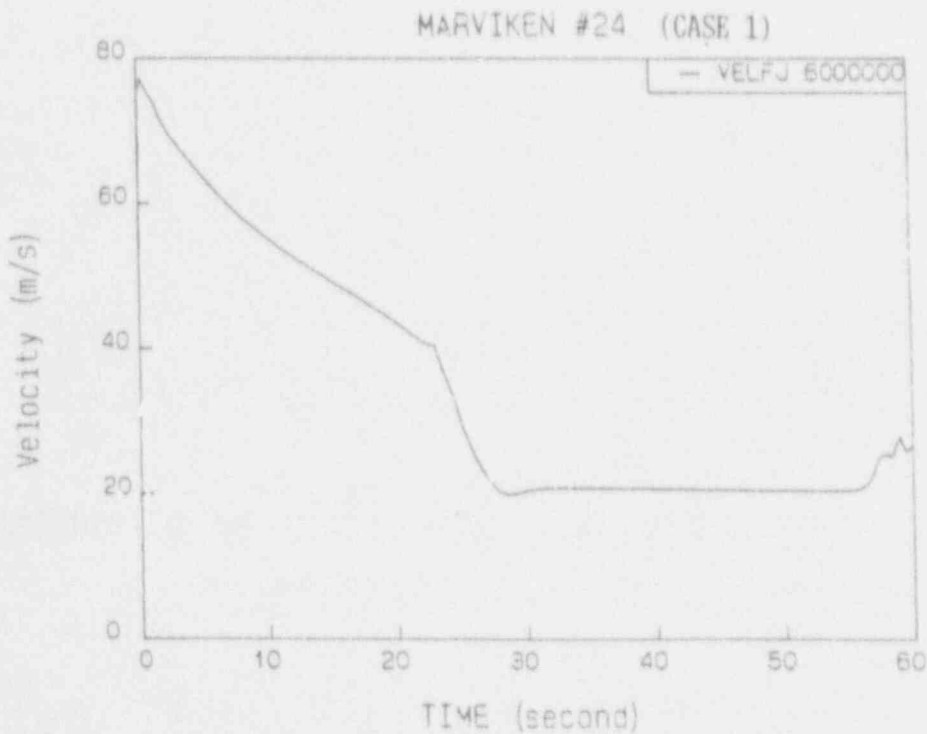


Fig. 4-34 Critical velocity at break junction for CFT 24(CASE 1)

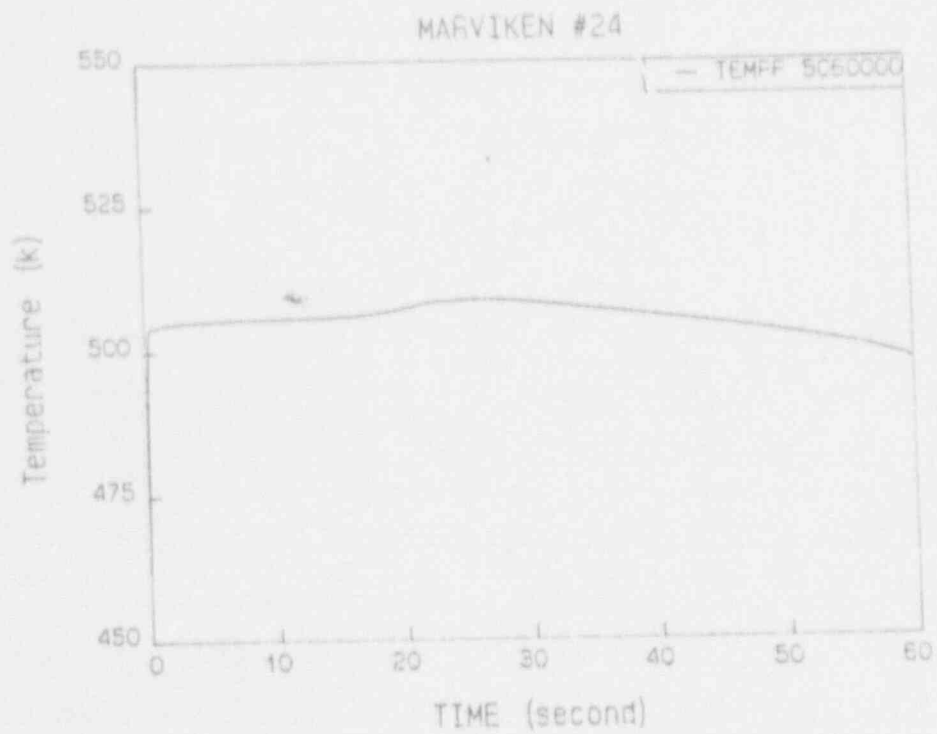


Fig. 4-35 Liquid temperature at nozzle for CFT 24(CASE 1)

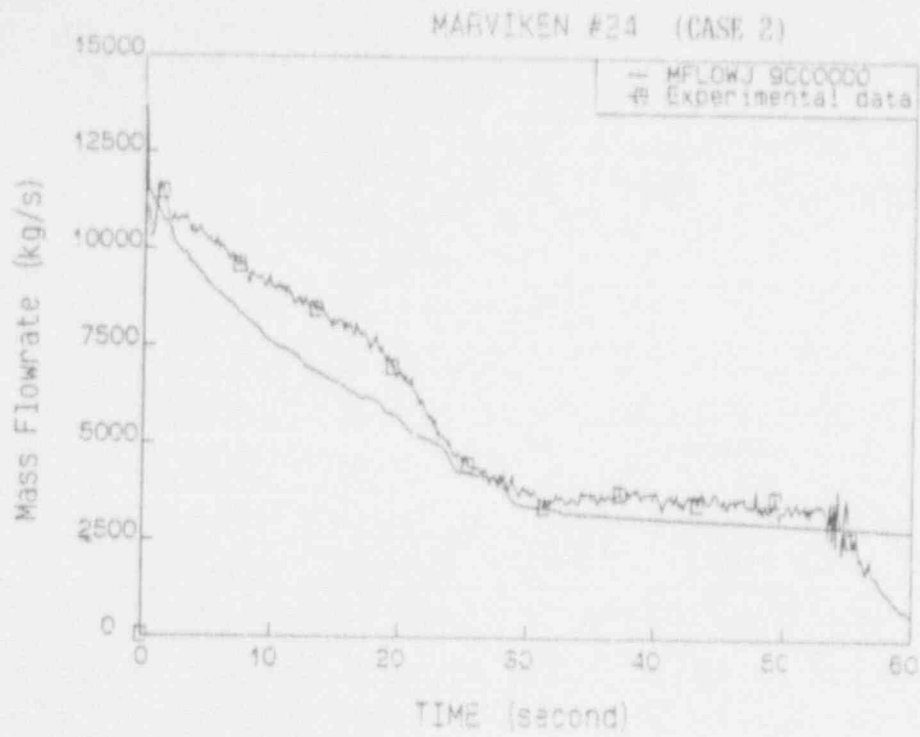


Fig. 4-36 Comparison of calculated and measured mass flowrate for CFT 24(CASE 2)

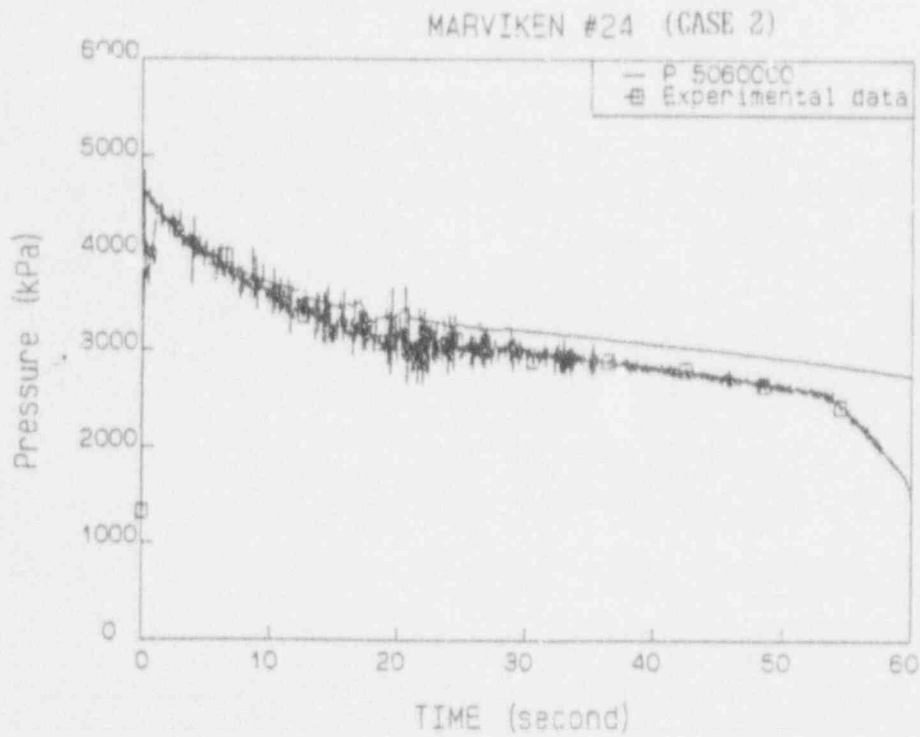


Fig. 4-37 Comparison of calculated and measured pressure at nozzle inlet for CFT 24(CASE 2)

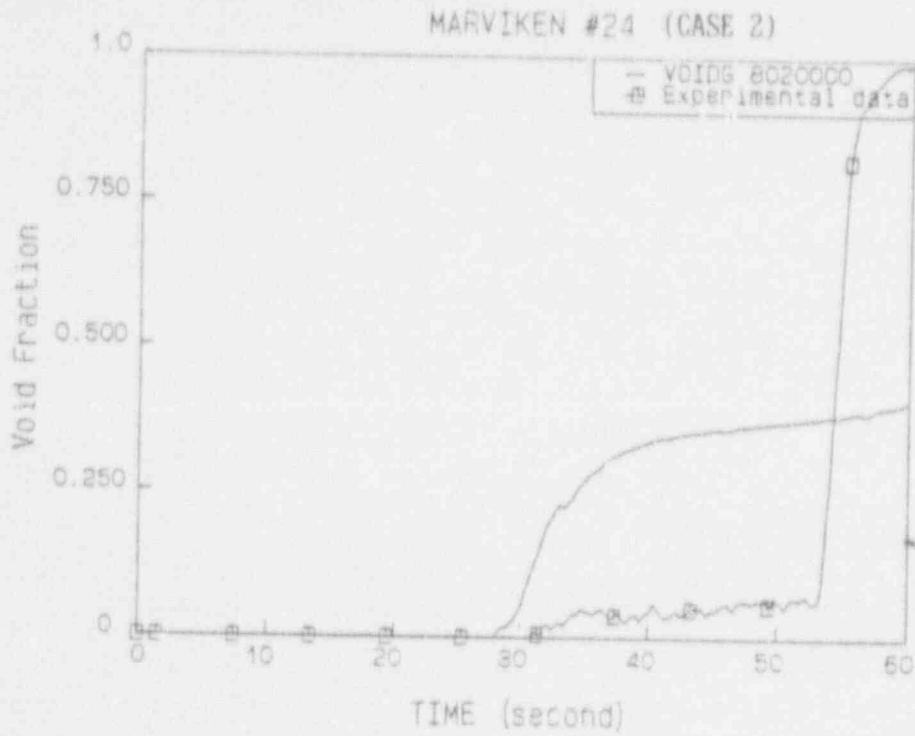


Fig. 4-38 Comparison of calculated and measured void fraction at nozzle inlet for CFT 24(CASE 2)

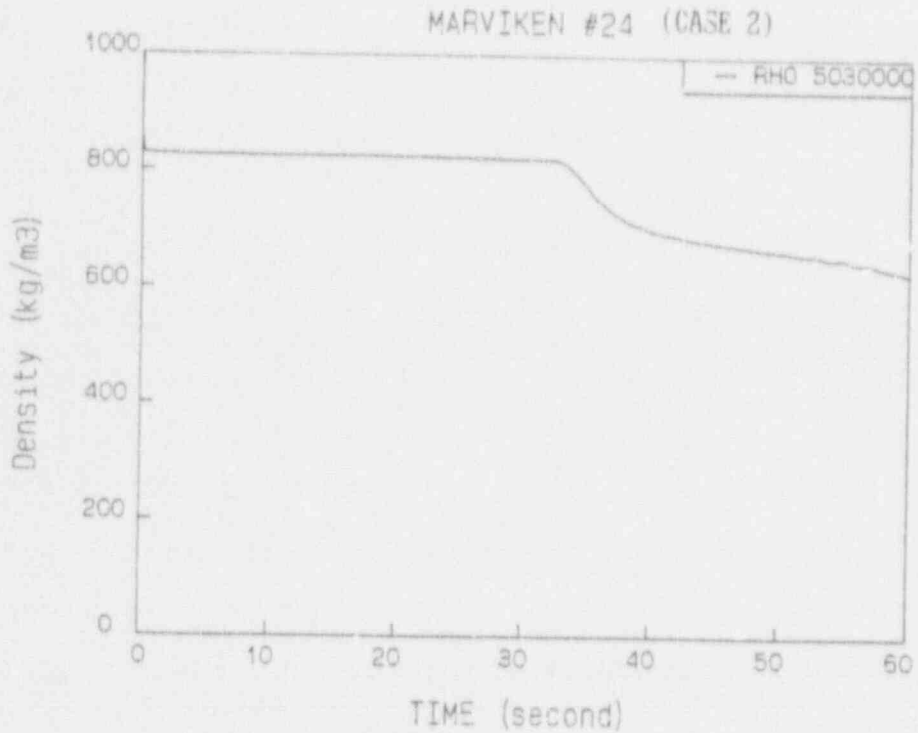


Fig. 4-39 Comparison of calculated and measured density at discharge pipe for CFT 24(CASE 2)

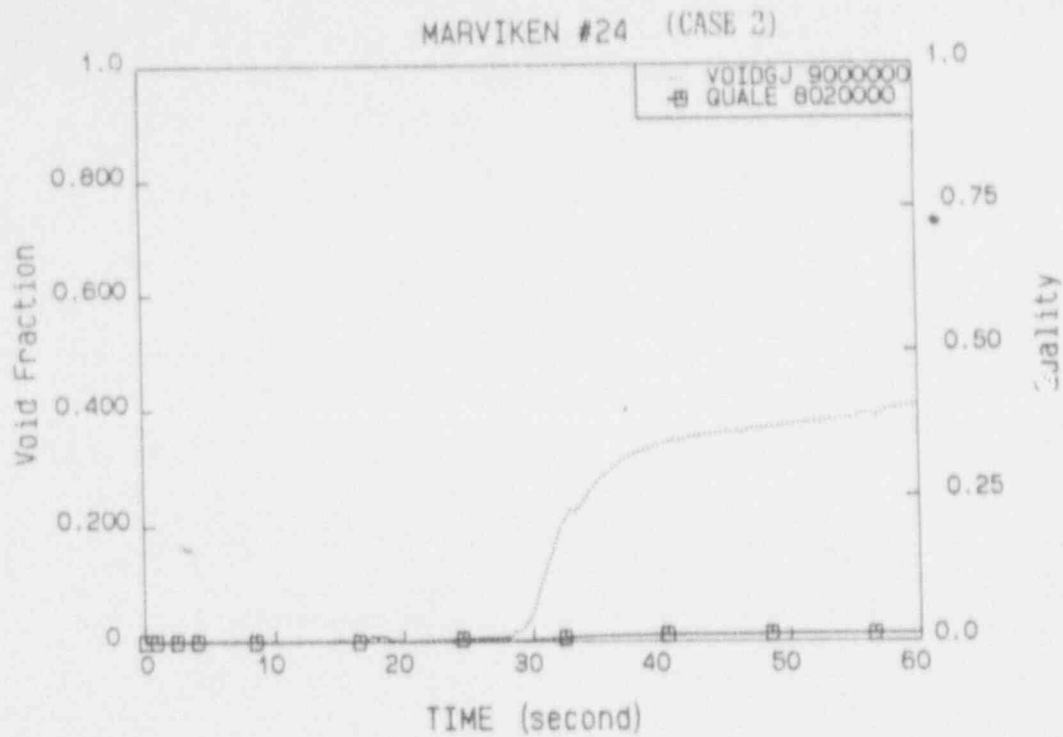


Fig. 4-40 Void fraction and quality at break for CFT 24(CASE 2)

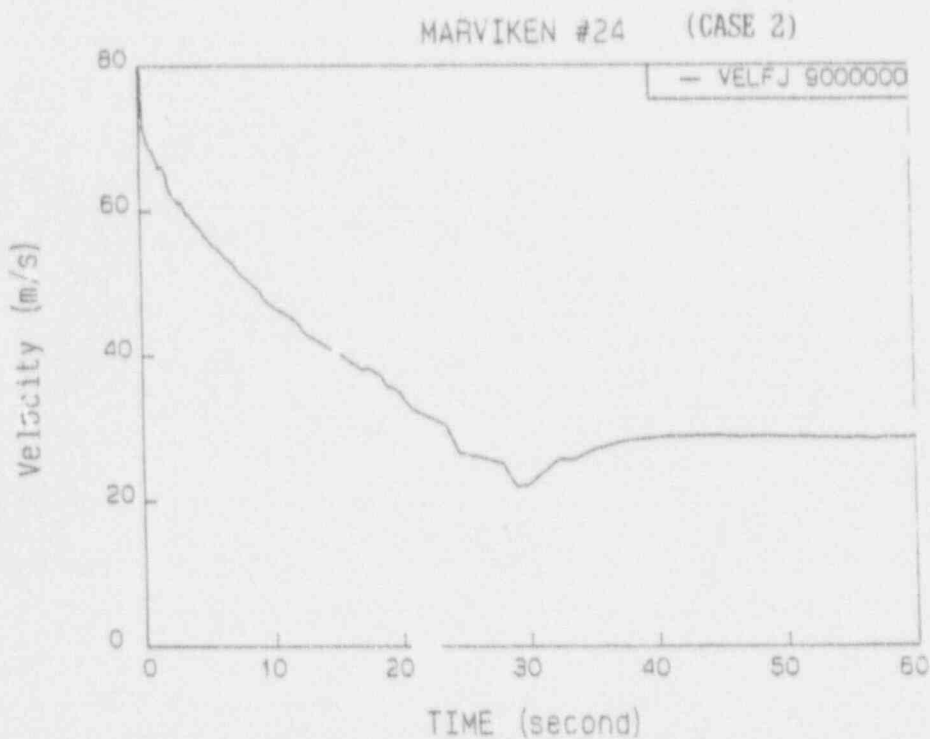


Fig. 4-41 Critical velocity at break junction for CFT 24(CASE 2)

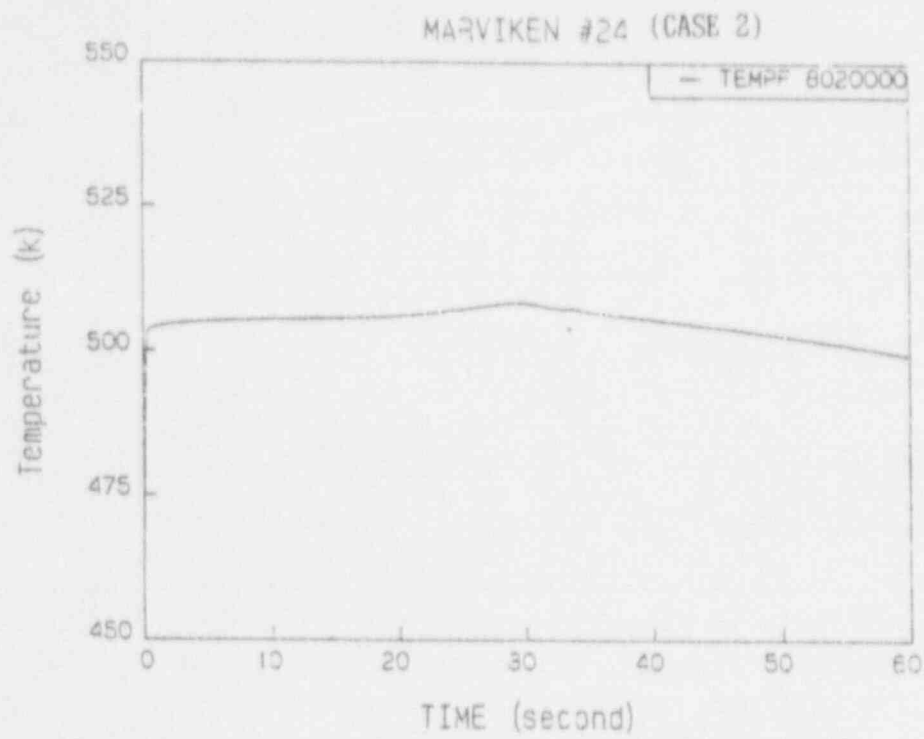


Fig. 4-42 Liquid temperature at nozzle for CFT 24(CASE 2)

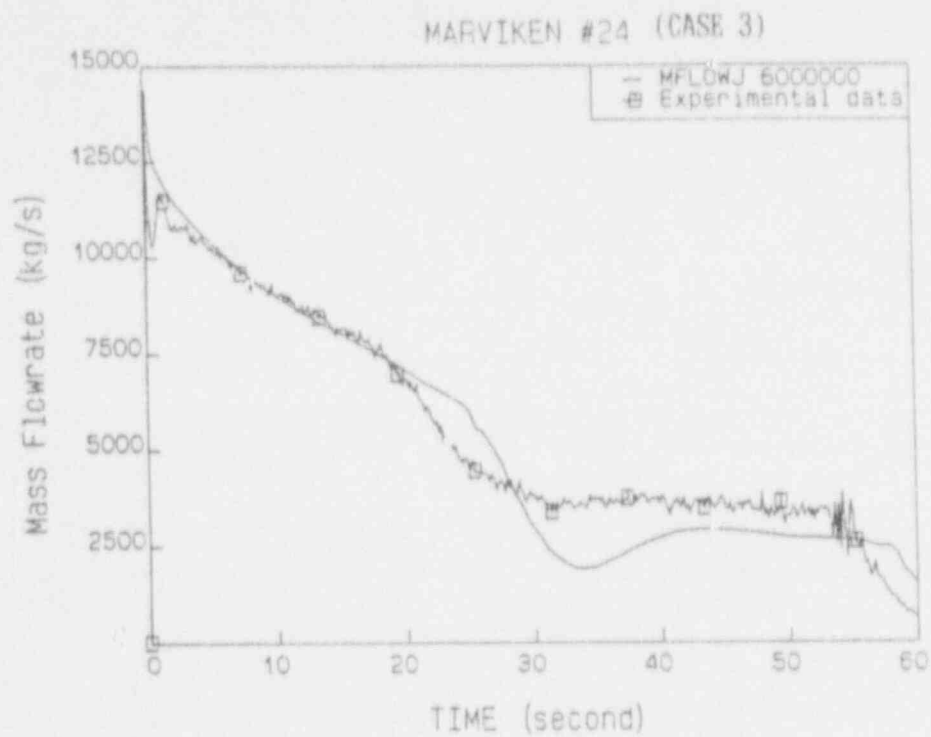


Fig. 4-43 Comparison of calculated and measured mass flowrate for CFT 24(CASE 3)

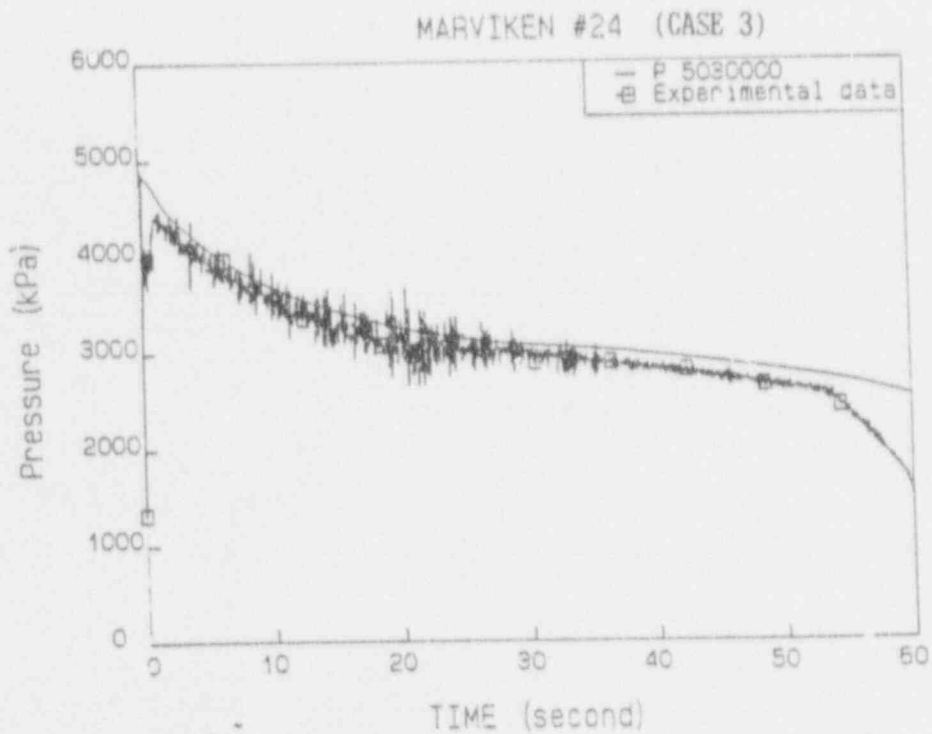


Fig. 4-44 Comparison of calculated and measured pressure at nozzle inlet for CFT 24(CASE 3)

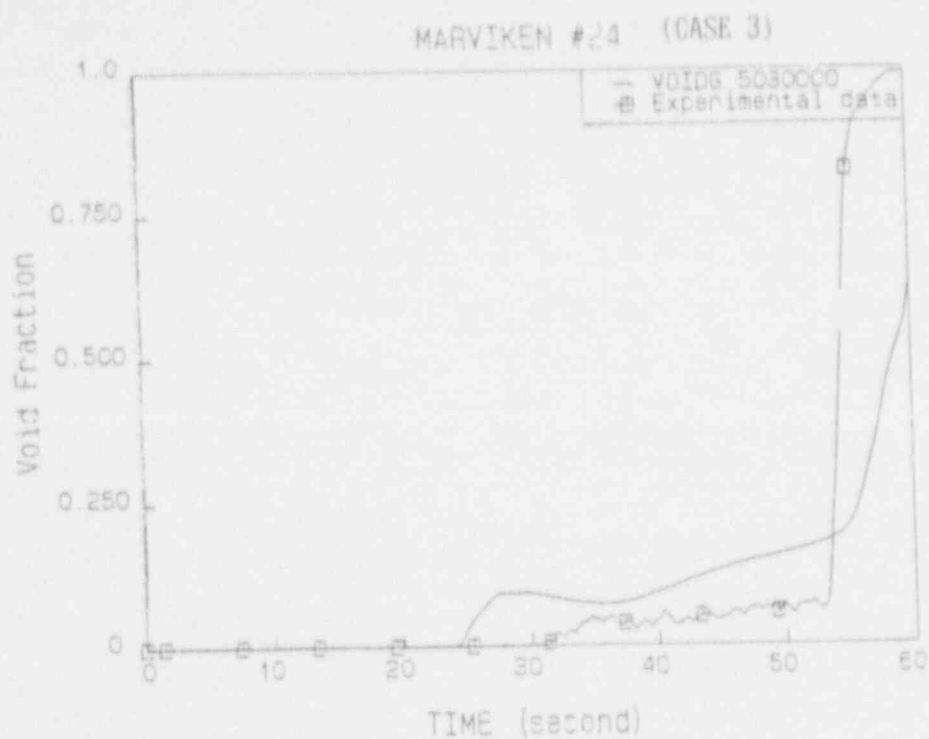


Fig. 4-45 Comparison of calculated and measured void fraction at nozzle inlet for CFT 24(CASE 3)

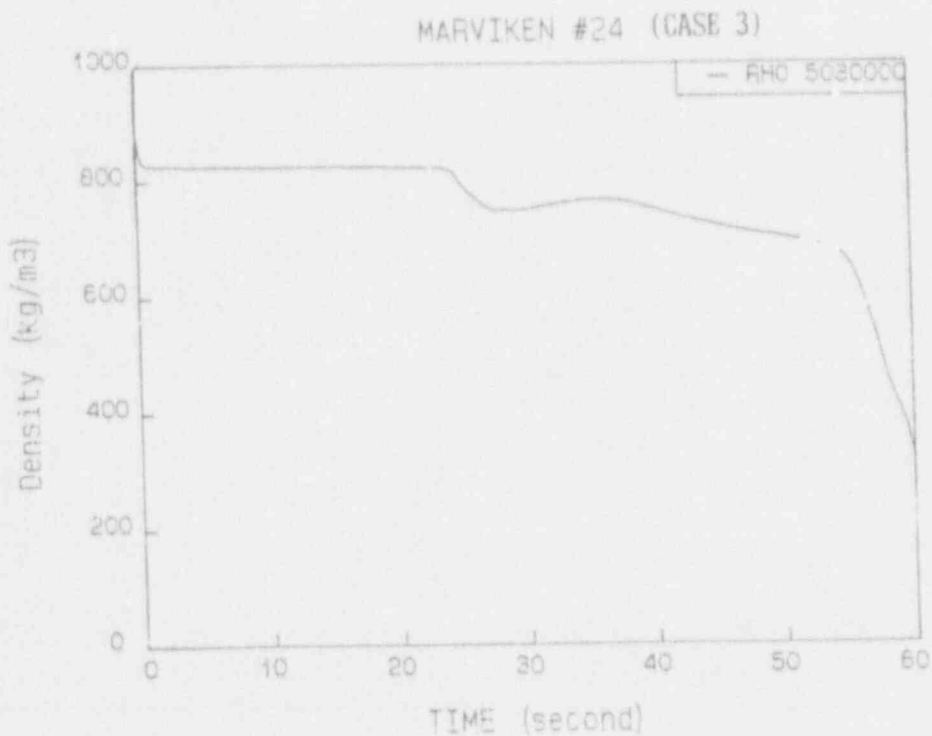


Fig. 4-46 Comparison of calculated and measured density at discharge pipe for CFT 24(CASE 3)

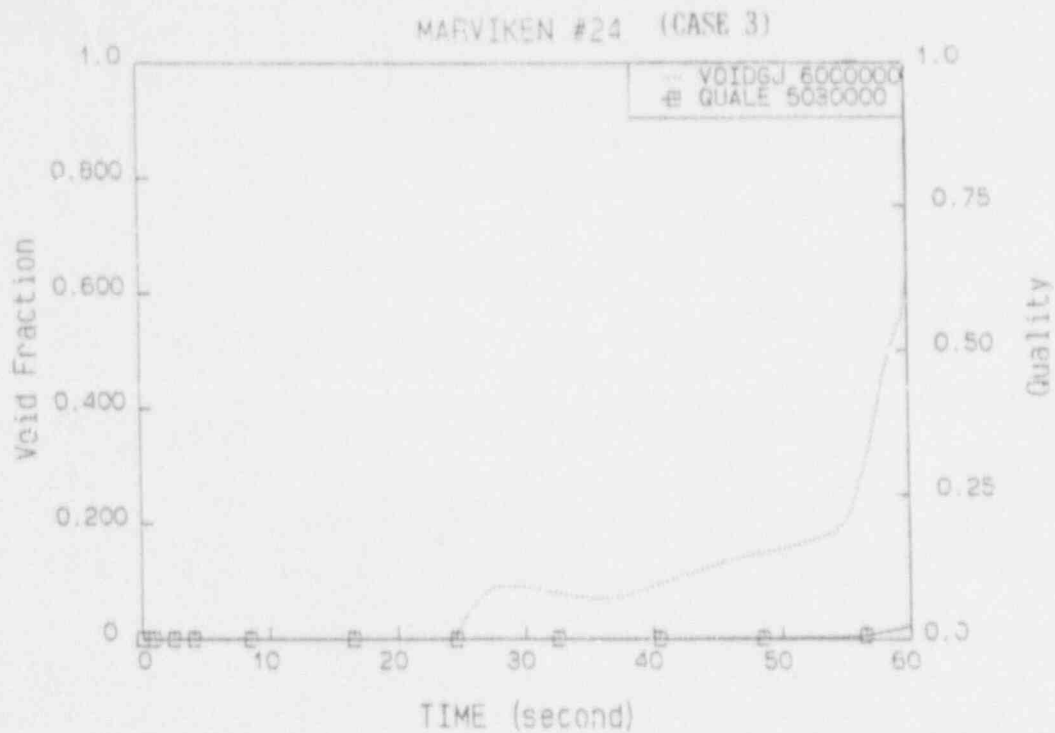


Fig. 4-47 Void fraction and quality at break for CFT 24(CASE 3)

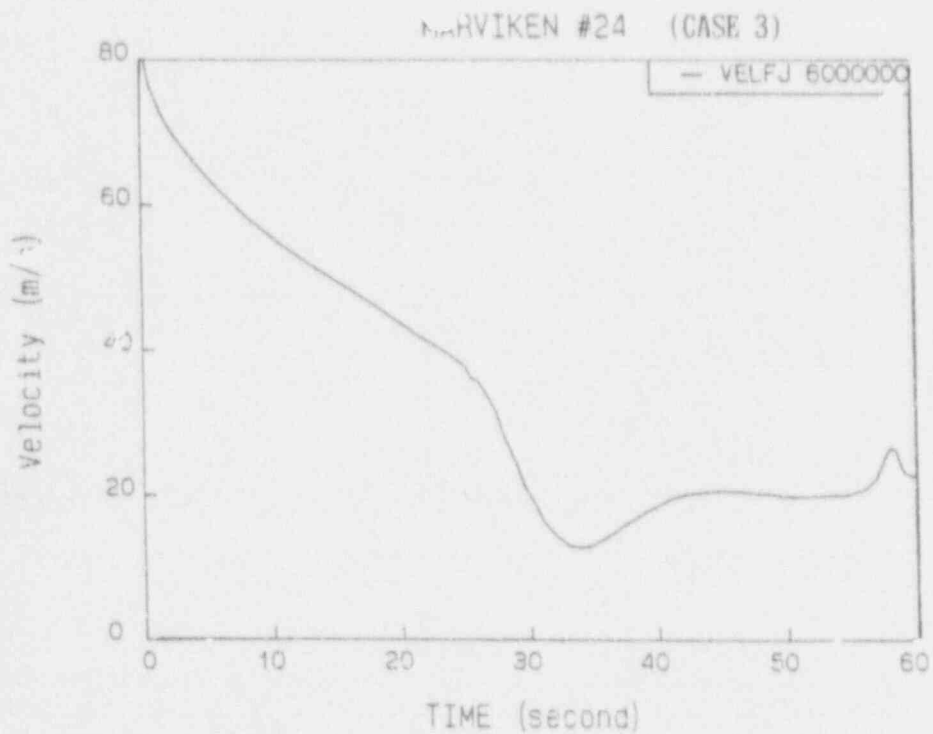


Fig. 4-48 Critical velocity at break junction for CFT 24(CASE 3)

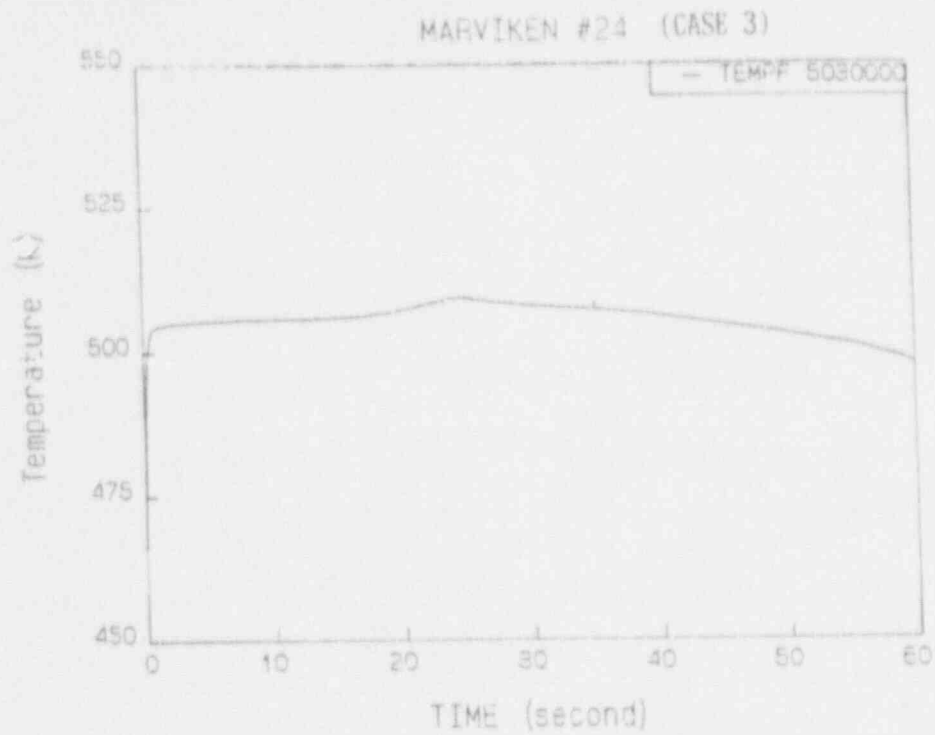


Fig. 4-49 Liquid temperature at nozzle for CFT 24(CASE 3)

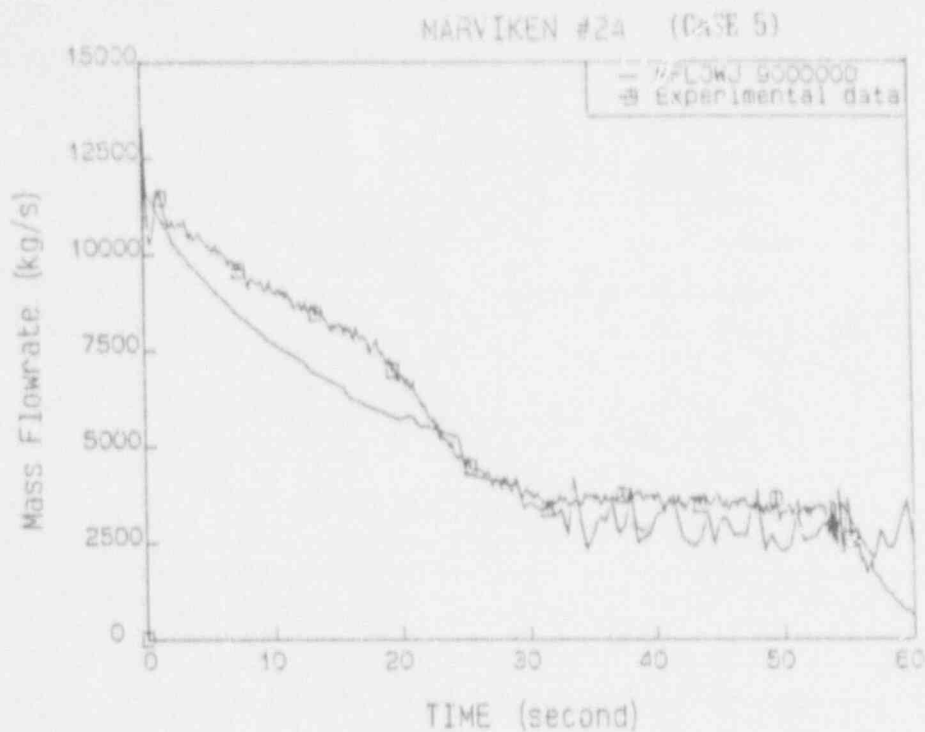


Fig. 4-50 Comparison of calculated and measured mass flowrate for CFT 24(CASE 5)

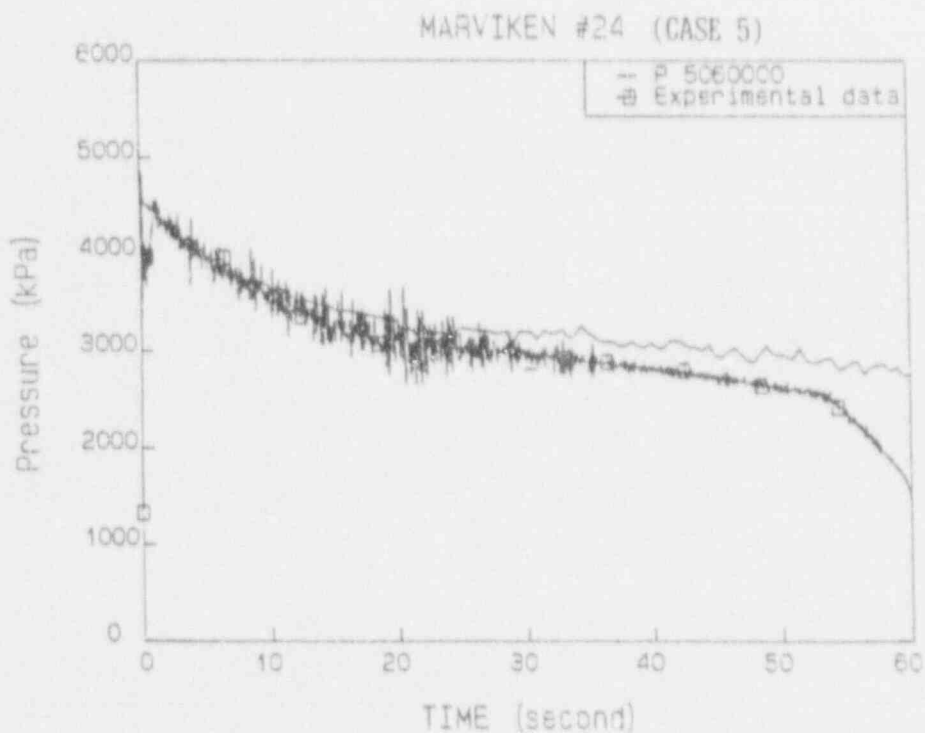


Fig. 4-51 Comparison of calculated and measured pressure at nozzle inlet for CFT 24(CASE 5)

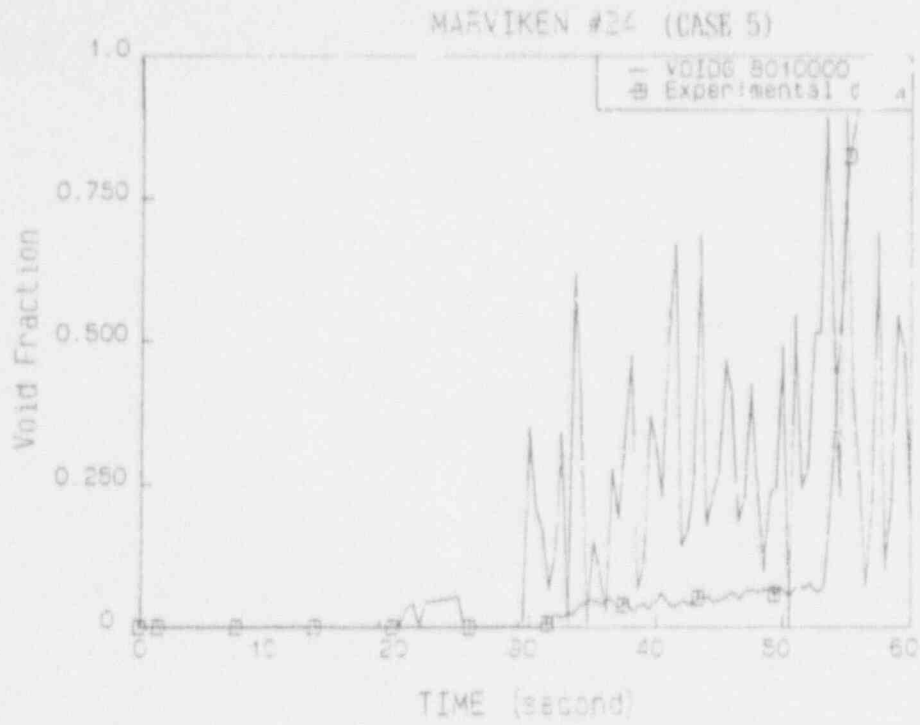


Fig. 4-52 Comparison of calculated and measured void fraction at nozzle inlet for CFT 24(CASE 5)

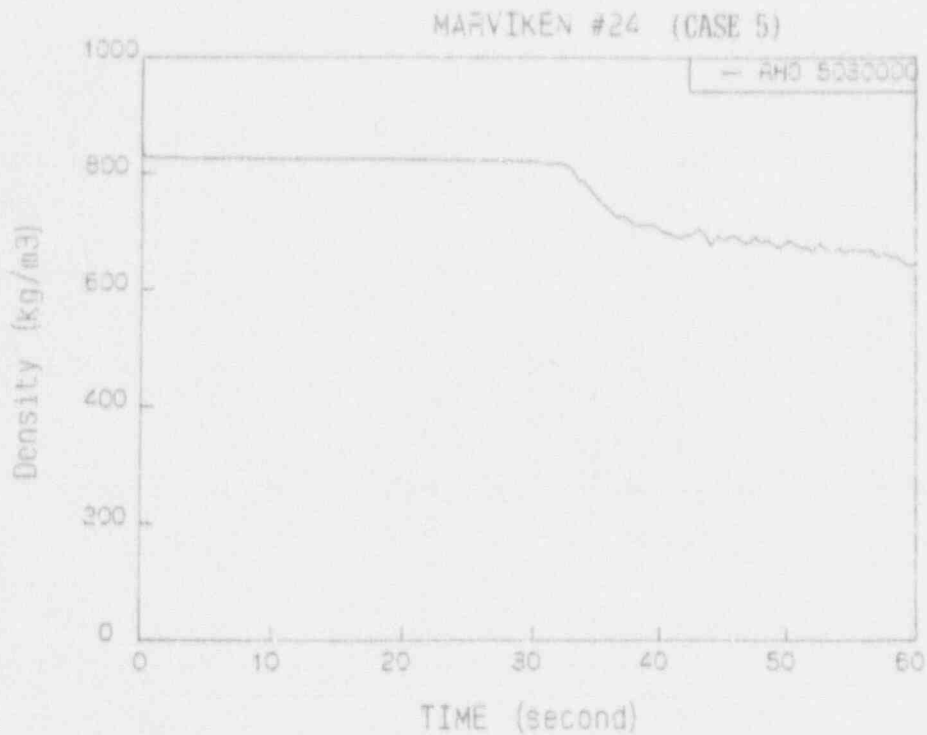


Fig. 4-53 Comparison of calculated and measured density at discharge pipe for CFT 24(CASE 5)

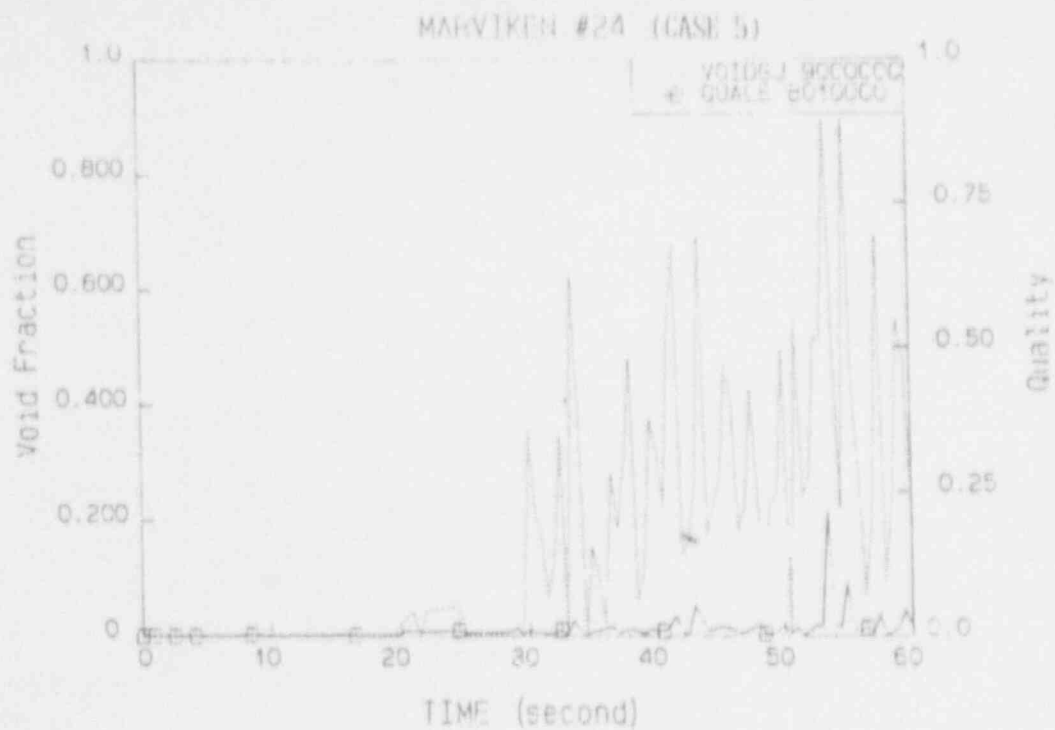


Fig. 4-54 Void fraction and quality at break for CFT 24(CASE 5)

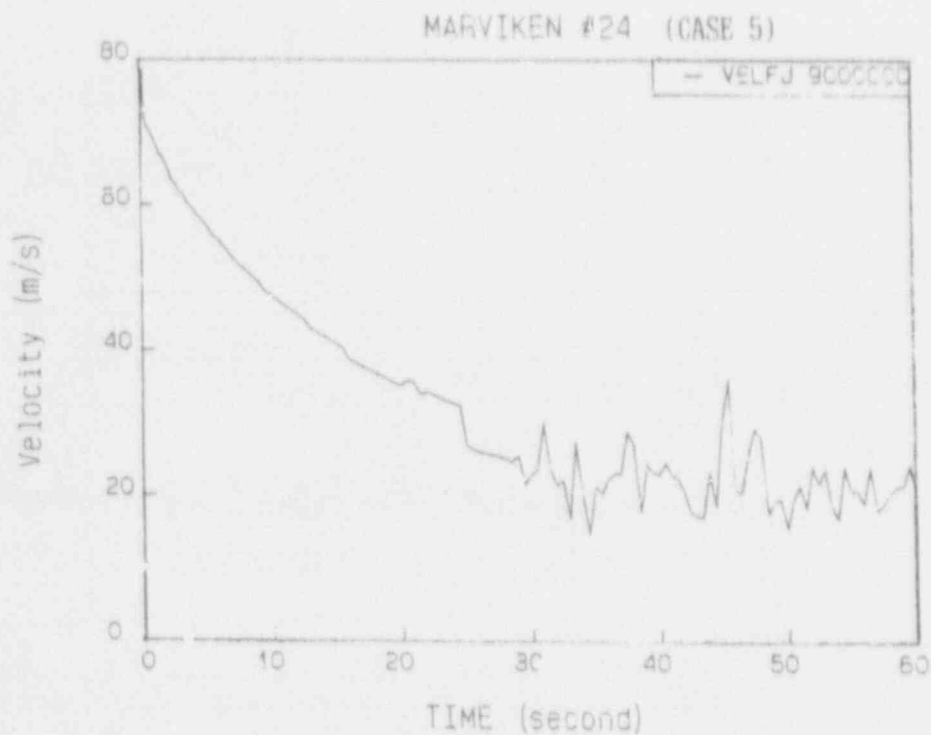


Fig. 4-55 Critical velocity at break junction for CFT 24(CASE 5)

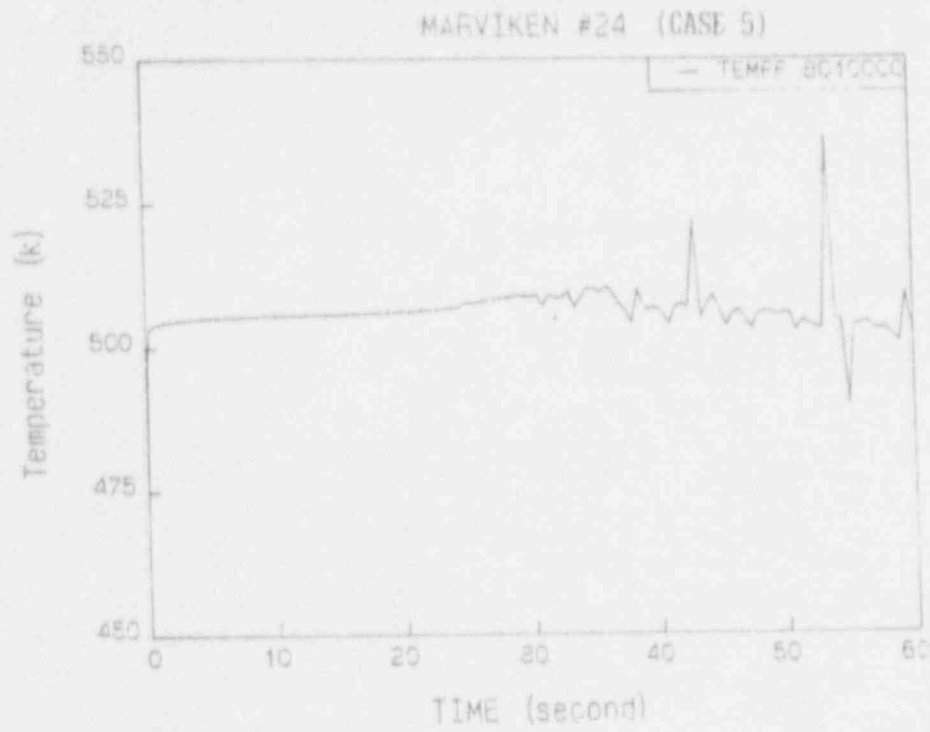


Fig. 4-56 Liquid temperature at nozzle for CFT 24(CASE 5)

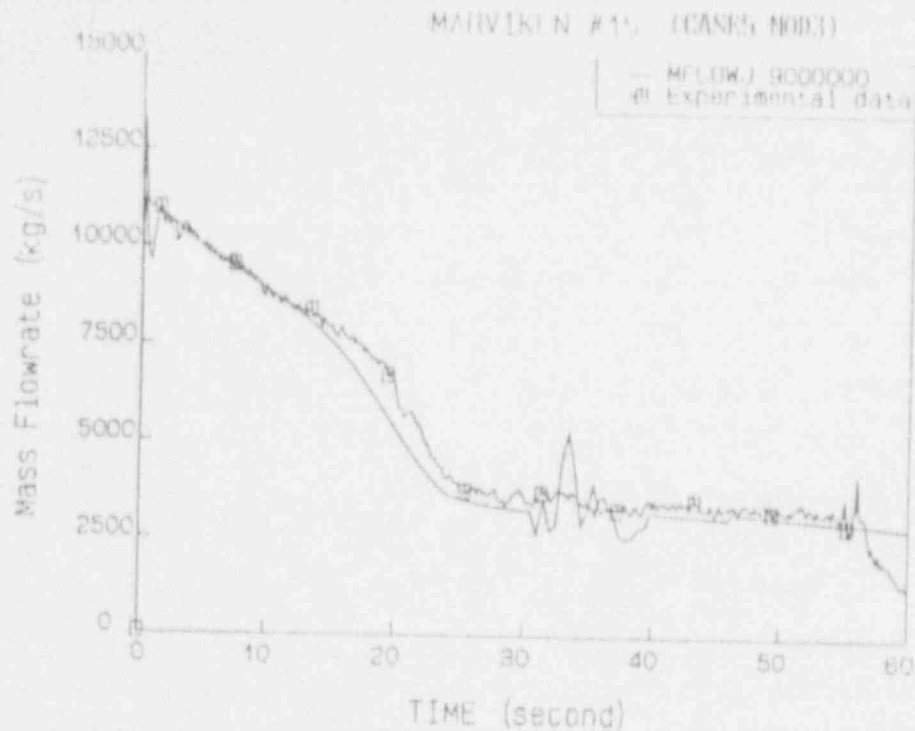


Fig. 4-57 Comparison of calculated and measured mass flowrate for CFT 15(CASE5-MOD3)

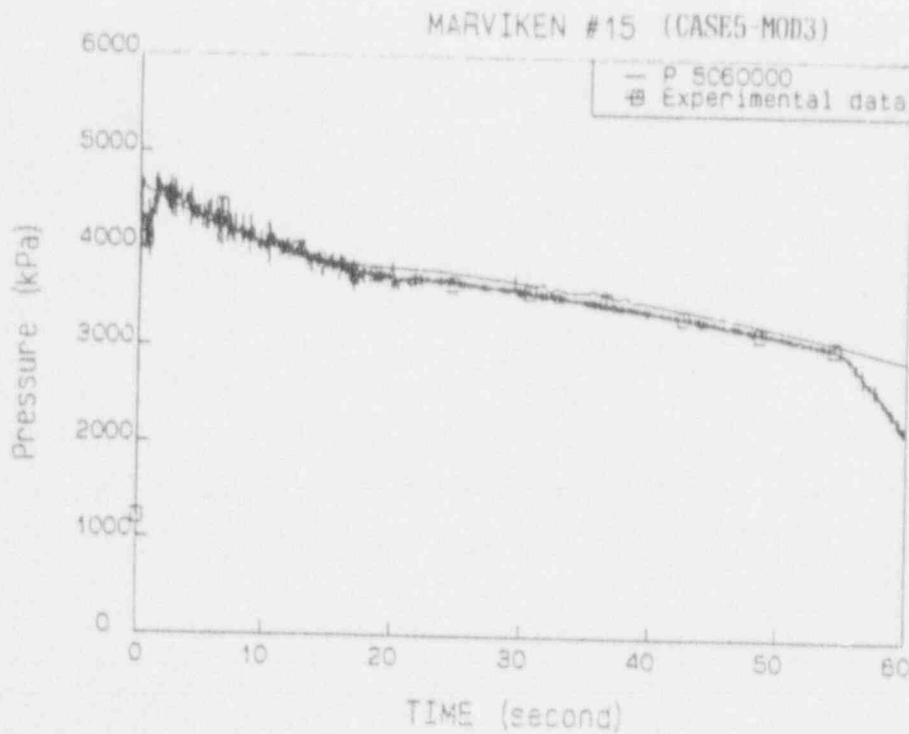


Fig. 4-58 Comparison of calculated and measured pressure at nozzle inlet for CFT 15(CASE5-MOD3)

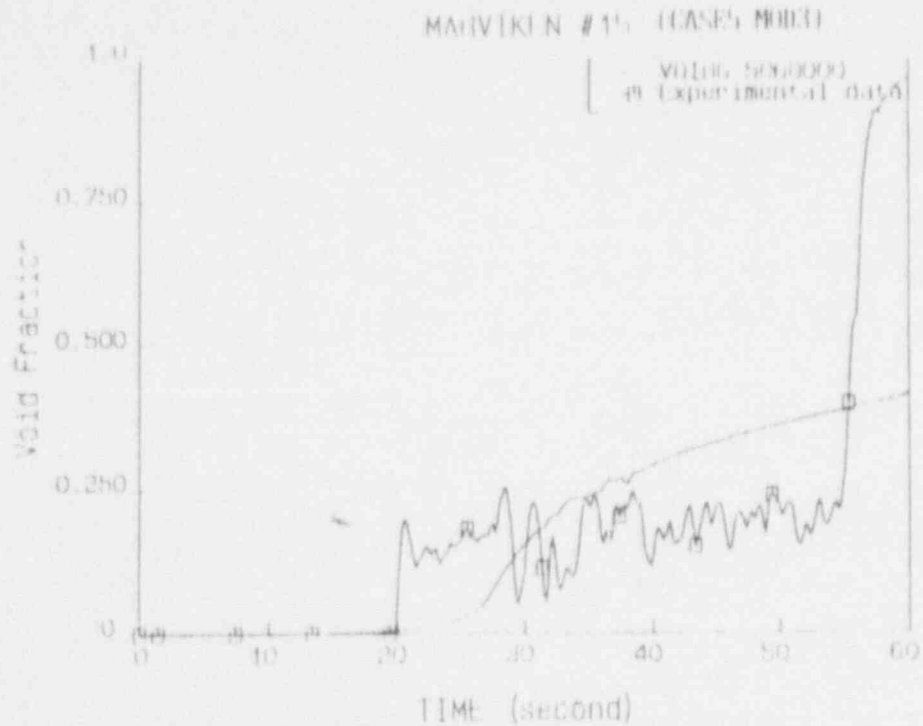


Fig. 4-59 Comparison of calculated and measured void fraction at nozzle inlet for CFT 15(CASE5 MOD3)

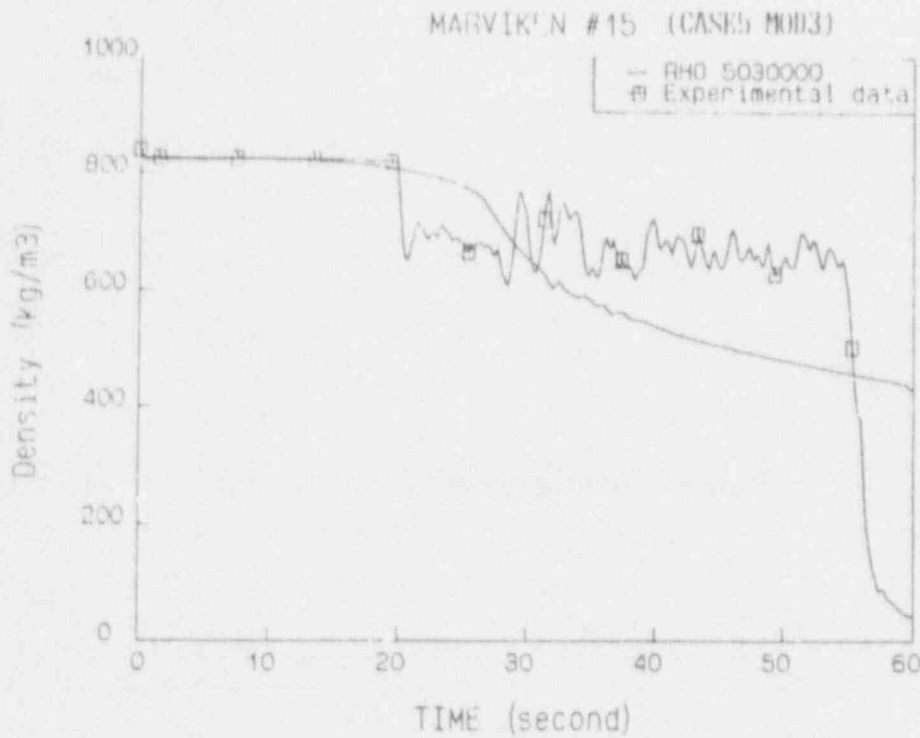


Fig. 4-60 Comparison of calculated and measured density at discharge pipe for CFT 15(CASE5-MOD3)

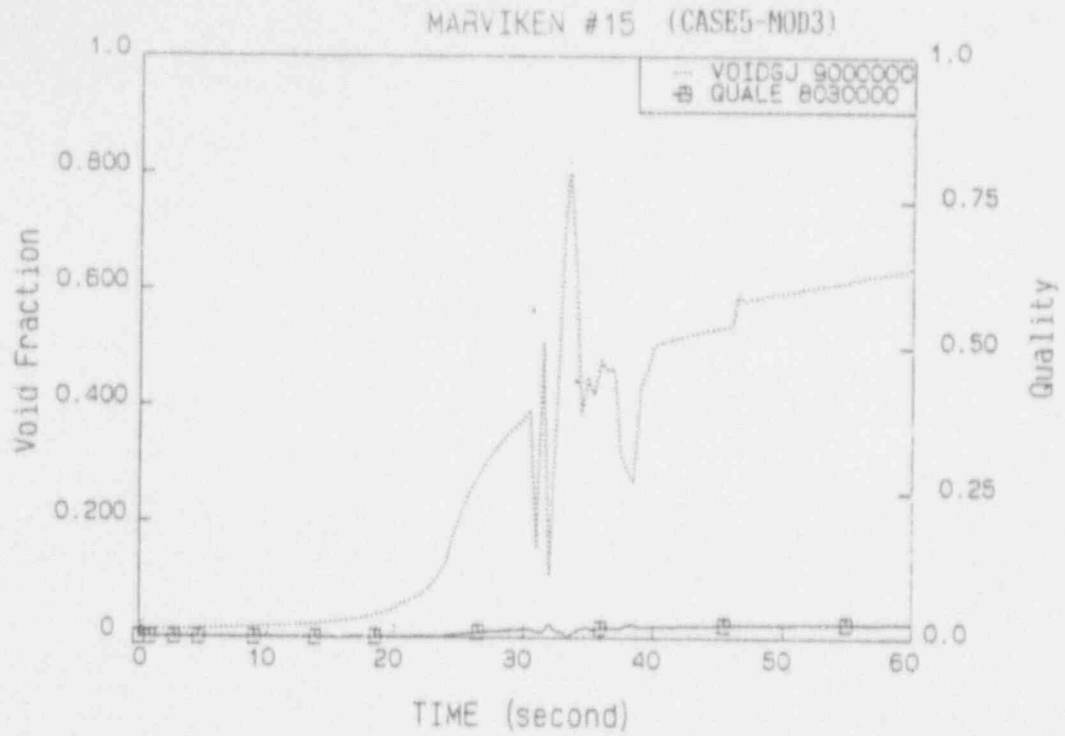


Fig. 4-61 Void fraction and quality at break for CFT 15(CASE5-MOD3)

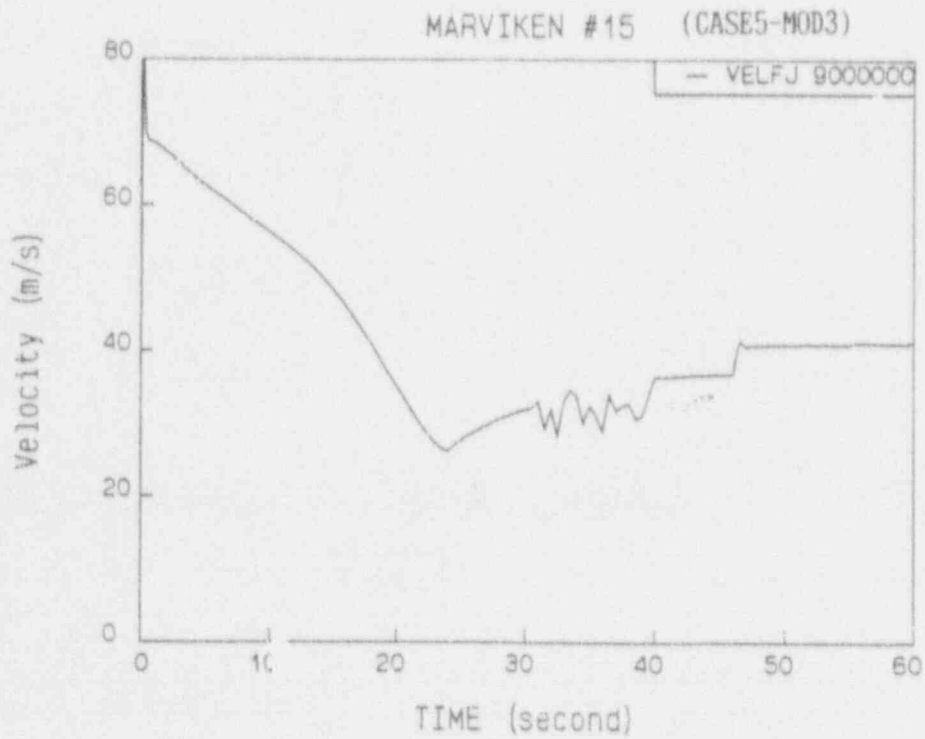


Fig. 4-62 Critical velocity at break junction for CFT 15(CASE5-MOD3)

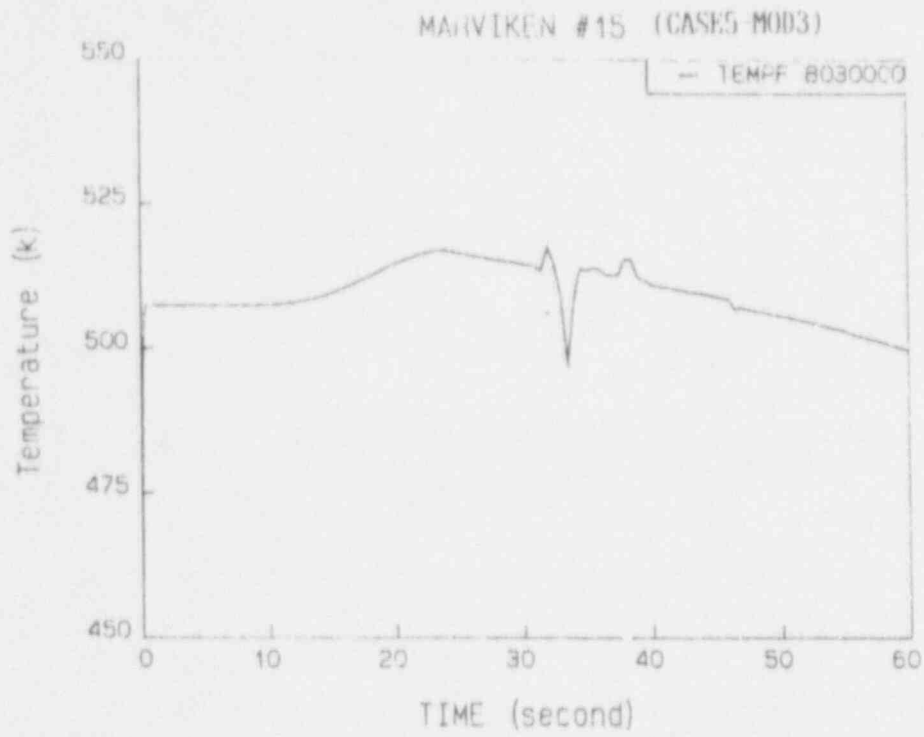


Fig. 4-63 Liquid temperature at nozzle for CFT 15(CASE5-MOD3)

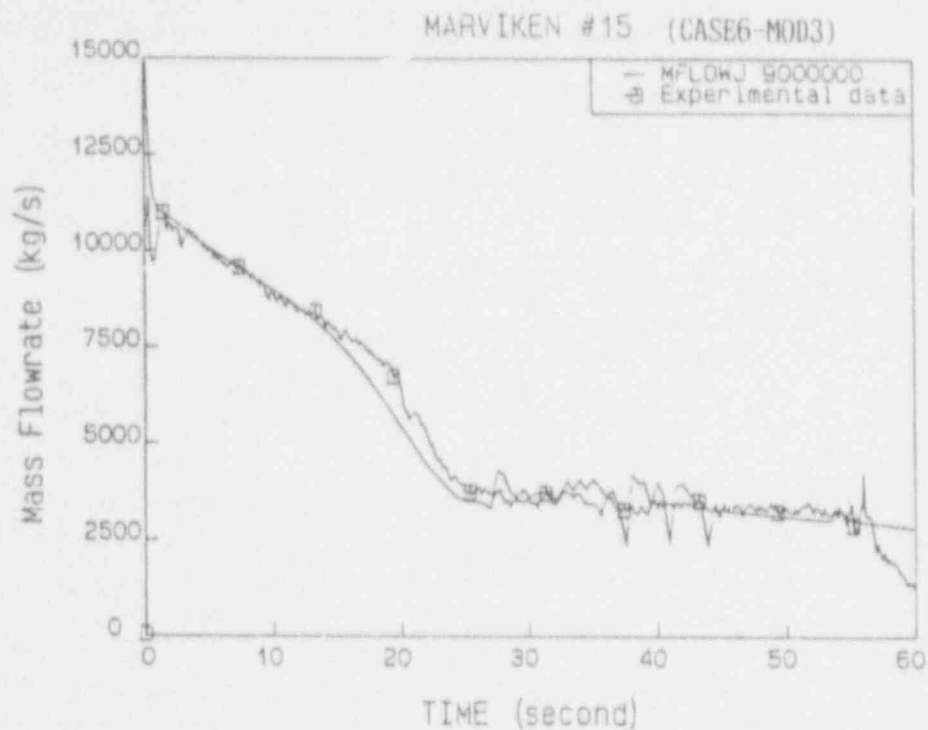


Fig. 4-64 Comparison of calculated and measured mass flowrate for CFT 15(CASE6-MOD3)

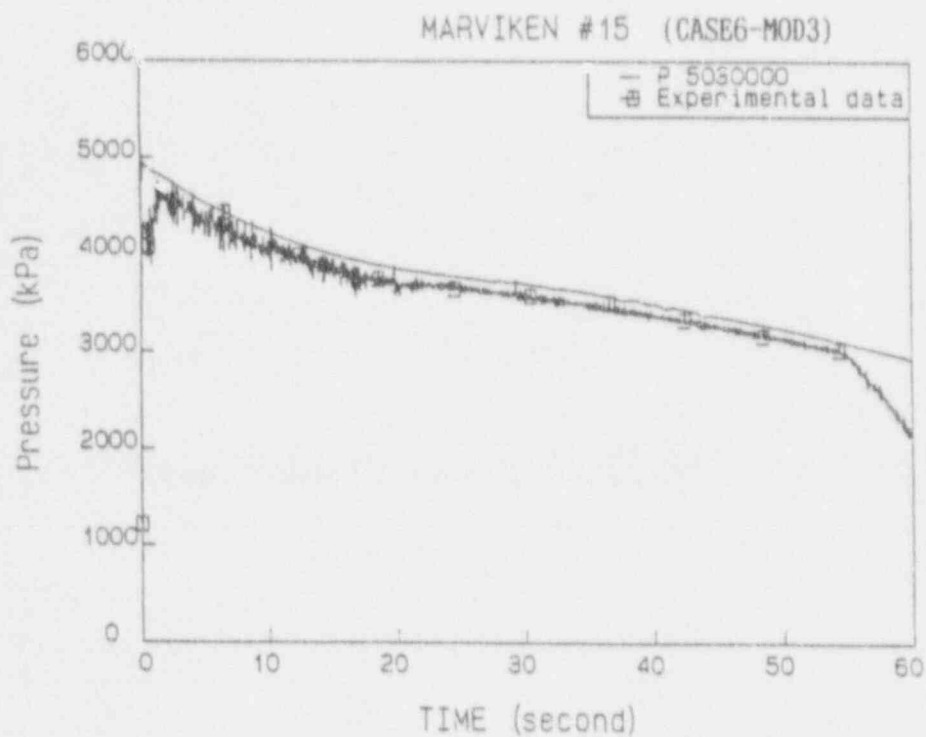


Fig. 4-65 Comparison of calculated and measured pressure at nozzle inlet for CFT 15(CASE6-MOD3)

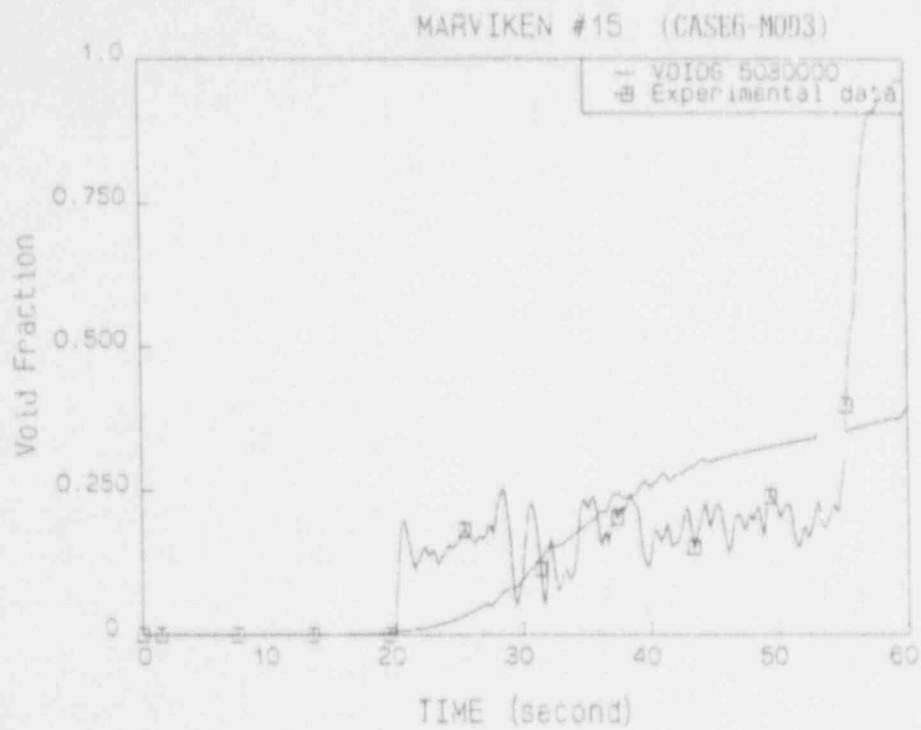


Fig. 4-66 Comparison of calculated and measured void fraction at nozzle inlet for CFT 15(CASE6-MOD3)

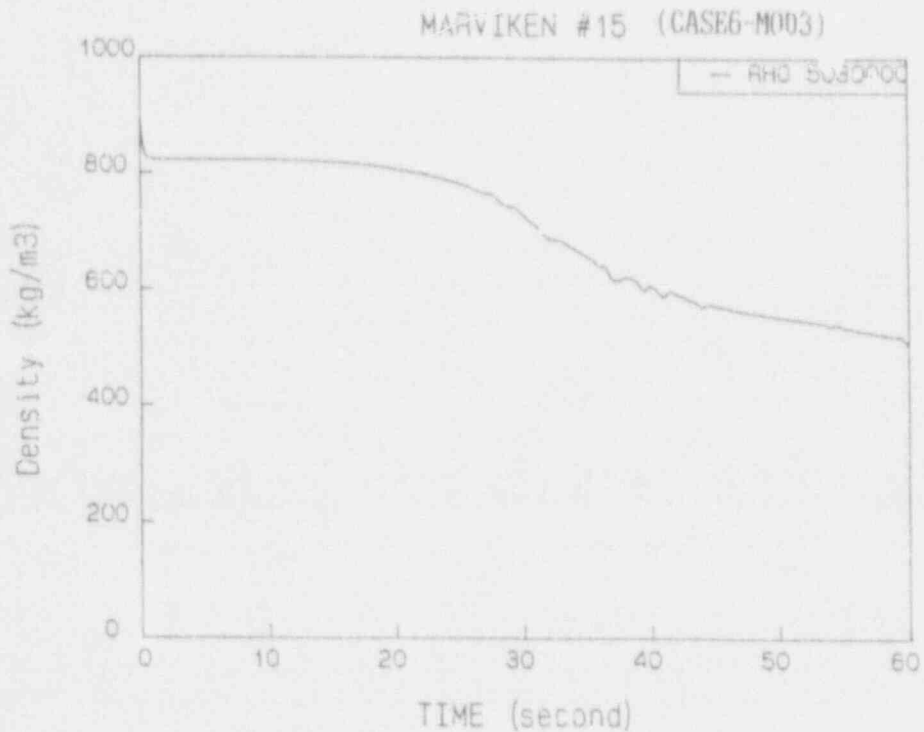


Fig. 4-67 Comparison of calculated and measured density at discharge pipe for CFT 15(CASE6-MOD3)

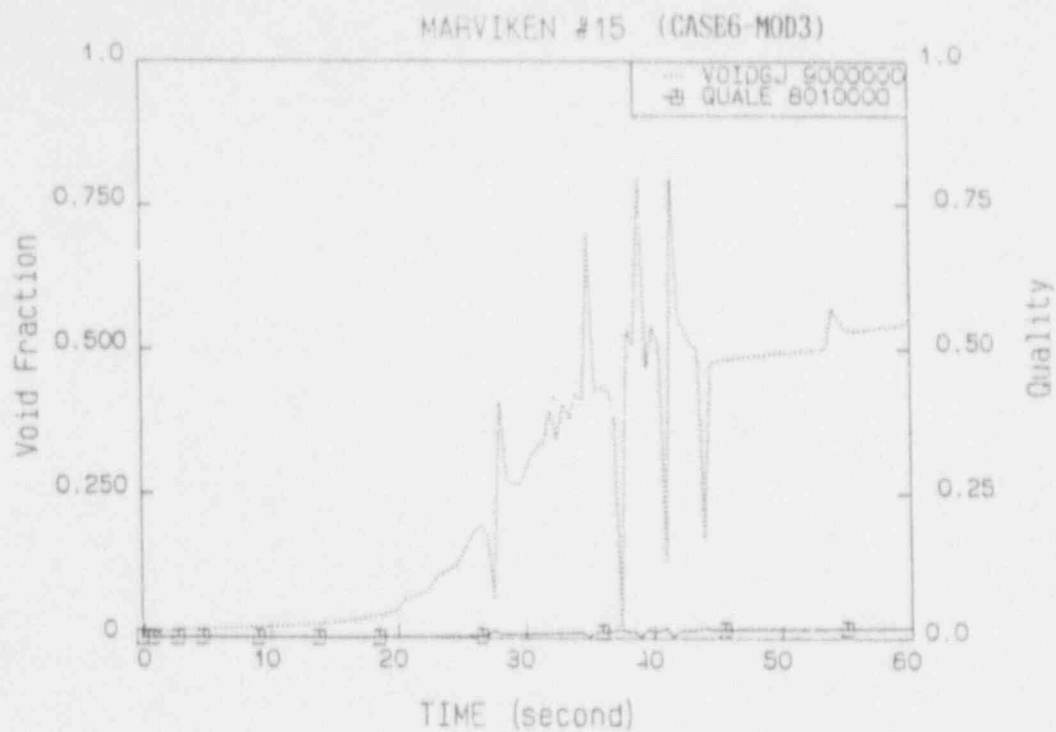


Fig. 4-68 Void fraction and quality at break for CFT 15(CASE6-MOD3)

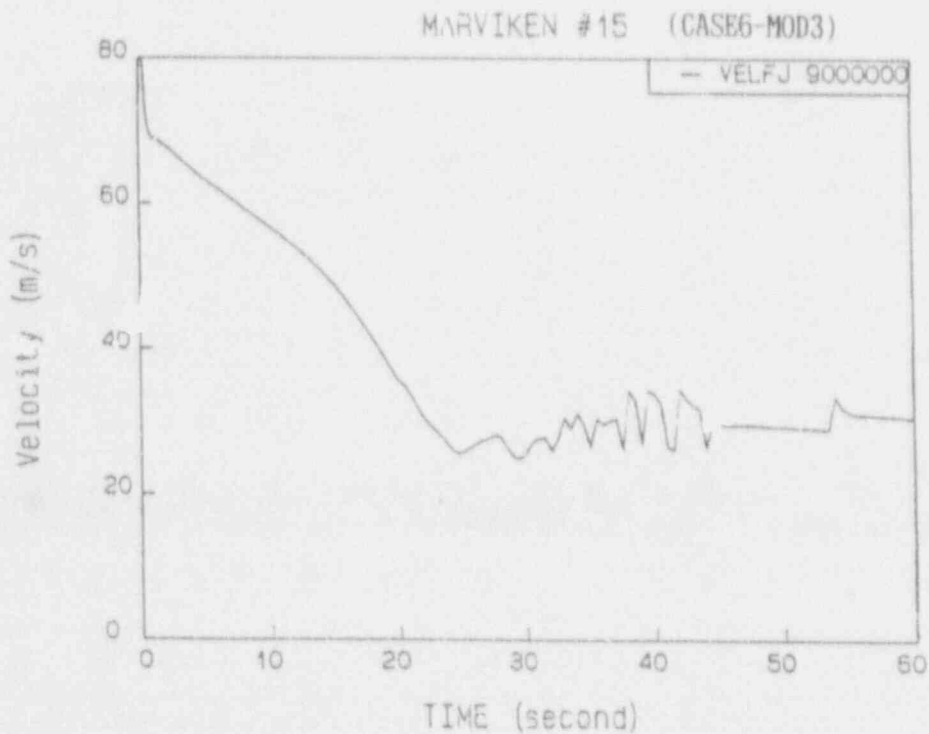


Fig. 4-69 Critical velocity at break junction for CFT 15(CASE6-MOD3)

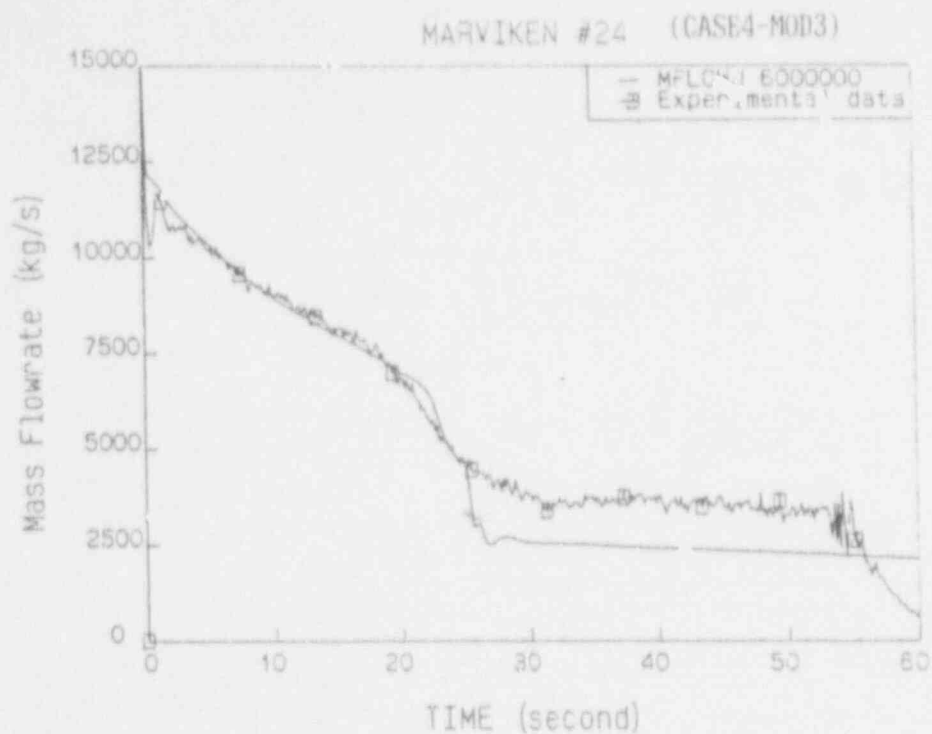


Fig. 4-70 Comparison of calculated and measured mass flowrate for CFT 24(CASE4-MOD3)

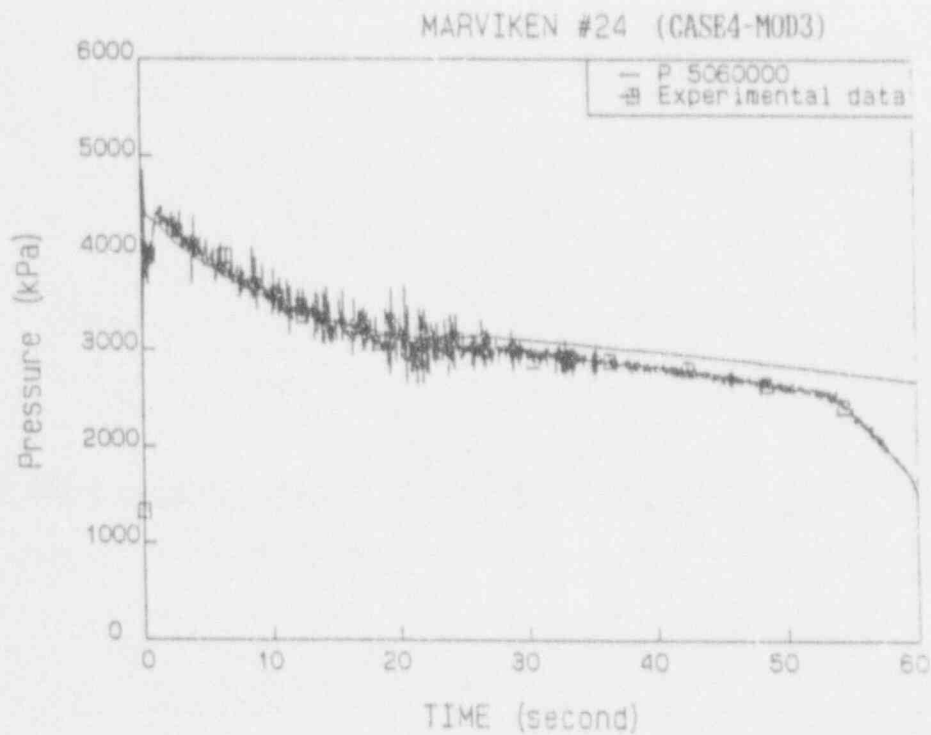


Fig. 4-71 Comparison of calculated and measured pressure at nozzle inlet for CFT 24(CASE4-MOD3)

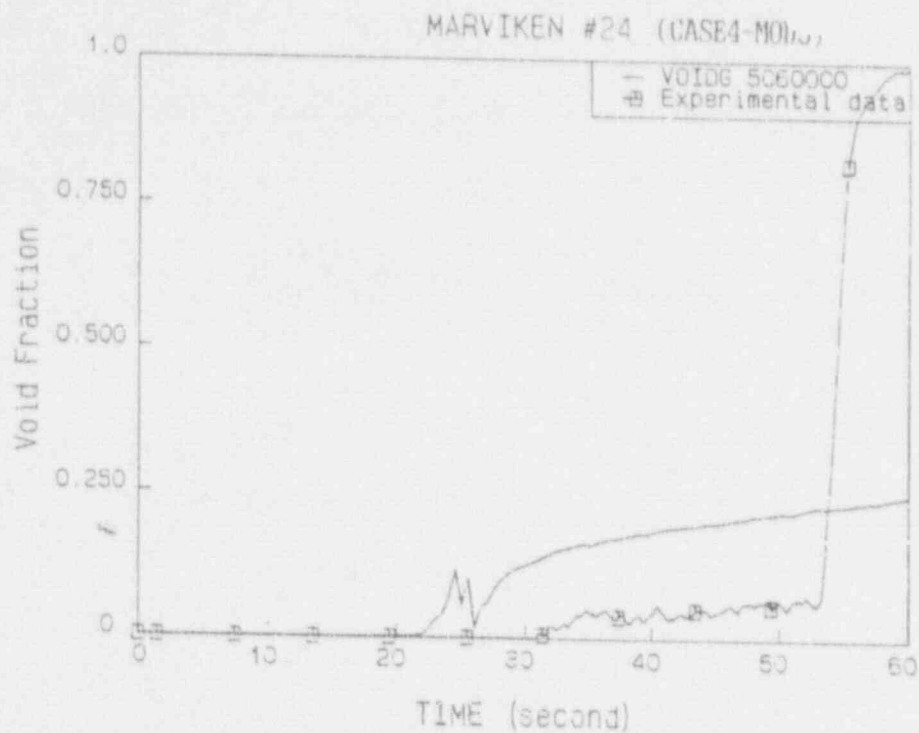


Fig. 4-72 Comparison of calculated and measured void fraction at nozzle inlet for CFT 24(CASE4-MOD3)

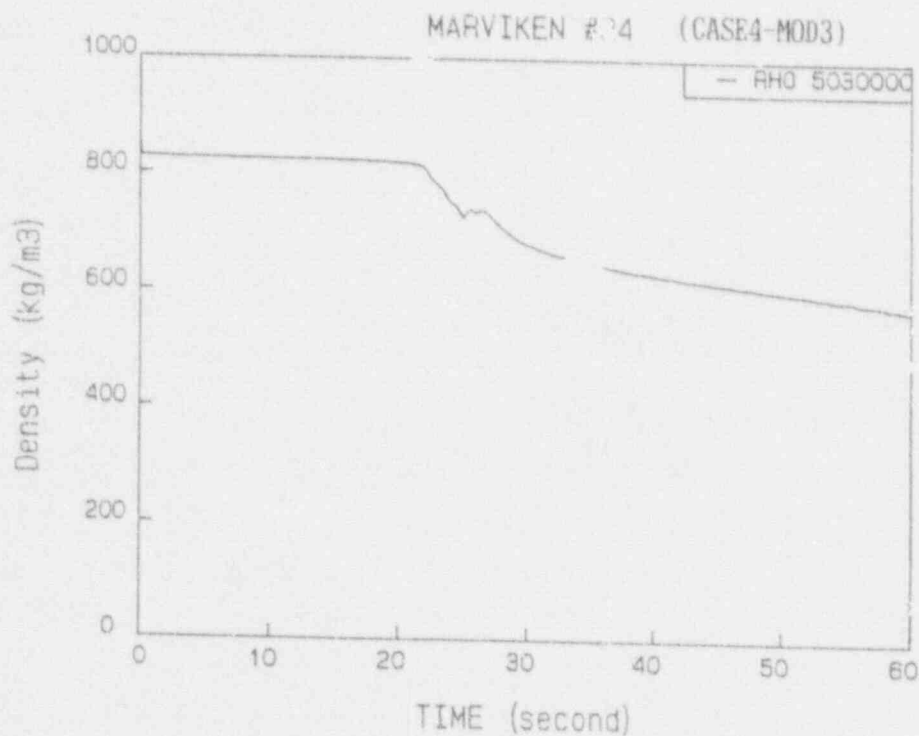


Fig. 4-73 Comparison of calculated and measured density at discharge pipe for CFT 24(CASE4-MOD3)

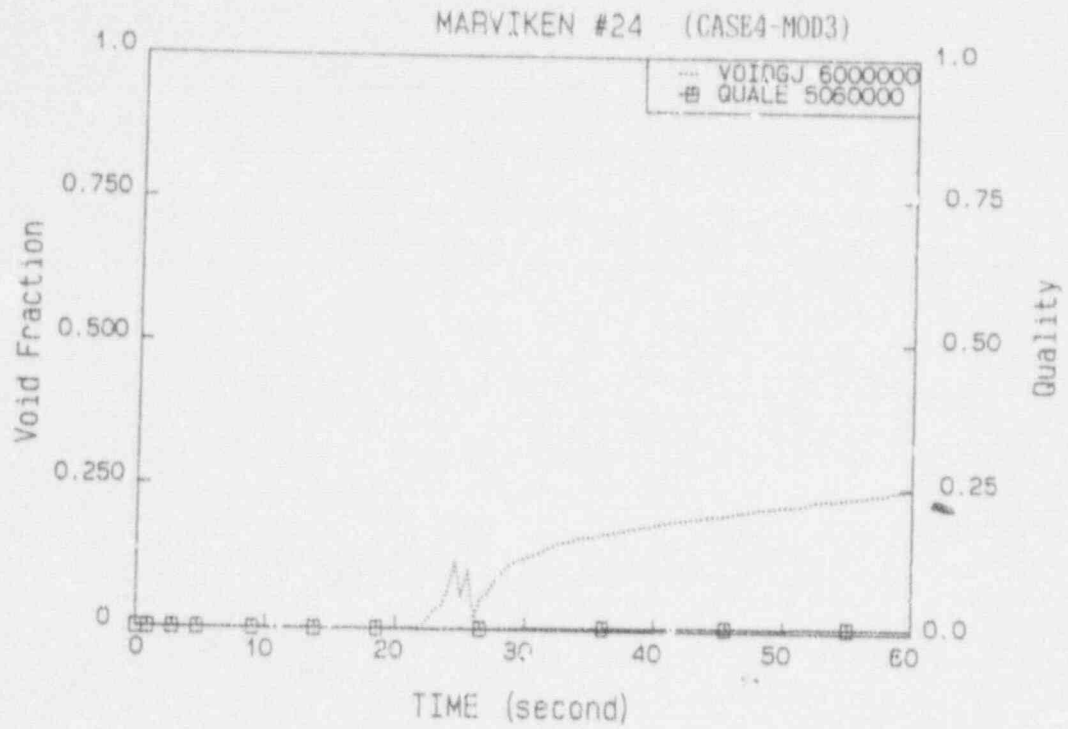


Fig. 4-74 Void fraction and quality at break for CFT 24(CASE4-MOD3)

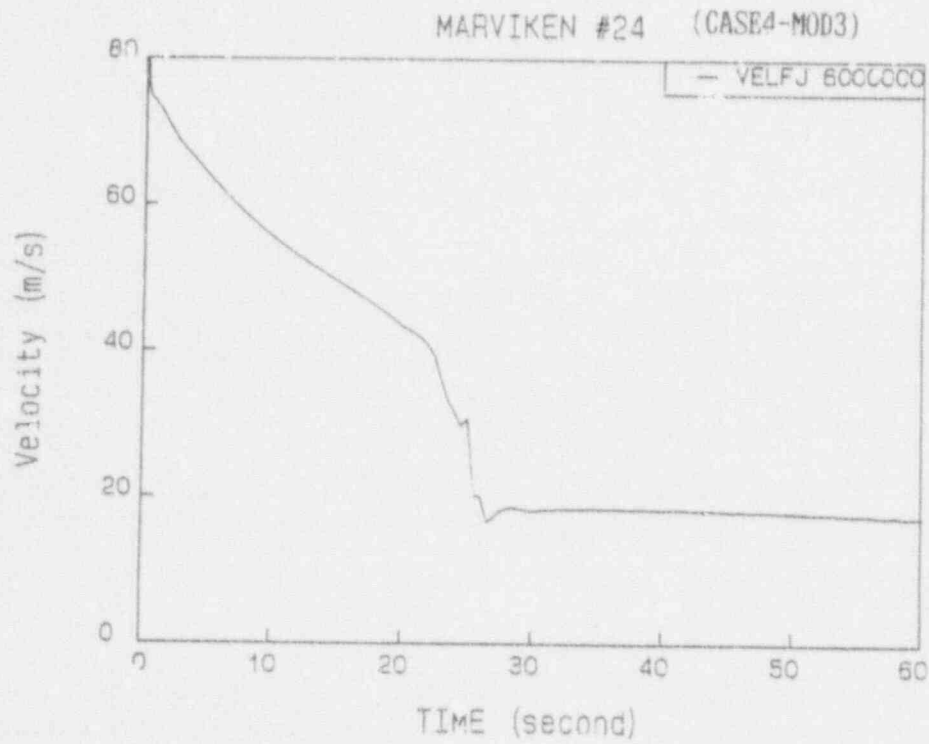


Fig. 4-75 Critical velocity at break junction for CFT 24(CASE4-MOD3)

5. Computational Efficiency

The computer conducting the simulation is CDC 170-875 Series with NOS Version 2.6.1. The simulation using RELAP5/MOD3 is conducted by CRAY-2S with UNIX Version. The computational efficiency is summarized in table 5-1 and 5-2.

Table 5-1. Run Statistics For CFT 15 Simulations

	DT Max.	Actual Time Step	CPU(s)	CPU/CELL /STEP
CASE 1	0.005 (t < 20) 0.25 (20 < t < 60)	8240	687.401	0.0017
CASE 2	0.005 (t < 20) 0.25 (20 < t < 60)	5243	387.512	0.0015
CASE 3	0.005 (t < 20) 0.25 (20 < t < 60)	8035	625.759	0.0017
CASE 4	0.005 (t < 20) 0.25 (20 < t < 60)	4712	328.972	0.0015
CASE 5	0.005 (t < 20) 0.25 (20 < t < 60)	6001	111.106	0.0003
CASE 6	0.005 (t < 20) 0.25 (20 < t < 60)	4581	77.724	0.0003
CASE 7	0.005 (t < 20) 0.25 (20 < t < 60)	11530	1054.46	0.0018
CASE 8	0.005 (t < 20) 0.25 (20 < t < 60)	5177	388.752	0.0016

Table 5-2 Run Statistics For CFT 24 Simulations

Case	DT Max.	Actual Time Step	CPU(s)	CPU/CELL /STEP
CASE 1	0.005 (t < 20) 0.25 (20 < t < 60)	4718	307.553	0.0014
CASE 2	0.005 (t < 20) 0.25 (20 < t < 60)	58002	5409.98	0.0019
CASE 3	0.005 (t < 20) 0.25 (20 < t < 60)	4204	248.668	0.0014
CASE 4	0.005 (t < 20) 0.25 (20 < t < 60)	4370	76.862	0.0003
CASE 5	0.005 (t < 20) 0.25 (20 < t < 60)	19632	2344.08	0.0027

6. Conclusions

RELAP5/MOD2 critical flow model is assessed using Marviken CFT 15 and 24. In order to evaluate the effects of the nodalization change for a nozzle and a discharge pipe, the sensitivity calculations are performed. The conclusions of this assessment are followings:

- 1) For the CFT 15 simulation, it may be recommended that a nozzle is modeled as PIPE or SINGLVOL. In case of the modeling of nozzle as PIPE, uniform length of each volume may present better results with respect to mass flowrate. With more than 3 cells the simulation may be failed because the mismatch between fast flow and a short nozzle length causes the water properties errors.
- 2) For the CFT 15 simulation, it is found that the calculated pressure at nozzle inlet is overpredicted in the case of rough subdivision of discharge pipe. And, in the case that L/D of one cell for discharge pipe exceeds 1.6, it is found that strong fluctuation is feasible to occur in two-phase region.
- 3) For the CFT 24 simulation, RELAP5 critical flow model agrees well with test data in subcooled choked flow region, but underpredicts the two phase critical mass flowrate by 10 to 20 %.

- 4) For the CFT 24 simulation, the modeling of nozzle as PIPE may present rather bad results of mass flowrate, than as a junction. It may be considered, in RELAP5, that the pressure drop due to friction loss in a pipe is overpredicted relative to actual nozzle.

- 5) It is considered that internal choking may provide the fluctuation of critical flow behavior, because the critical flowrate at upstream junction restricts that at break junction. It is recommended that the use of choking option is excluded at all junctions except a break junction.

The critical flow model in RELAP5/MOD3 is assessed to evaluate the adequacy of the improvements with respect to the model in RELAP5/MOD2. The critical flow model in RELAP5/MOD3 underpredicts about 5 % the mass flowrate and shows the oscillations during two-phase region, although it predicts smoothly in transition region.

REFERENCES

1. V. H. Ransom, et al., RELAP5/MOD2 Code Manuals, NUREG/CR-4312, EGG-2396, EG&G Idaho Inc., Dec. 1985.
2. USNRC, The Marviken Full Scale Critical Flow Tests, Summary Report., NUREG/CR-2671, MXC-301, Dec. 1979.
3. S. LEVY, Critical Flow Data Review and Analysis, EPRI-NP-2192, Jan. 1982.
4. Walter L. Weaver, Improvements to The RELAP5/MOD3 Choking Model, EGG-FAST-8822, Dec. 1989.
5. Dimenna, R. A., et al., RELAP5/MOD2 Models and Correlations, NUREG/CR-5194, Aug. 1988.

Appendix A
RELAP5 INPUT DECK FOR CFT 15

=MARVIKEN TEST 15 (CASE 1)

** PROBLEM TYPE AND OPTION

*CARD # TYPE OPTION
0000100 NEW TRANSNT

*

** UNITS SELECTION

*CARD # INPUT-UNITS OUTPUT-UNITS
0000102 SI SI

*

* RSTPLT CONTROL

0000105 3.0 4.0

*

** TIME STEP CONTROL CARDS

*CARD #	T-END	DTMIN	DTMAX	CONTROL	MINOR	MAJOR	RESTART
0000201	5.00	1.0E-7	0.005	1	20	200	4096
0000202	20.0	1.0E-7	0.005	1	50	1000	4096
0000203	60.0	1.0E-7	0.250	1	2	40	4096

*

** MINOR EDIT REQUESTS

0000301 P 3010000
 0000302 F 3390000
 0000303 P 5060000
 0000304 RHO 3390000
 0000305 RHO 5030000
 0000306 VOIDG 3390000
 0000307 VOIDG 5060000
 0000308 MFLOWJ 9000000
 0000309 MFLOWJ 5050000
 0000310 TEMPF 8030000
 0000311 TEMPG 8030000
 0000312 P 8020000
 0000313 P 8030000
 0000314 VOIDG 8020000
 0000315 VOIDG 8030000
 0000316 RHOF 8030000
 0000317 RHOG 8030000
 0000318 SOUNDE 8030000
 0000319 VOIDGJ 8020000
 0000320 VOIDGJ 9000000
 0000321 SATTEMP 8030000
 0000322 VELFJ 9000000
 0000323 QUALE 8030000
 0000324 CPUTIME

```

*
** HYDRODYNAMIC COMPONENTS
*
** VESSEL COMPONENT *****
*CARD#  NAME  TYPE
0030000  VESSEL  PIPE
*
*CARD #  NO.VOLS
0030001   39
*
** PIPE FLOW AREA
*CARD #  AVOL  VOL.NO
0030101   0.0   39
*
** PIPE JUNCTION FLOW AREAS
*CARD #  AJUN  JUN.NO
0030201   0.0   37  17.0  38
*
** PIPE VOLUME LENGTHS
*CARD #  LENGTH  VOL.NO
0030301  3.55  1  1.0  2  0.5  38  1.26  39
*
** PIPE VOLUMES
**CARD #  VOLUME  VOL.NO
0030401  8.547  1  13.9  2  10.036  3  10.501  4  10.8125  13
0030402  10.767  17  10.373  18  10.76  19  9.05  20
0030403  10.5  24  10.45  28  10.319  37  10.098  38  19.68  39
*
** PIPE VOLUME HORIZONTAL ANGLE
*CARD #  H-ANGLE  VOL.NO
0030601  -90.0  39
*
** PIPE VOLUME FRICTION DATA
**CARD #  ROUGHNESS  HYD.DIA  VOL.NO
0030801  0.0  0.0  39
*
** PIPE VOLUME CONTROL FLAG
*CARD #  CONTROL  VOL.NO
0031001  0  39
*
** PIPE JUNCTION CONTROL FLAG
*CARD #  CONTROL  JUN.NO
0031101  000  38
*

```

** PIPE VOLUME INITIAL CONDITIONS

*CARD #	CONTROL	PRESSURE	QUALS	ZERO	ZERO	ZERO	VOL. NO
0031201	2	5.04E6	1.0	0.0	0.0	0.0	1
0031202	2	5.04E6	1.0	0.0	0.0	0.0	2
0031203	2	5.04E6	0.00504	0.0	0.0	0.0	3
0031204	2	5.046E6	0.0	0.0	0.0	0.0	4
0031205	2	5.050E6	0.0	0.0	0.0	0.0	5
0031206	2	5.053E6	0.0	0.0	0.0	0.0	6
0031207	2	5.058E6	0.0	0.0	0.0	0.0	7
0031208	2	5.061E6	0.0	0.0	0.0	0.0	8

*CARD #	CONTROL	PRESSURE	TEMP	ZERO	ZERO	ZERO	VOL. NO
0031209	3	5.065E6	537.0	0.0	0.0	0.0	9
0031210	3	5.069E6	536.5	0.0	0.0	0.0	10
0031211	3	5.073E6	536.3	0.0	0.0	0.0	11
0031212	3	5.077E6	536.0	0.0	0.0	0.0	12
0031213	3	5.080E6	535.0	0.0	0.0	0.0	13
0031214	3	5.084E6	534.2	0.0	0.0	0.0	14
0031215	3	5.088E6	532.4	0.0	0.0	0.0	15
0031216	3	5.092E6	530.5	0.0	0.0	0.0	16
0031217	3	5.096E6	521.9	0.0	0.0	0.0	17
0031218	3	5.100E6	513.3	0.0	0.0	0.0	18
0031219	3	5.104E6	508.9	0.0	0.0	0.0	19
0031220	3	5.108E6	508.9	0.0	0.0	0.0	20
0031221	3	5.112E6	508.9	0.0	0.0	0.0	21
0031222	3	5.116E6	508.5	0.0	0.0	0.0	22
0031223	3	5.120E6	508.5	0.0	0.0	0.0	23
0031224	3	5.124E6	508.5	0.0	0.0	0.0	24
0031225	3	5.128E6	508.5	0.0	0.0	0.0	25
0031226	3	5.132E6	508.0	0.0	0.0	0.0	26
0031227	3	5.136E6	508.0	0.0	0.0	0.0	27
0031228	3	5.140E6	508.0	0.0	0.0	0.0	28
0031229	3	5.144E6	508.0	0.0	0.0	0.0	29
0031230	3	5.148E6	508.0	0.0	0.0	0.0	30
0031231	3	5.152E6	508.0	0.0	0.0	0.0	31
0031232	3	5.156E6	508.0	0.0	0.0	0.0	32
0031233	3	5.160E6	508.0	0.0	0.0	0.0	33
0031234	3	5.164E6	508.0	0.0	0.0	0.0	34
0031235	3	5.168E6	508.0	0.0	0.0	0.0	35
0031236	3	5.172E6	508.0	0.0	0.0	0.0	36
0031237	3	5.176E6	508.0	0.0	0.0	0.0	37
0031238	3	5.180E6	508.0	0.0	0.0	0.0	38
0031239	3	5.188E6	508.0	0.0	0.0	0.0	39

*
** PIPE JUNCTION INITIAL CONDITIONS

*CARD #	VELF	VELG	VJUN	JUN.NO
0031301	0.0	0.0	0.0	3S

*

** SINGLE JUNCTION OUTLET FROM VESSEL *****

*CARD # NAME TYPE
0040000 OUTLETJ SNGLJUN

*

** SINGLE JUNCTION GEOMETRY CARD

*CARD # FROM TO AJUN KF KR FLAG
0040101 003010000 005000000 2.0 0.0 0.0 1000

*

** SINGLE JUNCTION INITIAL CONDITIONS

*CARD # CONTROL VELFJ VELGJ VELJUN
0040201 0 0.0 0.0 0.0

*

** PIPE COMPONENT *****

*CARD # NAME TYPE
0050000 DISCHARGE PIPE

*

** PIPE INFORMATION

*CARD # NO.VOLS
0050001 6

*

** PIPE FLOW AREA

*CARD # AVOL VOL.NO
0050102 0.4441 3
0050103 0.4778 5
0050104 0.4441 6

*

** PIPE JUNCTION FLOW AREAS

*CARD # AJUN JUN.NO
0050201 0.0 5

*

** PIPE VOLUME LENGTHS

*CARD # LENGTH VOL.NO
0050304 1.1770 3
0050305 0.8890 5
0050306 1.0000 6

*

** PIPE VOLUME HORIZONTAL ANGLE

*CARD # H-ANGLE VOL.NO
0050501 0.0 6

*

** PIPE VOLUME VERTICAL ANGLE

*CARD # V-ANGLE VOL.NO
0050601 -90.0 6

*

** PIPE VOLUME FRICTION DATA

*CARD # ROUGHNESS HYD.DIA VOL.NO
0050801 0.0 0.0 6

*

** PIPE JUNCTION LOSS COEFFICIENTS

*CARD # KF KR JUN.NO
0050901 0.0 0.0 5

*

** PIPE VOLUME CONTROL FLAG

*CARD # CONTROL VOL.NO
0051001 0 6

*

** PIPE JUNCTION CONTROL FLAG

*CARD # CONTROL JUN.NO
0051103 1000 2
0051104 1100 3
0051105 1000 4
0051106 1100 5

*

** PIPE VOLUME INITIAL CONDITIONS

*CARD #	CONTROL	PRESSURE	TEMP	ZERO	ZERO	ZERO	VOL. NO
0051221	3	5.197E+6	503.50	0.0	0.0	0.0	1
0051222	3	5.207E+6	499.00	0.0	0.0	0.0	2
0051223	3	5.217E+6	488.00	0.0	0.0	0.0	3
0051224	3	5.225E+6	477.00	0.0	0.0	0.0	4
0051225	3	5.233E+6	460.80	0.0	0.0	0.0	5
0051227	3	5.241E+6	450.50	0.0	0.0	0.0	6

*

** PIPE JUNCTION CONTROL WORD

*CARD # CONTROL
0051300 0

*

** PIPE JUNCTION INITIAL CONDITIONS

*CARD # VELF VELG VJUN JUN.NO
0051301 0.0 0.0 0.0 5

*

** SINGLE JUNCTION FROM DISCHARGE TO NOZZLE *****

*CARD # NAME TYPE
0060000 DISCHJ SNGLJUN

*

** SINGLE JUNCTION GEOMETRY CARD

*CARD # FROM TO AJUN KF KR FLAG
0060101 5010000 8000000 0.19634954 0 0 1000

*

** SINGLE JUNCTION INITIAL CONDITIONS

*CARD # CONTROL VELFJ VELGJ VELJUN
0060201 0 0.0 0.0 0.0

*

** NOZZLE COMPONENT *****

*CARD # NAME TYPE
0080000 NOZZLE PIPE

*

```

*
** PIPE INFORMATION
*CARD # NO.VOLS
0080001 3
*
** PIPE FLOW AREA
*CARD # AVOL VOL.NO
0080101 0.196349541 3
*
** PIPE JUNCTION FLOW AREAS
*CARD # AJUN JUN.NO
0080201 0.196349541 2
*
** PIPE VOLUME LENGTHS
*CARD # LENGTH VOL.NO
0080301 0.6000 1
0080302 0.6000 2
0080303 0.6090 3
*
** PIPE VOLUME VOLUMES
*CARD # VOLUME VOL.NO
0080401 0. 3
*
** PIPE VOLUME HORIZONTAL ANGLE
*CARD # H-ANGLE VOL.NO
0080501 0.0 3
*
** PIPE VOLUME VERTICAL ANGLE
*CARD # V-ANGLE VOL.NO
0080601 -90.0 3
*
** PIPE VOLUME FRICTION DATA
**CARD # ROUGHNESS HYD.DIA VOL.NO
0080801 0.0 0.0 3
*
** PIPE JUNCTION LOSS COEFFICIENTS
*CARD # KF KR JUN.NO
0080901 0.0 0.0 2
*
** PIPE VOLUME CONTROL FLAG
*CARD # CONTROL VOL.NO
0081001 0 3
*
** PIPE JUNCTION CONTROL FLAG
*CARD # CONTROL JUN.NO
0081101 1000 2
*

```



```

** PIPE VOLUME INITIAL CONDITIONS
*CARD # CONTROL PRESSURE TEMPF ZERO ZERO ZERO VOL. NO
0081201 3 5.246E+6 450.5 0.0 0.0 0.0 1
0081202 3 5.252E+6 450.5 0.0 0.0 0.0 2
0081203 3 5.259E+6 450.5 0.0 0.0 0.0 3
*
** PIPE JUNCTION CONTROL WORD
*CARD # CONTROL
0081300 0
*
** PIPE JUNCTION INITIAL CONDITIONS
*CARD # VELF VELG VJUN JUN.NO
0081301 0.0 0.0 0.0 2
*
** SINGLE JUNCTION OUTLET FROM NOZZLE *****
*CARD # NAME TYPE
0090000 OUTLTJ SNGLJUN
*
** SINGLE JUNCTION GEOMETRY CARD
*CARD # FROM IO AJUN KF KR FLAG
0090101 8010000 7000000 0.19634954 0 0 000
*
** SINGLE JUNCTION INITIAL CONDITIONS
*CARD # CONTROL VELFJ VELGJ VELJUN
0090201 0 0.0 0.0 0.0
*
** TIME DEPENDENT OUTLET VOLUME *****
*CARD # NAME TYPE
0070000 OUTLTV TMDPVOL
*
** TIME DEPENDENT VOLUME GEOMETRY CARDS
*CARD # AVOL LNG VOL HANGLE VANGLE DEL-Z ROUGH DHY FLAG
0070101 0.2035 1.0 0.0 0.0 -90.0 -1.0 0.0 0.0 0
*
** TIME DEPENDENT VOLUME DATA CONTROL WORD
*CARD # CONTROL
0070200 2
*
** TIME DEPENDENT VOLUME DATA CARDS
*CARD # TIME PRESSURE QUALS
0070201 0.0 1.0+5 1.0

```

Appendix B
RELAP5 INPUT DECK FOR CFT 2J

=MARVIKEN TEST 24 (CASE 1)

*

** PROBLEM TYPE AND OPTION

*CARD # TYPE OPTION

0000100 NEW TRANSNT

*

** UNITS SELECTION

*CARD # INPUT-UNITS OUTPUT-UNITS

0000102 SI SI

*

* RSTPLT CONTROL

0000105 3.0 4.0

*

** TIME STEP CONTROL CARDS

*CARD #	T-END	DTMIN	DTMAX	CONTROL	MINOR	MAJOR	REST ART
0000201	5.00	1.0E-7	0.005	1	20	200	4096
0000202	20.0	1.0E-7	0.005	1	50	1000	4096
0000203	60.0	1.0E-7	0.250	1	2	40	4096

*

** MINOR EDIT REQUESTS

0000301 P 3010000
 0000302 P 3390000
 0000303 P 5060000
 0000304 RHO 3390000
 0000305 RHO 5030000
 0000306 VOIDF 3390000
 0000307 VOIDF 5060000
 0000308 MFLOWJ 6000000
 0000309 MFLOWJ 5050000
 0000310 TEMPF 5060000
 0000311 VOIDG 5060000
 0000312 RHOF 5060000
 0000313 RHOG 5060000
 0000314 SOUNDE 5060000
 0000315 VOIDGJ 6000000
 0000316 SATTEMP 5060000
 0000317 VELFJ 6000000
 0000318 QUALE 5060000
 0000319 CPUTIME

*

*

** HYDRODYNAMIC COMPONENTS

*

** VESSEL COMPONENT *****

*CARD# NAME TYPE
0030000 VESSEL PIPE

*

*CARD # NO.VOLS
0030001 39

*

** PIPE FLOW AREA

*CARD # AVOL VOL.NO
0030101 0.0 39

*

** PIPE JUNCTION FLOW AREAS

*CARD # AJUN JUN.NO
0030201 0.0 37 17.0 38

*

** PIPE VOLUME LENGTHS

*CARD # LENGTH VOL.NO
0030301 3.55 1 1.0 2 0.5 38 1.26 39

*

** PIPE VOLUMES

**CARD # VOLUME VOL.NO
0030401 8.547 1 13.9 2 10.036 3 10.501 4 10.8125 13
0030402 10.767 17 10.373 18 10.76 19 9.05 20
0030403 10.5 24 10.45 28 10.319 37 10.098 38 19.68 39

*

** PIPE VOLUME HORIZONTAL ANGLE

*CARD # H-ANGLE VOL.NO
0030601 -90.0 39

*

** PIPE VOLUME FRICTION DATA

**CARD # ROUGHNESS HYD.DIA VOL.NO
0030801 0.0 0.0 39

*

** PIPE VOLUME CONTROL FLAG

*CARD # CONTROL VOL.NO
0031001 0 39

*

** PIPE JUNCTION CONTROL FLAG

*CARD # CONTROL JUN.NO
0031101 000 38

*

** PIPE VOLUME INITIAL CONDITIONS

*CARD #	CONTROL	PRESSURE	QUALS	ZERO	ZERO	ZERO	VOL. NO
0031201	2	4.96E6	1.0	0.0	0.0	0.0	1
0031202	2	4.96E6	1.0	0.0	0.0	0.0	2
0031203	2	4.96E6	0.01004	0.0	0.0	0.0	3
0031204	2	4.964E6	0.0	0.0	0.0	0.0	4
0031205	2	4.968E6	0.0	0.0	0.0	0.0	5
0031206	2	4.971E6	0.0	0.0	0.0	0.0	6
0031207	2	4.975E6	0.0	0.0	0.0	0.0	7
0031208	2	4.979E6	0.0	0.0	0.0	0.0	8

*CARD #	CONTROL	PRESSURE	TEMP	ZERO	ZERO	ZERO	VOL. NO
0031209	3	4.983E6	531.0	0.0	0.0	0.0	9
0031210	3	4.987E6	525.0	0.0	0.0	0.0	10
0031211	3	4.991E6	519.0	0.0	0.0	0.0	11
0031212	3	4.995E6	506.5	0.0	0.0	0.0	12
0031213	3	4.999E6	506.5	0.0	0.0	0.0	13
0031214	3	5.003E6	506.5	0.0	0.0	0.0	14
0031215	3	5.007E6	506.5	0.0	0.0	0.0	15
0031216	3	5.011E6	506.5	0.0	0.0	0.0	16
0031217	3	5.015E6	506.5	0.0	0.0	0.0	17
0031218	3	5.019E6	506.5	0.0	0.0	0.0	18
0031219	3	5.023E6	506.5	0.0	0.0	0.0	19
0031220	3	5.027E6	506.5	0.0	0.0	0.0	20
0031221	3	5.031E6	506.0	0.0	0.0	0.0	21
0031222	3	5.035E6	506.0	0.0	0.0	0.0	22
0031223	3	5.039E6	506.0	0.0	0.0	0.0	23
0031224	3	5.043E6	506.0	0.0	0.0	0.0	24
0031225	3	5.048E6	506.0	0.0	0.0	0.0	25
0031226	3	5.052E6	506.0	0.0	0.0	0.0	26
0031227	3	5.056E6	506.0	0.0	0.0	0.0	27
0031228	3	5.060E6	506.0	0.0	0.0	0.0	28
0031229	3	5.064E6	506.0	0.0	0.0	0.0	29
0031230	3	5.068E6	506.0	0.0	0.0	0.0	30
0031231	3	5.072E6	506.0	0.0	0.0	0.0	31
0031232	3	5.076E6	505.5	0.0	0.0	0.0	32
0031233	3	5.080E6	505.5	0.0	0.0	0.0	33
0031234	3	5.084E6	505.5	0.0	0.0	0.0	34
0031235	3	5.088E6	505.5	0.0	0.0	0.0	35
0031236	3	5.092E6	505.5	0.0	0.0	0.0	36
0031237	3	5.096E6	505.5	0.0	0.0	0.0	37
0031238	3	5.100E6	505.0	0.0	0.0	0.0	38
0031239	3	5.108E6	504.0	0.0	0.0	0.0	39

*

** PIPE JUNCTION INITIAL CONDITIONS

*CARD #	VELF	VELG	VJUN	JUN.NO
0031301	0.0	0.0	0.0	38

*

** SINGLE JUNCTION OUTLET FROM VESSEL *****

*CARD # NAME TYPE
0040000 OUTLETJ SNGJ JUN

*

** SINGLE JUNCTION GEOMETRY CARD

*CARD # FROM TO AJUN KF KR FLAG
0040101 003010000 005000000 2.0 0.0 0.0 1000

*

** SINGLE JUNCTION INITIAL CONDITIONS

*CARD # CONTROL VELFJ VELGJ VELJUN
0040201 0 0.0 0.0 0.0

*

** PIPE COMPONENT *****

*CARD # NAME TYPE
0050000 DISCHARGE PIPE

*

** PIPE INFORMATION

*CARD # NO.VOLS
0050001 6

*

** PIPE FLOW AREA

*CARD # AVOL VOL.NO
0050102 0.4441 3
0050103 0.4778 5
0050104 0.4441 6

*

** PIPE JUNCTION FLOW AREAS

*CARD # AJUN JUN.NO
0050201 0.0 5

*

** PIPE VOLUME LENGTHS

*CARD # LENGTH VOL.NO
0050304 1.1770 3
0050305 0.8890 5
0050306 1.0000 6

*

** PIPE VOLUME HORIZONTAL ANGLE

*CARD # H-ANGLE VOL.NO
0050501 0.0 6

*

** PIPE VOLUME VERTICAL ANGLE

*CARD # V-ANGLE VOL.NO
0050601 -90.0 6

*

** PIPE VOLUME FRICTION DATA

*CARD # ROUGHNESS HYD.DIA VOL.NO
0050801 0.0 0.0 6

*

** PIPE JUNCTION LOSS COEFFICIENTS

*CARD # KF KR JUN.NO
0050901 0.0 0.0 5

*

** PIPE VOLUME CONTROL FLAG

*CARD # CONTROL VOL.NO
0051001 0 6

*

** PIPE JUNCTION CONTROL FLAG

*CARD # CONTROL JUN.NO
0051103 1000 2
0051104 1100 3
0051105 1000 4
0051106 1100 5

*

** PIPE VOLUME INITIAL CONDITIONS

*CARD #	CONTROL	PRESSURE	TEMP	ZERO	ZERO	ZERO	VOL. NO
0051221	3	5.122E+6	501.00	0.0	0.0	0.0	1
0051222	3	5.133E+6	496.00	0.0	0.0	0.0	2
0051223	3	5.139E+6	484.00	0.0	0.0	0.0	3
0051224	3	5.147E+6	476.00	0.0	0.0	0.0	4
0051225	3	5.155E+6	469.00	0.0	0.0	0.0	5
0051227	3	5.163E+6	462.00	0.0	0.0	0.0	6

** PIPE JUNCTION CONTROL WORD

*CARD # CONTROL
0051300 0

*

** PIPE JUNCTION INITIAL CONDITIONS

*CARD # VELF VELG VJUN JUN.NO
0051301 0.0 0.0 0.0 5

*

** SINGLE JUNCTION OUTLET FROM NOZZLE *****

*CARD # NAME TYPE
0060000 OUTLTJ SNGLJUN

*

** SINGLE JUNCTION GEOMETRY CARD

*CARD # FROM TO AJUN KF KR FLAG
0060101 5010000 7000000 0.1963 0 0 000

*

** SINGLE JUNCTION INITIAL CONDITIONS

*CARD # CONTROL VELFJ VELGJ VELJUN
0060201 0 0.0 0.0 0.0

*

** TIME DEPENDENT OUTLET VOLUME *****

*CARD # NAME TYPE
0070000 OUTLTV TMDPVOL

*

** TIME DEPENDENT VOLUME GEOMETRY CARDS
*CARD # A:OL LNG VOL HANGLE VANGLE DEL-Z ROUGH DHY FLAG
0070101 0.2035 1.0 0.0 0.0 -90.0 -1.0 0.0 0.0 0

*
** TIME DEPENDENT VOLUME DATA CONTROL WORD
*CARD # CONTROL
0070200 2

*
** TIME DEPENDENT VOLUME DATA CARDS
*CAPD # TIME PRESSURE QVALS
0070201 0.0 1.0+5 1.0

BIBLIOGRAPHIC DATA SHEET

(See instructions on the reverse)

1. REPORT NUMBER
(Assigned by NRC. Add Vol., Supp., Rev.,
and Addendum Numbers, if any.)

NUREG/IA-0086

2. TITLE AND SUBTITLE

Assessment of RELAP5/MOD2 Critical Flow Model Using
Marviken Test Data 15 and 24

3. DATE REPORT PUBLISHED

MONTH | YEAR

April | 1992

4. FIN OR GRANT NUMBER

A4682

5. AUTHOR(S)

K. Kim, H.-J. Kim

6. TYPE OF REPORT

Technical

7. PERIOD COVERED (Inclusive Dates)

8. PERFORMING ORGANIZATION - NAME AND ADDRESS (If NRC, provide Division, Office or Region, U.S. Nuclear Regulatory Commission, and mailing address; if contractor, provide name and mailing address.)

Korea Institute of Nuclear Safety
Safety Analysis Department
P. O. Box 16, Daeduk-Danji
Taejon, Korea

9. SPONSORING ORGANIZATION - NAME AND ADDRESS (If NRC, type "Same as above"; if contractor, provide NRC Division, Office or Region, U.S. Nuclear Regulatory Commission, and mailing address.)

Office of Nuclear Regulatory Research
U.S. Nuclear Regulatory Commission
Washington, DC 20555

10. SUPPLEMENTARY NOTES

11. ABSTRACT (200 words or less)

The simulations of Marviken CFT 15 and 24 have been performed using RELAP5/MOD2. For the modeling of a nozzle as a pipe, the results of simulations and the CFT 15 test data are in good agreement, but the simulations underpredict by about 5 to 10% in transition region between subcooled and two-phase. In the two-phase region, there happens the fluctuations of the calculated mass flowrate for the case of using the critical flow model in RELAP5/MOD3. It seems that the improvement of the critical flow model in RELAP5 during the transition period is necessary. RELAP5 critical flow model underpredicts the CFT 24 data by 10 to 20% in two-phase choked flow region, while its predictions are in good agreement with subcooled choked flowrate data. The modeling of a nozzle as a pipe in the case of CFT 24 may give rise of unreasonable results in subcooled critical flow region.

12. KEY WORDS/DESCRIPTORS (List words or phrases that will assist researchers in locating the report.)

Assessment of RELAP5/MOD2
Critical Flow Model
Marviken Test Data 15 and 24

13. AVAILABILITY STATEMENT

Unlimited

14. SECURITY CLASSIFICATION

(This Page)

Unclassified

(This Report)

Unclassified

15. NUMBER OF PAGES

16. PRICE

THIS DOCUMENT WAS PRINTED USING RECYCLED PAPER

UNITED STATES
NUCLEAR REGULATORY COMMISSION
WASHINGTON, D.C. 20555

SPECIAL FOURTH-CLASS RATE
POSTAGE AND FEES PAID
USNRC
PERMIT NO. G-67

OFFICIAL BUSINESS
PENALTY FOR PRIVATE USE, \$300

120555139531 1 JAN10
US NRC-04DM
DIV FOIA & PUBLICATIONS SVCS
TDS-PDR-NUREG
P-211
WASHINGTON DC 20555